CVJ CLUJ VETERINARY JOURNAL

Research article

Hepato and nephroprotective effects of aqueous extract of *Citrullus lanatus (Linn.)* juice in gentamicin-overdosed commercial broiler chickens

Olukayode G Akintunde [1*], Christianah O Korede [1], Samson A Rahman [1], Ademola A Oyagbemi [2] and Salihu A Ameen [3]

[1] Department of Veterinary Physiology and Biochemistry, College of Veterinary Medicine, Federal University of Agriculture, Abeokuta; akintundeog@funaab.edu.ng, koredechristianah00@gmail.com, rahmansa@funaab.edu.ng
[2] Department of Veterinary Physiology and Biochemistry, Faculty of Veterinary Medicine, University of Ibadan; ademolaoyagbemi@yahoo.com
[3] Department of Veterinary Medicine, Faculty of Veterinary Medicine, University of Ilorin; ameen.sa@unilorin.edu.ng
* Corresponding author: akintundeog@funaab.edu.ng.

Abstract This study evaluated hepato- and nephroprotective potentials of *Citrullus lanatus* juice (CLJ) on gentamicin-overdosed broilers. Eighty broilers were used for this experiment; fifty broilers were used to confirm gentamicin toxic dose with liver function assay. While thirty broilers were reared from day old to thirty-five days, randomly distributed into six groups with five birds per group. Broilers in group A received 1.0mL/kg normal saline; group B received 45mg/kg gentamicin intramuscularly; group C received 200mg/kg Vitamin C orally, groups D, E, and F received 100, 200, and 400mg/kg of CLJ respectively orally for 14 days later received single dose 45mg/kg gentamicin intramuscularly. Statistical analysis was performed to assess significant differences among groups. Body weights were compared on days 35 and 49. Blood chemistry for liver and kidney functions were examined, liver and kidney pathologies were evaluated at day 49. There was significant increase in body weight of 400-treated birds unlike decreased body weight in GM-treated birds at day 49. There were significant decrease in Na^+, Creatinine and Uric acids but increase in K^+ in 400 mg/kg CLJ–treated birds compared with gentamicin-treated birds. There were liver and kidney pathological damages in gentamicin-treated birds. These impairments were resolved in 400 mg/kg CLJ-treated birds. The hepatoprotection and nephroprotection may be due to ascorbic acids and flavonoids present in CLJ. This may have provided antioxidant effects for restoration of liver and kidney pathological changes in 400 mg/kg CLJ-treated birds. This study shows that 400mg/kg CLJ may improve body weight and reversed gentamicin-overdose damages in liver and kidney of broilers.

Keywords: *Citrullus lanatus*, Gentamicin, Hepatoprotective, Nephroprotective, Broilers.

Received: 15.08.2025
Accepted: 01.12.2025
Published: 09.03.2026

DOI:10.52331/vol31i2w863

1.Introdcution

Gentamicin sulfate is an aminoglycoside antibiotic that is commonly used in poultry production. Gentamicin residue arising from overdose in poultry products is of great public health importance worldwide, which can lead to antibiotic resistance if it is not controlled. Gentamicin residue and or overdose can be associated with health risks in clinical cases such as hepatotoxic, nephrotoxic, and ototoxic effects [1]. The damages seen in kidney due to abuse of gentamicin in poultry industry in our community leading to nephrotoxicity requires great attention [2]. Gentamicin overdose can cause metabolic and nutritional abnormalities, hepatotoxicity, kidney failure as well as cancer leading to death.

Some studies have revealed that drug-induced toxicity had resulted in major causes of renal injury [3]. Gentamicin is normally used for treatment of different poultry diseases such as chronic respiratory disease, fowl cholera, salmonellosis to mention but a few [4,5] Gentamicin can be used to prevent early chick mortality due to bacterial infections by administration of gentamicin in day-old chicks. Although, in day old

chicks there are no observable effects of gentamicin at a dose of 10 mg/kg body weight, but, at higher dose different pathological changes such as enlarged and swollen kidneys, swollen liver, decreased serum total protein, albumin and higher concentrations of serum alanine aminotransferase (ALT), creatinine and urea were observed in dose dependent manners [6,7].

Serum electrolytes such as increased sodium, potassium and chloride are indication of nephrotoxicity which can be resolved with fruit juice [8,9]. Creatinine is produced in liver and it is breakdown to creatine phosphate in muscle. Creatinine is a good indicator of kidney damage [10]. Creatinine is removed mainly through the kidney, and the concentration in biological system is altered by various muscle toxicants or decreased muscular activity [11]. An increase in serum creatinine concentration is a biomarker of nephrotoxicity [12]. Uric acid is the final oxidative product of purine metabolism and is ready excreted by the kidney [13]. Thus, increased serum uric acid levels are seen in patients with reduced glomerular filtration rate (GFR) as well as in kidney failure [10].

Overdose of gentamicin causes nephrotoxicity arising from fat accumulation seen in renal proximal convoluted tubules could have led to loss of brush border integrity [14]. Although it is technically absurd to observe some farmers doing co-administration of gentamicin with killed vaccines for the treatment and prevention of bacterial infections. Major causes of kidney disease in birds are infectious nephritis, vitamins A and or C deficiency, heavy metal toxicity, and kidney tumor. This normally manifest with elevated blood uric acid in kidney disease when there is abnormality in the integrity of the urinary tract or blockade of urine flow [15]. Increased serum uric acid levels are a main risk factor for renal failure, which is the most nitrogenous metabolic product in birds [16, 17].

Measurement of blood creatinine concentration in mammals is used to evaluate the glomerular filtration rate [15]. Creatinine value is a vital test that can be used for examination of renal failure in birds [18]. This situation can arise due to increase in use of drugs, chemical toxins, and microbial agents, which can cause increase in serum biochemical indicators [15,19, 20].

Plants have been used for treatment and prevention of hepatotoxicity and nephrototoxicity in domestic animals [21]. The use of plants for treatment can serve as future approach to ethnopharmacology research and clinical sciences exploiting the knowledge of phytochemicals present in plants [22]. Watermelon also known as *Citrullus lanatus* fruit is a flowering plant belonging to the family, *Cucurbitaceae*. *Citrullus lanatus* seed has been shown to possess hepatoprotective effect in Wistar rats [23] and cardioprotective effects in rats [24]. *Citrullus lanatus* juice is rich in beta-carotene, vitamin C, and lycopene, which counteract free radicals effect in the body [25, 26]

Watermelon is a fruit with a juicy pulp that is red or pink with many seeds, the fruit is consumed worldwide due to the wellbeing benefits. Watermelon fruit contains water (91%) and sugar (6%), and is low in fat. Watermelon fruit has been identified as a good source of vitamin C [27]. The fresh watermelon juice contains 3.72 mg/100 g of Vitamin C in watermelon which varies with the difference in watermelon cultivars and environmental factors [28].

Vitamin C is found in Citrus fruit, vegetables and adrenal glands as hexuronic acid as a natural source. It is an essential nutrient that cannot be synthesized by the human body therefore, it has to be incorporated in the body through diet [28]. Vitamin C is a water-soluble essential nutrient that is frequently added to a variety of food products for nutrient enhancement and supplementation important for biosynthesis of collagen and certain hormones [29, 30]. Ascorbic acid is also an anticancer agent [31].

This study evaluated the hepatoprotective and nephroprotective potentials of *C. lanatus* juice in commercial broilers with gentamicin overdose.

2.Materials and Methods

2.1 Fruit collection and identification of C. lanatus fruit.

The *C. lanatus* fruit was collected from a fruit market in Alabata area very close to Federal University of Agriculture, Abeokuta. The *C. lanatus* fruit was deposited for authentication in the Herbarium unit of the Botany Department, University of Ibadan, Oyo State Nigeria and the voucher number UIH 22872 was issued.

2.2. Preparation of aqueous extract of C. lanatus Juice (CLJ).

The aqueous extract of CLJ was prepared from whole *C. lanatus* fruit while the rind and seeds were carefully removed. The CLJ was blended while water was removed using rotary evaporator until a

constant weight of aqueous extract of CLJ was obtained. This was done in the laboratory, Department of Veterinary Physiology and Biochemistry, Federal University of Agriculture, Abeokuta. The aqueous extract of CLJ was prepared according to the procedure previously described by Sofowora [32], it was stored in refrigerator at 4^0c until it was used.

2.3 Ethical statement

This research was carried out with the approval of the ethical committee in the College of Veterinary Medicine, Federal University of Agriculture, Abeokuta, Nigeria with approval number FUNAAB / COLVET / CREC / 2021/09/01.

2.4. Experimental design: Birds Management

A total of Eighty (80) day-old commercial Arbor Acre broiler chicks were acquired from a reputable hatchery in Ibadan. The birds were kept in Poultry section of Teaching and Research Farm, College of Veterinary Medicine, Federal University of Agriculture Abeokuta, Ogun State, Nigeria, with longitude of 3°25'29"E, latitude of 7°13'27"N and an altitude of 76m above sea level. This is located in the tropical rainforest vegetation zone of South-Western Nigeria. The experimental site was a humid climate with mean annual rainfall of about 1037 mm, mean humidity and temperature of 83 % and 24.7 °C, respectively.

This experiment was divided into two studies, study one (1) was used to confirm the toxic dose of gentamicin with 50 pieces of day old broilers randomly distributed into 5 groups with 10 birds per group were observed for clinical signs, mortality twice daily for 28 days and evaluation of the liver function enzymes (Aspartate aminotransferase, AST; Alanine aminotransferase, ALT and Alkaline phosphatase, ALP). These groups were administered the following doses: 0, 40, 50, 60 and 80mg/kg body weight of gentamicin respectively according to the study of Javed [5] modified. The birds in study 1 were raised on deep litter management, fed with chick marsh and administered different doses of gentamicin at day old, the birds were observed for clinical signs, mortality and blood sample was collected on 28th day to evaluate liver function tests of the birds in different groups.

Birds in study 2, thirty (30) broilers were reared from day-old on deep litter management and later placed them in battery cage on day 30 for close monitoring. The study 2 was used to check protective effects of aqueous extract of CLJ on gentamicin-overdosed broilers. The birds in study 2 were initially given chick marsh from day old to 28th day and later fed with broiler finisher from 29th to 48th day, water and feed were provided *ad libitum* throughout the period of study. The birds in study 2, on day 33rd, were weighed and randomly distributed into six groups (A, B, C, D, E and F) with five birds per group in a battery cage system. The birds' weight was repeated on day 35th before extract administration at the onset of study 2. These thirty (30) pieces of broilers were observed and evaluated on day 49.

- Group A was given 1.0 mL/kg normal saline in pectoral muscles as control negative, NS.
- Group B was given 45 mg/kg gentamicin only, GM.
- Group C was given 200mg/kg of Vitamin C, VTM (Positive control).
- Group D was given 100 mg/kg of CLJ and 45 mg/kg gentamicin, GM.
- Group E was given 200 mg/kg of CLJ and 45 mg/kg gentamicin, GM.
- Group F was given 400 mg/kg of CLJ and 45 mg/kg gentamicin, GM.

On 35th day, birds in groups D, E and F were given different doses of aqueous extract of CLJ orally for fourteen (14) days, and later given 45mg/kg of Gentamicin (GM) intramuscularly on 42nd day. The birds in groups B were given 45mg/kg of Gentamicin intramuscularly while birds in group C were given 200mg/kg of Vitamin C (Ascorbic acid) on 42nd day, as described in section 2.5 below). This study was terminated on the forty-ninth (49th) day with samples collection. This experiment was designed with slight modification to the studies of [5, 6].

2.5. Drugs/ Vaccines administered

The birds were given antibiotics (ArserylR) for the first five days (days 1 to 5) to remove any known or unknown microbial infection, vaccinations were administered using Newcastle disease (Lasota strain) vaccine with Vaksimune NDR, 100 doses, batch number 201AL24801 was given on day 7. While Infectious bursal disease (Gumboro) vaccine B.P vet intermediate strain, 100 doses, batch number A19107 was administered twice on days 14 and 21 to the birds orally. The vaccinations were done to improve the immune status of the birds. GentanorR 100 (Gentamicin injectable containing Gentamicin 100mg/ml) (GM) was used to induce the broilers with mean body weight ranging from 1.38 to 1.50kg were given 0.62 to

0.68ml of GM intramuscularly that delivered 45mg/kg of GM in this study. While VcnorR Water Soluble Preparation (Vitamin C 100,000mg) in 100g per sachet, a multivitamin and supplement referred to as Vitamin (VTM) was given orally, broilers with mean body weight ranging from 1.38 to 1.5 kg were given 0.14 to 0.15ml, the stock solution was prepared by reconstituting 2,500mg/L of water that delivered 200mg/kg of Vitamin C to the broilers in this study. Arseryl, Gentamicin and Vcnor were manufactured and sold by Jubaili Animal Health, Nigeria.

2.6. Sample collection

At the end of the study, on 49th day all the birds were weighed, blood sample was collected from the jugular vein of each bird in plain sample bottle from each birds in all the groups. The blood samples, were held on ice until centrifugation at 5,000 revolutions at 0°C for 20 min. The serum biochemical evaluations (Total protein (TP), Albumin (Alb), Aspartate aminotransferase (AST), Alanine aminotransferase (ALT), Alkaline phosphatase (ALP), and Creatinine activities were determined according to enzymatic procedures described in commercial test kits manufactured by Randox Laboratories, Crumlin, England. The serum uric acid was evaluated with PriestTM SYS kit manufactured by Robonik (India) PVT LTD. While the electrolyte analysis for Sodium, Potassium, Calcium and Chloride were determined using commercial colorimetric kits (Quimica ClinicaAplicada S A Amposta, Spain).

2.7. Histopathology of liver and Kidney

The birds were humanely sacrificed liver and kidney were carefully collected into 10% formalin solution for histopathological examination. The liver and kidney histopathology analysis were done in the laboratory of Department of Veterinary Pathology, Federal University of Agriculture, Abeokuta, Nigeria.

2.8. Statistical Analysis

The data obtained were statistically analyzed with one-way ANOVA in Graph pad Instat software version 7.0, California USA. The mean differences were considered statistically significant differences at $P<0.05$ using the Tukey comparison postdoc test. The data generated were expressed as mean ± Standard Error of Mean and presented in tables and graphical forms.

3.0. Results

3.1. Mortality rate of commercial broilers treated with different doses of gentamicin, Study 1.

There was no mortality % in the broilers administered with 0 to 40 mg/kg body weight of gentamicin. There was single mortality on different days (9 and 18) in broiler given 50mg/kg body weight of gentamicin; two broilers died on day 26 this made 25% mortality in broilers given 50mg/kg body weight of gentamicin in study 1, (Table 1). Meanwhile broilers given 60mg/kg body weight of gentamicin showed 50% mortality with one mortality in day 4th, two died on day 9th, one died on day 17th and one died on day 22nd. Finally, broilers given 80mg/kg body weight of gentamicin showed 90% mortality rate with three mortalities on day 2, one on day 9, two on day 17 and three on day 24 in this group, (Table 1).

Table 1. Mortality rate of commercial broilers treated with different doses of gentamicin, Study 1.

Group	Day 0- 7	Day 8- 14	Day 15- 21	Day 22- 28	Nr. of total mortality	% of total mortality
A (0mg/kg)	0	0	0	0	0	0
B (40mg/kg)	0	0	0	0	0	0
C (50mg/kg)	0	1	1	2	4	25
D (60mg/kg)	1	2	1	1	5	50
E (80mg/kg)	3	1	2	3	9	90

3.2 Clinical Signs of commercial broilers treated with different doses of gentamicin, Study 1.

The broilers given 0 to 40mg/kg body weight gentamicin did not exhibit any clinical signs with no change in their behavior throughout the study period. Their interest in the feed and drinking water of these groups was normal. The broilers that received 50 to 60 mg/kg body weight of gentamicin showed depression with slight increased water intake. These signs were serious in broilers given 80 mg/kg body weight of GM with severe depression, sitting on hock joints shortly with 90% mortality after gentamicin

administration, (Table 1). Water intake was increased throughout the period of study and watery diarrhea was a regular feature. The birds progressively became emaciated and had prominent keel bone.

3.3. Result of serum liver function test of broilers treated with different doses of gentamicin, (Study 1).

The Aspartate aminotransferase, (AST) values of broilers treated with 50 and 60 mg/kg GM were significantly (P<0.05) high when compared with broilers given normal saline (NS) and 40mg/kg GM , but the Alanine aminotransferase, (ALT) values was significantly (P<0.05) high in broilers given 60mg/kg GM compared with broilers given normal saline (NS) and 40mg/kg GM. Considering Alkaline Phosphatase, ALP values the broilers given 60mg/kg GM were significantly (P<0.05) high than broilers given normal saline (NS), (Fig. 1).

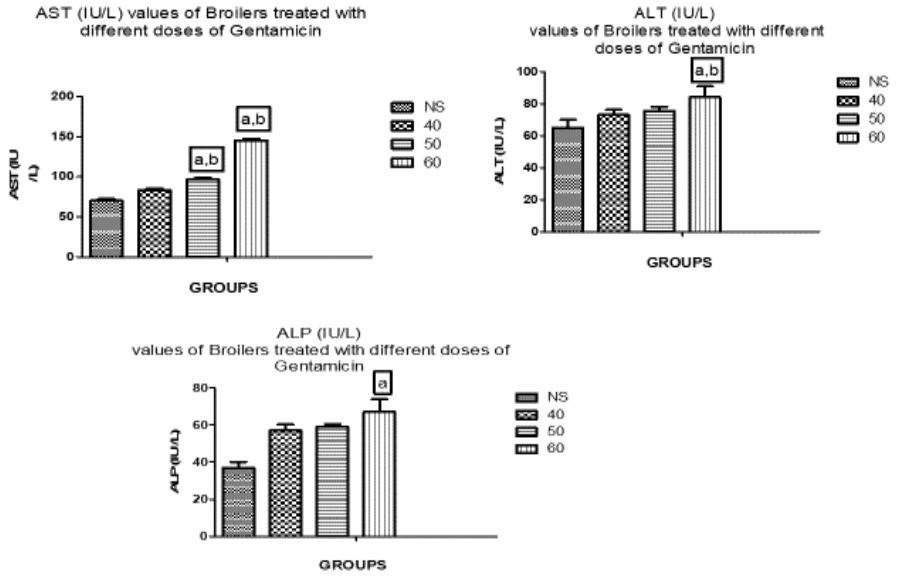

Figure 1. Serum liver test of broilers treated with different doses of gentamicin, (Study 1). NS= Normal saline; AST= Aspartate Aminotransferase; ALT= Alanine Aminotransferase; ALP= Alkaline Phosphatase. n= Number of Broilers used were 5 per group; a and b were significantly different (P<0.05) compared with NS and 40mg/kg groups respectively.

3.4 Result of body weight of gentamicin-overdosed Broilers within two week (35th and 49th day) treated with and without CLJ, (Study 2).

There was a significant (P<0.05) increase in body weight change in birds treated with 400 mg/kg/body weight of CLJ extract (14.67 %) on day 49 when compared with the body weight of birds on day 35. This similar trend was seen in VTM group, which showed a slight increase in body weight change (4.23%) when comparing body weight of these birds on days 35 and 49. While, there was a slight decrease in body weight change of birds treated with GM (4.17%) when compared birds on days 35 and 49. There was significant (P<0.05) increase in body weight of birds treated with 400 mg/kg/BW of CLJ extract (14.67%) when compared body weight of GM- treated birds (4.17%) at day 49. As well as significant increase in body weight change in 400 mg/kg/BW of CLJ extract (14.67%) compared with body weight change in normal saline-treated birds (5.63%), (Table 2).

Table 2. Result of mean weight of gentamicin- induced Broilers within 14 days (35th and 49th day) treated with and without CLJ, (Study 2).

Group/Weight (gm)	35th day (Before Treatment) kg	49th day (After Treatment) kg	Differences in weight between 35th and 49th day (%)
NS	1.42± 0.05	1.50±0.00	5.63% (Increase)
GM	1.44± 0.02	1.38±0.07	4.17% (Decrease)

VTM	1.42± 0.02	1.48±0.04	4.23 % (Increase)
100 CLJ	1.38±0.05	1.38±0.04	No difference
200CLJ	1.40±0.06	1.44±0.02	2.86% (Increase)
400 CLJ	1.500± 0.00	1.72±0.00	14.67% [a, b] (Increase)

Mean± SEM; n= number of broilers per group is 5. The superscript a and b were significantly ($P < 0.05$) different when compared with NS and GM groups respectively. NS= Normal saline; GM= Gentamicin.

3.5. Result of Serum Liver Function Test values of GM-overdose Broiler treated with and without CLJ, Study 2.

The total protein concentration was significantly ($P<0.05$) increased in 200mg/kg of CLJ-treated broilers (5.60±0.24mg/dl) when compared with GM-treated broilers (4.6±0.24mg/dl), (Fig. 2). The albumin concentration was significantly ($P<0.05$) increased in broilers treated with 100, 200 and 400mg/kg of CLJ (3.10±0.7; 3.00±0.04 and 3.62±0.09mg/dl) respectively when compared with broilers treated with GM (2.6±0.24mg/dl) and severely significantly ($P<0.05$) decrease in albumin concentration when compared with broilers treated with normal saline (4.60±0.24 mg/dl). The ALT concentration was significantly ($P<0.05$) low in broilers treated with 400mg/kg CLJ (66.60±0.51 IU/L) when compared with GM-treated broilers (77.40±0.93 IU/L); AST concentration were significantly ($P<0.05$) low in broilers treated with 400mg/kg CLJ (88.40±0.51 IU/L) when compared with broilers treated with GM (112.4±2.58 IU/L); While the ALP concentration was significantly ($P<0.05$) low in broilers treated with 400mg/kg CLJ (46.4±0.24 IU/L) when compared with GM-treated broilers (57.60±0.24 IU/L), (Fig. 2).

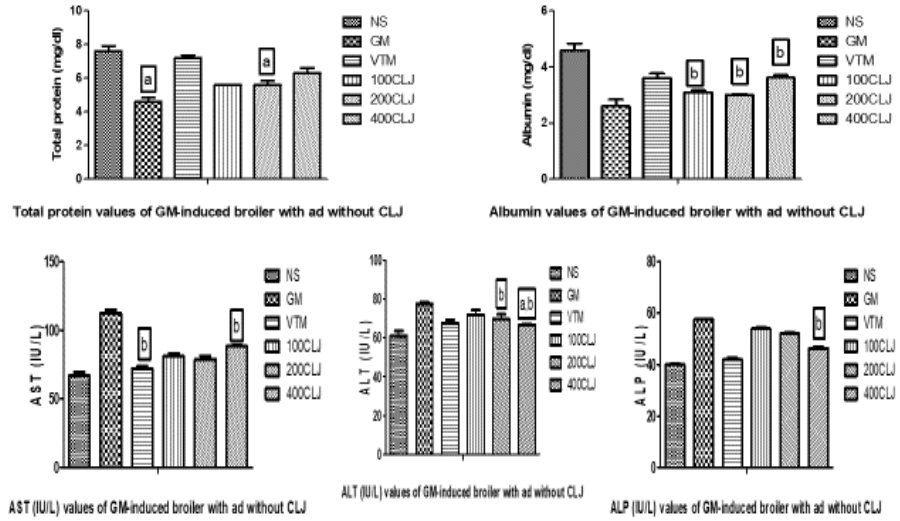

Figure 2. Serum Liver Function Test concentration of GM-overdosed Broiler treated with and without CLJ. NS= Normal saline; GM=Gentamicin; VTM=Vitamin; CLJ= *Citrullus lanatus* juice; 100CLJ= 100mg/kg of CLJ +GM; 200 CLJ = 200mg/kg of CLJ +GM; 400 CLJ = 400mg/kg of CLJ +GM; AST= Aspartate aminotransferase; ALT=Alanine aminotransferase; ALP= Alkaline phosphatase. a= significantly different compared to NS; b= significantly different compared to GM.

3.6. Result of Serum Kidney function Tests of gentamicin-overdosed broilers treated with and without CLJ.

There were significant ($P<0.05$) decrease in serum Na^+ concentration of broilers treated with 400mg/kg of CLJ (142.2±0.51mEq/L) when compared with serum Na^+ concentration of GM-treated broilers (158.0±0.89mEq/L). It was observed that the serum K^+ concentration of broilers treated with 200 and 400mg/kg of CLJ (3.8±0.2 and 3.4±0.24mEq/L) respectively were significantly high when compared with serum K^+ concentration of gentamicin-treated broilers (2.5±0.24mEq/L). The serum Ca^{2+} concentration of broilers treated with 400mg/kg CLJ (7.20±0.20mEq/L) was significantly ($P<0.05$) higher than the serum Ca^{2+} concentration in normal saline-treated broilers (4.2±0.2 mEq/L) but lower than the serum Ca^{2+} concentration of gentamicin-treated broilers (6.2±0.37 mEq/L). Meanwhile the serum Cl^- concentration of broilers treated with 400mg/kg CLJ (63.00±1.54 mEq/L) was significantly ($P<0.05$) higher than the serum Cl^- concentration of broilers treated with GM (55.83±1.22mEq/L), (Fig. 3). Considering creatinine, the serum

creatinine concentration of broilers treated with 400mg/kg CLJ (1.12.00±0.04 mg/dl) was significantly (P<0.05) lower than the serum creatinine concentration of GM-treated broilers (1.86±0.05 mg/dl). While the serum uric acid concentration of 200 and 400mg/kg treated broilers (5.74±0.16mg/dl and 5.78±0.04 mg/dl) respectively were significantly (P < 0.05) lowered than the serum uric acid concentration of gentamicin-treated broilers (8.40±0.12 mg/dl), (Fig. 4).

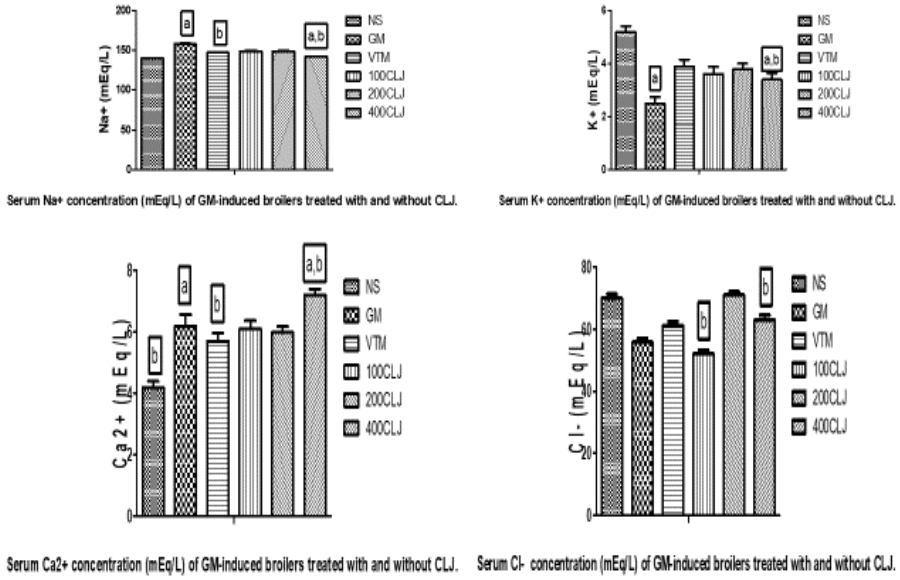

Figure 3. Serum electrolyte concentration of gentamicin-overdosed broilers treated with and without CLJ. NS=Normal saline; GM=Gentamicin only; VTM=Vitamin; CLJ= *Citrullus lanatus* juice; 100CLJ= 100mg/kg of CLJ+GM; 200CLJ = 200mg/kg of CLJ +GM; 400CLJ = 400mg/kg of CLJ +GM; Mean ± SEM with significant difference of P>0.05 with a and b showed significant difference compared with NS and GM respectively.

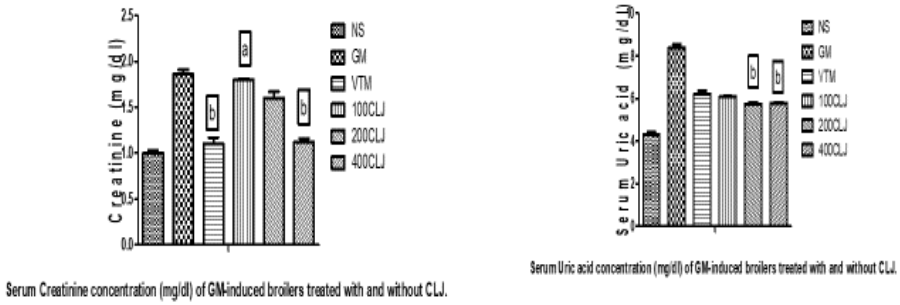

Figure 4. Serum Creatinine and uric acid concentration of gentamicin-overdosed nephrotoxic broilers treated with CLJ. NS= Normal saline; GM=Gentamicin; VTM=Vitamin; CLJ= *Citrullus lanatus* juice; 100CLJ= 100mg/kg of CLJ+GM; 200CLJ = 200mg/kg of CLJ+GM; 400CLJ = 400mg/kg of CLJ +GM; Mean ± SEM with significant difference of P>0.05 with a and b showed significant difference compared with NS and GM respectively.

3.7. Histopathology of Liver in gentamicin-overdosed broilers treated with and without aqueous extract of CLJ.

There were no pathological lesions in the liver treated with normal saline and VTM. Liver treated with gentamicin showed moderate hyperplasia of the bile duct epithelial cells and moderate hepatic congestion. Meanwhile the liver treated with 100mg/kg of CLJ showed enlarged and congested central vein with mild mononuclear infiltration of the portal area. There were moderate congestion in liver of broilers treated with 200mg/kg CLJ with little or no pathological lesion in the liver of broilers treated with 400mg/kg CLJ, (Fig. 5).

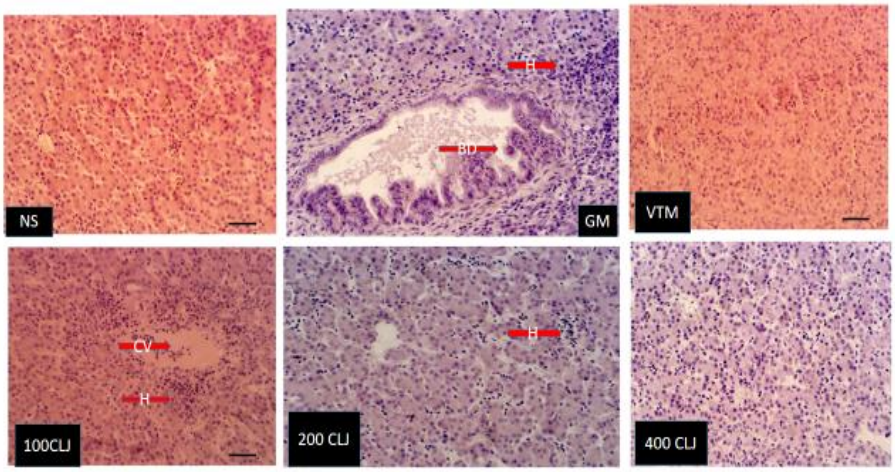

Figure 5. Histopathology of Liver in gentamicin-overdosed broilers treated with and without aqueous extract of CLJ. H&E Stain. Scale bar=50µm. NS=Control group; GM= Gentamicin-induced group; VTM= Vitamin C; 100CLJ= 100mg/kg of CLJ +GM; 200 CLJ = 200mg/kg of CLJ +GM; 400 CLJ = 400mg/kg of CLJ +GM; CV= Central vein; H=Hepatic; S= Sinusoid; Red Marked= Pathological CV, H and Bile duct, BD.

3.8. Histopathology of Kidney in gentamicin-overdosed broilers treated with and without aqueous extract of CLJ.

The kidney of broiler treated with GM showed presence of severe eosinophilic material on the intraluminal wall of the tubule indicated with thin red arrow. There were moderate eosinophilic materials around the tubular lumen and walls in kidney of broiler treated with 100mg/kg of CLJ. Meanwhile there were mild eosinophilic materials around the intraluminal wall of the kidney tubules in the broilers treated with 400mg/kg of CLJ. While there was no pathological lesion in the glomeruli and kidney tubules of broiler treated with normal saline and VTM, (Fig. 6).

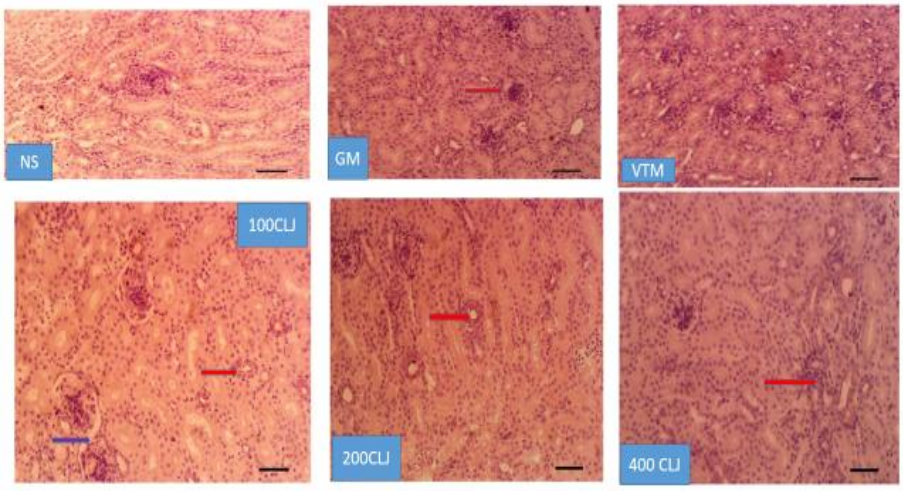

Figure 6. Histopathology of Kidney in gentamicin-overdosed broilers treated with and without aqueous extract of CLJ. H&E Stain. Scale bar=50µm. NS: Normal saline (NS) showing glomerulus and the renal tubules with no pathological lesion; GM: Gentamicin only (GM) showing eosinophilic material in the tubular lumen and haemorrhages in the interstitium, (red arrow); VTM: Vitamin C (VTM) showing the glomeruli and tubules with no pathological lesion. 100CLJ: 100mg/kg CLJ + GM showing mild presence of eosinophilic material in the tubular lumen and walls (red arrow); 200CLJ: 200mg/kg CLJ + GM showing mild presence of eosinophilic material on the intraluminal wall of the tubules (red arrow); 400CLJ: 400mg/kg CLJ + GM showing no pathological lesion.

4. Discussion

The clinical signs of low feed intake, emaciation, increased water intake, and watery diarrhea seen in this study 1 of broilers treated with 60mg/kg of gentamicin were similar to the observation seen by Javed

[5] when broilers when were treated with 70 to 100mg/kg of gentamicin. The high mortality of broilers treated with 60 and 80mg/kg of gentamicin in study 1 may be due to hepatic and or renal failure [18]. This confirmed the investigation and clinical signs seen during gentamicin toxicity in white leghorn birds by Islam [20] that reported increased mortality and toxicopathological alterations in the birds' kidneys and liver. The significant increase in body weight of birds treated with 400 mg/kg/ CLJ compared with the body weight of gentamicin-treated and normal saline-treated birds in this study. This may be attributed to the phytochemical compounds found in aqueous extract of CLJ such as ascorbic acids, flavonoids, phenolics, alkaloids, terpenes, triterpenoids, steroidal glycosides and vitamins [29, 30]. There could have been initiation of some antioxidant effects by the ascorbic acids found in CLJ that may have effected some improved biological activities in broilers treated with 400 mg/kg CLJ. This is similar to the previous observation by Rabiu [7] in rats treated with C. lanatus seed in lead-induced nephrotoxicity that showed increased body weight with some antioxidant effects on the rats.

Liver disease may occur due to hepatic membrane disruption that can lead to leakage of some enzymatic cytosolic contents which can invariably lead to increased serum liver function enzymes such as aspartate aminotransferase, alanine aminotransferase and alkaline phosphatase that are biomarkers of liver damage [7]. The increased in serum liver function enzymes values of gentamicin-treated broilers in study two of this experiment may be due to liver damage. This was invariably reduced in 400mg/kg CLJ- treated broilers which may be due to the ameroliative effects of some phytochemical substances like ascorbic acids, Citrulline, lycopene, alkaloids, glycosides, saponins, flavonoids, phenols, tannins and terpenes found in CLJ that may have caused some antioxidant activities in broilers administered with CLJ. This is similar to the assertions of Ebhohon [12] in investigation of hepato-and nephro-protective effects of methanol extract of CL rind in Wistar rats by relieving damages caused with motor engine oil in contaminated feed of Wistar rats with different doses of CL rinds

The significant decrease in serum electrolytes of broilers treated with 400mg/kg of CLJ such as Na+ and Ca2+concentration in study two of this experiment still suggests the ameroliative effects on the kidney of 400mg/kg CLJ-treated broilers. This is similar to the assertion of Onwuka [8] and Anacletus [9] that showed increased serum electrolytes in nephrotoxicity which were resolved with fruit juice. The serum concentration of creatinine of broilers treated with 400mg/kg CLJ was significantly lower than the serum concentration of creatinine of GM- treated broilers in this study. This may have been caused by antioxidants effects of CLJ that is rich in beta-carotene, vitamin C, and lycopene [25, 30]. This is confirming the assertion that creatinine is a good indicator of kidney damage leading to an increase in serum creatinine concentration as a biomarker of nephrotoxicity [12].

The reduction in serum creatinine in 400mg/kg CLJ-treated broilers may suggests that CLJ may be used to relieve nephrotoxicity in broilers. The serum uric acid values of 200 and 400mg/kg CLJ treated-broilers which were significantly lowered than serum uric acid values of gentamicin-treated broilers seen in this study. This may suggest that 200 and 400mg/kg CLJ-treated broilers may have reduced the serum uric acid levels in broilers by resolving the kidney damage since serum uric acids is known to be the major biomarker of most nitrogenous metabolic product in birds indicating kidney damage birds [16, 17]. The knowledge that optimal dosages and supplementation with Watermelon fruit as a good source of vitamin C, can be used in disease prevention [30]. This may be due to the phytochemistry nutraceutical importance of Ascorbic acids found in CLJ. This may be involved in liver drug and chemical metabolism that may relieve some hepatic damages in the body according to Takahashi [31] assertion that high-dose of intravenous vitamin C can improve quality of life in cancer patients. This was confirmed in this present study that the hepatic pathological lesions seen in gentamicin-treated broilers compared with expressions in liver of 200mg/kg CLJ-treated broilers totally disappeared in 400mg/kg CLJ-treated broilers. This is similar to the affirmation of Bazabang [23] that Citrullus lanatus had hepatoprotective effects in Wistar rats, while Akintunde [24] emphasized it is cardioprotective effects in rats.

Some of the major causes of kidney disease in birds are infectious nephritis, vitamins A and or C deficiency, heavy metal toxicity, and kidney tumor. Also overdose of gentamicin can cause nephrotoxicity seen in this study that arised from fat accumulation in renal proximal convoluted tubules could have led to loss of brush border integrity as seen in previous study [14]. This present study revealed that kidney of broilers treated with gentamicin showed presence of severe eosinophilic material on the intraluminal wall of the tubules. The disappearance of these lesions seen in 400mg/kg CLJ treated-broilers and Vitamin C-treated broilers in this present study may be due to the presence of phytochemical substances like beta-

carotene, ascorbic acids and lycopene found in CLJ which may have played some antioxidant effects in the biological activities of the broilers kidney [31].

5. Conclusions

It may be concluded from this study that supplementation of aqueous extract of CLJ can cause increased body weight in commercial broilers. As well as involved in hepatoprotective and nephroprotective activities in gentamicin overdosed broilers. This is suggestive that aqueous extract of CLJ may be incorporated as a supplement in ameliorating gentamicin overdosed broilers.

Author Contributions: conceptualization, O.G.A. and A.A.O.; methodology: S.A.R.; validation, O.G.A. and A.A.O.; data analysis, O.G.A.; investigation, C.O.K.; resources, O.G.A. and C.O.K.; writing – original draft preparation, O.G.A. and K.C.O., writing – review & editing, S.A.A. and A.A.O.; visualization, O.G.A.; supervision, A.A.O.; project administration, O.G.A.

Funding: This research was funded by the authors (OGA, COK and SAR).

Institutional Review Board Statement: The Ethical Committee of College of Veterinary Medicine, Federal University of Agriculture, Abeokuta Nigeria, (Ethical number: FUNAAB / COLVET / CREC / 2021/09/01) approved the use of experimental animals in this study.

Data Availability Statement: All the relevant data are available in the manuscript.

Acknowledgements: Special thanks to Mr Apantaku and Dr Morenikeji Oladipo both are staff of Department of Veterinary Pathology, College of Veterinary Medicine, Federal University of Agriculture, Abeokuta, Nigeria for their assistance in the histopathological analysis.

Conflicts of Interest: The authors declare no conflict of interest.

References

1. Onyeanu, C.T.; Ezenduka, E.V.; Anaga, A.O. Determination of gentamicin use in poultry farms in Enugu state, Nigeria, and detection of its residue in slaughter commercial broilers. *Inter J One Health* **2020**, *6(1)*, 6-11. DOI.org/10.14202/IJOH.2020.6-11.
2. Oluwasile, B.B.; Agbaje, M. Antibiotic usage pattern in selected poultry farms in Ogun State. *Sokoto J Vet Sci* **2014**, *12(1)*, 45-504. DOI.10.4314/sokjvs.v12i1.7
3. Safa, J.; Argani, H.; Bastani, B. Protective effect of grape seed extract on gentamicin-induced acute kidney injury. *Iranian J Kid Dis* **2010**, *4(4)*, 285-291. DOI. ijkd.org/index.php/ijkd/article/view/227.
4. Booth, R.H.; Mcdonald, L.E. Jone's Veterinary Pharmacology and Therapeutics, 6th ed.; Iowa University Press, Ames, Iowa, USA. 1988. p 753.
5. Javed, U.; Khan, M.Z.; Saleemi, M.K.; Khan, A.; Javed, I.; Rafique, S. Toxico-pathological effects of parenteral administration of gentamicin in growing broilers. *Inter J Agric Biol* **2013**, 15: 529–534.
6. Saleemi, M.K.; Khan, M.Z.; Khan, A.; Javed, I. Pathological effects of gentamicin administered intramuscularly to day old broiler chicks. *Expert Toxic Path* **2009**, *61*, 425–432. DOI.org/10.1016/j.etp.2008.10.006.
7. Rabiu, S.; Bello, A.; Dandare, A.; Sadiq, M.E. Ameliorative effect of aqueous seed extract of Citrullus Lanatus (Water Melon) on liver function parameters and markers of oxidative stress in lead-treated rats. *Nig J Basic Appl Sci* **2019**, *27(1)*, 76-80. DOI.10.4314/njbas.v27i1.10.
8. Onwuka, F.C.; Erhabor, O.; Eteng, M.U.; Umoh, I.B. Ameliorative effect of cabbage extract on cadmium-induced changes on hematology and biochemical parameters of albino rats. *J Toxicol Environ Health Sci* **2010**, *2(2)*, 11-6. DOI.org/10.5897/JTEHS.9000004.
9. Anacletus, F.; Nwakaku, B.; Nwauche, K.; Monago-Ighorodje, C. Effect of Combined Fruit Juice of Citrullus lanatus and Cucumis sativus on Cadmium Induced Hepatotoxicity and Nephrotoxicity in Male Wister Rats. *Sch Acad J Biosci* **2017**, *5(10)*, 732-743.
10. Giordano, C.; Karasik, O.; King-Morris, K.; Asmar, A. Review Article: Uric Acid as a Marker of Kidney Disease: Review of Curr. Lit. Hindawi Publishing Corporation. *Dis Markers* **2015**, 6. DOI.org/10.1155/2015/382918.
11. Ndukaku, O.Y.; Ejiofor, E.U.; Loveth, U.E.; Oluchi, O.I. Valuation of some serum kidney functions and lipid profile of malaria patients in South Eastern Nigeria. *Rom J Biochem*, **2015**, *52*, 39–49. DOI: 10.9734/IJTDH/2015/17322.
12. Ebhohon, S.O.; Ibeh, R. C.; Ejiofor, U. E.; Abu, O. D.; Osegenna, S. C. Hepato-and nephro-protective effects of methanol extract of Citrullus lanatus rind in Wistar rats fed with used motor engine oil contaminated feed. *FUDMA J Sci* **2019**, *3(4)*, 246-250.
13. Johnson, R. J.; Lanaspa, M. A.; Gaucher, E. A. Uric acid: a danger signal from the RNA world that may have a role in the epidemic of obesity, metabolic syndrome, and cardiorenal disease: evolutionary considerations. *Semin Nephro* **2011**, *31(5)*, 394–399. DOI.org/10.1016/j.semnephrol.2011.08.002.
14. Lopez-Novoa, J.M.; Quiros, Y.; Vicente, L.; Morales, A.I.; Lopez-Hernandez, F.J. New insights into the mechanism of aminoglycoside nephrotoxicity: An integrative point of view. Kidney Inter **2011**, *79(1)*, 33–45. DOI:10.1038/ki.2010.337;

15. Alberton, S.; Vergneau-Grosset, C.; Summa, N. Advances in exotic animal clinical pathology. Veterinary Clinics of North Amer. *Exotic Ani Pract* **2019**, *22(3)*, 367-385. DOI:10.1016/j.cvex.2019.06.001
16. Gustafsson, D.; Unwin, R. The pathophysiology of hyperuricaemia and its possible relationship to cardiovascular disease, morbidity and mortality. *BMC Nephrol* **2013**, *14(164)*, 2–9. DOI: 10.1186/1471-2369-14-164.
17. Lin, Q.; Liang, R.; Williams, P. A.; Zhong, F. Factors affecting the bioaccessibility of β-carotene in lipid-based microcapsules: Digestive conditions, the composition, structure and physical state of microcapsules. *Food Hydrocoll*, **2018**. 77, 187-203. DOI.org/10.1016/j.foodhyd.2017.09.034.
18. Huang, S.C.; Fu, Y. F.; Lan, Y. F.; Rehman, M. U.; Tong, Z. X. Histopathological and biochemical evaluations of the kidney in broiler chickens under acute heat stress conditions. *Indian J Ani Research* **2018**, *52(4)*, 637–39. DOI.org/10.56093/ijans.v93i6.128912.
19. Etminan, P.S.; Jafarian, D. M.; Karimi, D. M. The effects of hyssop hydroalcoholic extract on the serum biochemical factors of rats. *Jour Med Herbs* **2021**, *12(3)*, 23–9. DOI: 10.30495/medherb.2021.686161
20. Islam, N.U.; Khan, M.Z. Clinicopathological studies on gentamicin toxicity in White Leghorn commercial layers. *Pakistan Vet J* **2011**, *31(4)*, 305-308.
21. Naz, A.; Butt, M. S.; Sultan, M. T.; Qayyum, M. N.; and Niaz, R. S. Watermelon Lycopene and Allied Health Claims. *Excli Jour* **2014**, *13*, 650–666. DOI. excli.de/excli/article/view/729.
22. Imam, M.Z.; Saleha Akter, S.; Musa paradisiaca L. and Musa sapientum L. A Phytochemical and Pharmacological Review. *J Appl Pharm Sci* **2011**, *01(05)*. 14-20. ISSN: 2231-3354. Available online at www.japsonline.com.
23. Bazabang, S.A.; Nwankwo, M.; Adebisi, S.S.; Makena,W.; Iliya, I.A. Hepatoprotective Effects of Aqueous Extract of Watermelon (Citrullus lanatus) Seeds on Ethanol-Induced Oxidative Damage in Wister Rats. *Sub Saharan Afric J Med* **2018**, *5(4)*, 129. DOI:10.4103/ssajm.ssajm_18_18.
24. Akintunde, O.G.; Abakpa, S.A.V.; Thomas, F.C.; Akeju, O.W.; Aremu, K.A. Ameliorative effects of aqueous extract of Citrullus lanatus fruit on phenylhydrazine-induced anaemia in male Wistar rats. *Alex J Vet Sci* **2020**, *64(1)*, 97-103. DOI: 10.5455/ajvs.39300.
25. Charoensiri, R.; Kongkachuichai, R.; Suknicom, S.; Sungpuag, P. Beta carotene, lycopene, and alpha-tocopherol contents of selected Thai fruits. *Food Chem* **2009**, *113*, 202-207. DOI.org/10.1016/j.foodchem.2008.07.074
26. Penuel, B.L.; Khan, E.M.; Maitera, M.O. Properties of proximate composition and elemental analysis of Citrullus Vulgaris (Guna) seed. *Bull Environ Pharmacol Life Sci* **2013**, *2(2)*, 39-46.
27. Jumde, A. D.; Shukla, R. N. Gousoddin.P. Development and Chemical Analysis of Watermelon Blends with Beetroot Juice during Storage. *Intern J Sci Eng Techn* **2015**, *3(4)* 2395–4752. 10.2348/ijset07150960
28. Oberoi, D. P. S.; Sogi, D. S. Prediction of lycopene degradation during dehydration of watermelon pomace (cv Sugar Baby). *J Saudi Soc Agric Sci* **2017**, *16(1)*, 97-103. DOI.org/10.1016/j.jssas.2015.03.003
29. Rodríguez-Roque, M. J.; de Ancos, B.; Sánchez-Moreno, C.; Cano, M. P.; Elez-Martínez, P.; Martín-Belloso, O. Impact of food matrix and processing on the in vitro bioaccessibility of vitamin C, phenolic compounds, and hydrophilic antioxidant activity from fruit juice-based beverages. *J Funct Foods* **2015**, *14*, 33-43. DOI.org/10.1016/j.jff.2015.01.020
30. Pacier, C.; Martirosyan, D. M. Vitamin C: Optimal Dosages, Supplementation and Use in Disease Prevention. *Funct Foods Health Dis* **2015**, *5*, 89–107.DOI.org/10.31989/ffhd.v5i3.174
31. Takahashi, H.; Mizuno, H.; Yanagisawa, A. High-dose intravenous vitamin C improves quality of life in cancer patients. *Pers Med Universe* **2012**, *1(1)*, 49-53. DOI.org/10.1016/j.pmu.2012.05.008
32. Sofowora, A. Phytochemical Screening of Medicinal Plants and Traditional Medicine in Africa. 1st ed.; Spectrum Books Ltd., Ibadan, Nigeria. 1993; pp. 150-156.

CVJ CLUJ VETERINARY JOURNAL

Research Article

Frequency of Favorable Alleles for Meat Quality, Litter Size, Adaptation, and Growth Traits in Closed Nucleus Population of Philippine Native Swine (*Sus philippensis var. markaduke*)

Giselle M. Perlas [1], Ester B. Flores [2] and Arnolfo M. Monleon [1*]

[1] College of Agriculture, Marinduque State University Torrijos Campus, Poctoy, Torrijos, Marinduque 4903, Philippines; giselle.perlas17@gmail.com;
[2] Department of Agriculture - Philippine Carabao Center National Headquarters and Gene Pool, Science City of Muñoz, Nueva Ecija, 3120, Philippines; esterflrs@gmail.com
* Correspondence: ammonleon@alum.up.edu.ph;

Abstract The Philippine native swine (PNS) represent valuable heritage genetic resources with significance for food security and geo-cultural traditions. Among these, the Markaduke breed is recognized for producing the "best lechón" and comminuted pork products, while also exhibiting moderate litter size (≥8) and adaptability to local conditions. To support the development of a breeding program suited for an optimal production system, its genetic properties were assessed. A total of 67 animals (17 males and 50 females) from 4.37 ± 0.12 generations, with an inbreeding coefficient of 0.1493 ± 0.0167, were genotyped using molecular markers. Seven gene markers for meat quality, three for litter size, two for adaptation, and one for growth were analyzed, with results tested under Hardy–Weinberg equilibrium and chi-square statistics. For meat quality, *rendement napole* (*RN*), *Cathepsin D* (*CTSD*), and *leptin receptor* (*LEPR*) exhibited genotype frequencies exceeding 50% in both sexes, with the *rn* allele fully expressed (100% rnrn, $p_{0.0001}<\alpha_{0.05}$). Regarding litter size, *prolactin receptor* (*PRLR*) was the major allele, with nearly equal frequencies of 0.77 in both sexes ($p_{0.05}=\alpha_{0.05}$). The N allele of the halothane gene, associated with stress tolerance, was observed at a frequency of 0.97 ($p_{0.80}>\alpha_{0.05}$). The favorable allele for growth (*MYOG*) appeared only in heterozygotes at low frequencies (0.08 in males, 0.14 in females, and 0.13 combined). These findings demonstrate that the closed nucleus population of Markaduke carries favorable alleles essential for genetic improvement, underscoring its potential for sustainable breeding strategies and conservation of native swine genetic resources.

Keywords: Allele, biomarker, genotype, homozygosity, Markaduke, meat quality

1. Introduction

The Philippine native swine (PNS) represent heritage domestic animal genetic resources that provide substantial economic utility as food sources while holding significant geo-cultural value. Although the precise progenitors of PNS remain uncertain, they are presumed to be products of interbreeding among wild pig species such as *Sus philippensis*, *Sus ahoenobarbus*, *Sus cebifrons*, *Sus oliveri*, and the subspecies *Sus philippensis mindanensis*, along with the introduced *Sus scrofa* [1-6]. Observations of neonates with striped, orange-brown coat coloration reveal phenotypes associated with wild pig ancestry, traits absent in commercial swine breeds. This distinctive characteristic offers a promising avenue for research into genetic lineages and interbreeding patterns between wild and introduced pig species. Several PNS breeds exhibit distinguishing physical traits that have evolved through community-based selection processes, reflecting both cultural practices and adaptive responses to local environments [5, 7]. These traits highlight the dynamic interaction between traditional husbandry and genetic adaptation, underscoring the importance of indigenous knowledge in shaping breed characteristics. Such processes have contributed to the resilience and uniqueness of PNS, positioning them as valuable resources for both food security and cultural heritage preservation.

Received: 29.01.2026
Accepted: 23.03.2026
Published: 01.04.2026

DOI:10.52331/v31i25p50

Among PNS, the Markaduke breed developed by Marinduque State University (13°19′57.8″N, 122°05′59.0″E) is officially listed in the Domestic Animal Diversity Information System (DAD-IS) of the Food and Agriculture Organization (FAO, https://www.fao.org/dad-is/browse-by-country-and-species/en/). It is highly sought after
for *lechón* (roast whole pork) and comminuted meat products such as *tocino*, *longganisa*, *sisig*, and smoked pork (*tapa*), owing to its distinct flavor, juiciness, and tenderness [8–9]. The breed has demonstrated resilience and productivity even during the *COVID-19* pandemic and outbreaks of African swine fever (ASF) [10]. Its reproductive performance is notable, particularly at the third and fourth parity, achieving a number born alive (NBA) of 10 or more piglets, with post-weaning growth averaging 92 g/day and carcass yield of 47.54% [11–12]. These attributes highlight the Markaduke's economic potential as a genetic resource for food security and income generation.

Molecular studies on swine genetics have largely prioritized commercial breeds with intensive selection histories [13–14]. In contrast, indigenous breeds such as the Markaduke are presumed to carry favorable alleles for meat quality, reproductive efficiency, environmental adaptation, and growth traits. These genetic resources remain underexplored, despite their potential to contribute to sustainable swine production systems. Research into the genetic architecture of PNS, particularly through molecular markers, can provide insights into their adaptability and productivity, ensuring that their unique traits are harnessed for long-term breeding strategies.

The application of marker-assisted selection and genomic analyses offers a promising approach to uncover the genetic potential of the Markaduke and other PNS breeds. Such strategies can guide breeding programs toward the enhancement of desirable traits while ensuring the preservation of genetic identity [7]. Incorporating genomic selection frameworks that balance productivity, adaptability, and cultural heritage will be critical for sustaining PNS populations. Ultimately, the conservation and strategic utilization of PNS genetic resources represent a pathway toward resilient, culturally grounded, and economically viable swine production in the Philippines.

2. Materials and Methods

2.1. Management of population

The closed nucleus population of Markaduke was established in 2012 and has been continuously maintained at the Research Center of Marinduque State University, Torrijos Campus, Marinduque, Philippines (13°19'57.8"N, 122°05'59.0"E). All individuals within the nucleus population were properly identified through ear-notching with coded numbers for data collection, recording, and performance evaluation. Breeding stock selection follows a phenotypic protocol, emphasizing qualitative traits such as pure black coat color, a signature of native swine, and quantitative traits including litter size and average daily gain (ADG). Selected individuals are raised to maturity and bred beginning at eight (8) months of age through a line-mating system designed to preserve desirable parental performance, particularly large litter sizes (>8 piglets born alive). Breeding stocks (sows and boars) are housed individually, while piglets and replacement stock are managed in groups of up to 50 heads in range systems with sheds. Feeding practices combine plant-based resources with commercially mixed feeds at ratios tailored to physiological requirements (e.g., 90:10 for boars, 70:30 for sows). Neonates receive iron dextran supplementation within the first week to prevent iron deficiency anemia. Overall, management practices adhere to prescribed husbandry standards under Republic Act No. 8485 and Republic Act No. 10631.

2.2. Sampling and laboratory analyses

The study sample consisted of 67 individuals, comprising 17 males (junior boars) and 50 females (replacement gilts). Pedigree analysis revealed an average of 4.35 ± 0.27 generations for males, with an inbreeding coefficient of 0.1480 ± 0.0302. Females showed a comparable pedigree of 4.38 ± 0.14 generations and an inbreeding coefficient of 0.1497 ± 0.0200. When combined, the pedigree data across sexes averaged 4.37 ± 0.12 generations back, with an overall inbreeding coefficient of 0.1493 ± 0.0167.

Biological samples including blood, hair follicles, and ear fragments were collected from each individual in strict adherence to standardized protocols to ensure sample integrity and ethical compliance. Blood was drawn via sterile venipuncture of the external jugular vein, hair follicles were plucked with intact roots, and ear fragments were obtained using approved punch techniques. All samples were systematically labeled and preserved under appropriate storage conditions (e.g., blood in vacutainers, hair follicles and ear fragments in sterile zip-lock pouches), and were handled in compliance with biosafety regulations and animal

welfare guidelines to safeguard reproducibility and reliability of subsequent analyses. During transport, samples were maintained under cold-chain conditions and subsequently stored in a bio-freezer at the Animal Breeding and Genomics Section, Department of Agriculture–Philippine Carabao Center (DA-PCC), National Headquarters, Science City of Muñoz, Nueva Ecija, Philippines (15°43′58″N, 120°55′52″E).

DNA Extraction. Genomic *DNA* was extracted from tissue samples (ear fragments and hair follicles) using the Qiagen DNeasy Blood and Tissue Kit with minor protocol modifications, wherein approximately 25 mg of ear tissue or 5–10 hair follicles were processed in 1.5 ml microcentrifuge tubes with Buffer *ATL* and proteinase *K*, incubated at 56 °C until complete lysis, followed by the addition of Buffer AL and ethanol, and subsequent purification on *DNeasy* mini spin columns with washes in Buffers AW1 and AW2 before final elution in Buffer AE and storage at 2–8 °C. Blood-derived genomic *DNA* was isolated using the Promega Wizard Genomic *DNA* Purification Kit with minor modifications, in which 500 µl of homogenized blood was treated with ammonium chloride to recover white blood cells, subjected to cell and nuclear lysis with protein precipitation, and processed by centrifugation; the supernatant was mixed with isopropanol, stored overnight, and centrifuged again to pellet *DNA*, which was washed with 70% ethanol, air-dried under laminar flow, rehydrated in 50 µl of *DNA* rehydration solution, gently mixed, and stored at 2–8 °C for downstream genotyping.

Mutagenically Separated Polymerase Chain Reaction and Gel Documentation. Seven meat quality markers of *rendement napole* (*RN*), *cathepsin D* (*CTSD*), *leptin receptor* (*LEPR*), *lipoprotein lipase* (*LPL*), *calpastatin* (*CAST*), *insulin-like growth factor binding protein intron 3* (*IGFBP3*), and *insulin-like growth factor binding protein intron 7* (*IGFBP7*) *genes* were analyzed using modified protocols of mutagenically separated polymerase chain reaction (MS-PCR). Similar procedures were applied to litter size (*PRLR, ESR, LIF*), adaptation (*HAL* and *FUT1*), and growth markers (*MYOG*). These targeted loci represent critical genetic determinants of productivity, resilience, and carcass quality in the closed nucleus population of Markaduke (Table A1, 15-24).

Amplification of specific genes (e.g., *ESR*, *FUT1*, *HAL*) was performed using MS-PCR under optimized laboratory conditions. PCR products were verified through 3.5% agarose gel electrophoresis (prepared with Pronadisa Agarose D1 Low EEO and Gel Red Biotium Solution) using the Mupid-exU submarine electrophoresis system. Gel documentation was conducted with the Enduro™ GDS system, and genotype scoring was performed through standard and manual computation. Sequencing provided further validation of gel products and enabled comparison with commercial swine breeds, ensuring accuracy and reproducibility of results (Table A1, 15–24).

2.3. Statistical analysis

The genotype and allele frequencies were tested in Hardy-Weinberg Equilibrium (HWE) and chi-square using an online HWE calculator (https://calculator.now/hardy-weinberg-equilibrium-calculator/). The p-value <0.05 indicates deviation from the HWE; otherwise, it conforms to the null hypothesis of stability in genotype and allele frequencies from one generation to the next.

3. Results

3.1. Meat quality markers

Seven gene markers associated with meat quality traits, namely: *rendement napole* (*RN*), *cathepsin D* (*CTSD*), *leptin receptor* (*LEPR*), *lipoprotein lipase* (*LPL*), *calpastatin* (*CAST*), *insulin-like growth factor binding protein 3* (*IGFBP3*), and *insulin-like growth factor binding protein 7* (*IGFBP7*) were identified in the closed nucleus population of Markaduke (Fig. 1 and Table A2). These loci represent critical genetic markers influencing muscle metabolism, fat deposition, tenderness, and overall carcass quality. The presence of favorable alleles across these biomarkers highlights the genetic potential of the population for producing high-quality pork.

Three biomarkers (*RN, CTSD*, and *LEPR*) exhibited genotypic frequencies exceeding 50% in both sexes. Remarkably, the sampled population (n = 67) expressed a homozygous recessive genotype (100% *rnrn*, 0.0001< 0.05) for rendement napole indicating near fixation of this allele within the population. This suggests strong selection for meat quality traits associated with RN, despite its known trade-offs with growth efficiency. In contrast, *CTSD* and *LEPR* conformed to Hardy–Weinberg equilibrium, indicating balanced allele distributions in the absence of active selection. Notably, *CTSD* showed higher favorable genotype and allele frequencies in females (0.90 > 0.50 and 0.95 > 0.75, respectively), whereas *LEPR* displayed relatively equal expression across sexes. These findings emphasize the need for targeted genotyping in males to increase the frequency of the favorable genotype and allele.

The favorable genotypes ***CC*** and ***DD*** for *LPL* and *CAST* were observed only in females, at frequencies of 0.20 and 0.06, respectively. Males acted solely as carriers of the favorable alleles, with frequencies of 0.25 for *C* and 0.13 for *D*. Both loci conformed to HWE ($p > 0.05$), suggesting stable transmission across generations. However, the relatively low frequencies of favorable genotypes necessitate deliberate breeding interventions. Genotyping to identify carriers and structured assortative mating are essential strategies to increase allele frequencies and achieve fixation within the population.

The favorable alleles, *A* and *C*, for *IGFBP3* and *IGFBP7*, were detected only in heterozygous individuals, with low frequencies of 0.12 and 0.07, respectively, across both sexes. Despite their rarity, both loci conformed to HWE, indicating genetic stability and the likelihood of persistence across generations. These insulin-like growth factor binding proteins are important regulators of muscle growth and fat deposition, traits directly linked to meat quality. Their presence, even at low frequencies, underscores the importance of genotyping and selective breeding to increase their prevalence and secure their contribution to carcass traits.

The combined expression of favorable alleles across *RN, CTSD, LEPR, LPL, CAST, IGFBP3,* and *IGFBP7* provides a strong genetic foundation for meat quality improvement in Markaduke. However, the varying frequencies and equilibrium statuses highlight the need for tailored breeding strategies. While *RN* appears fixed, *CTSD* and *LEPR* require sex-specific genotyping, and *LPL, CAST, IGFBP3*, and *IGFBP7* demand deliberate assortative mating to prevent allele loss. Integrating marker-assisted selection and genomic frameworks will be critical to balance fixation of favorable alleles with preservation of genetic diversity, ensuring sustainable improvement of meat quality traits in the population.

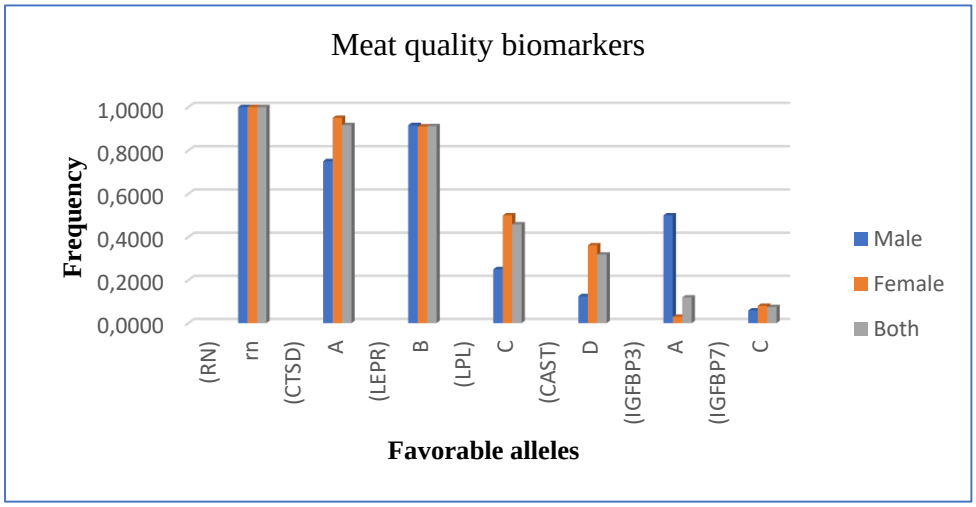

Figure 1. Frequency of favorable alleles of biomarkers (RN, $p<_{0.05}$; CTSD, $p>_{0.05}$; LPL, $p>_{0.05}$; CAST, $p>_{0.05}$; IGFBP3, $p>_{0.05}$; IGFBP7, $p>_{0.05}$) for meat quality traits.

3.2. Litter size markers

Three litter size biomarkers such as *prolactin receptor* (*PRLR*), *estrogen receptor* (*ESR*), and *leukemia inhibitory factor* (*LIF*) revealed the presence of favorable alleles within the closed nucleus population of Markaduke (Fig. 2 and Table A3). The most prominent allele was observed in *PRLR*, with nearly equal frequencies across sexes and a combined value of 0.77. This distribution deviated significantly from HWE ($p < 0.05$), suggesting possible non-random mating or directional selection favoring reproductive efficiency. In contrast, *ESR* exhibited lower allele frequencies (0.36 combined) but conformed to HWE, indicating genetic stability and the likelihood of consistent transmission of genotypes and alleles across generations.

The *LIF* gene was detected only in heterozygous form, with low allele frequencies (0.18), and deviated from HWE, indicating a high probability of allele loss within the population. Given *LIF's* critical role in uterine receptivity and embryo implantation, its potential disappearance poses risks to reproductive performance. The low frequency of favorable alleles suggests that without deliberate intervention, genetic drift or unfavorable selection pressures could accelerate their loss, thereby compromising reproductive success in the long term.

To mitigate these risks, deliberate interventions such as systematic genotyping and structured assortative mating are necessary to preserve favorable alleles. Incorporating genomic selection frameworks that

balance *PRLR, ESR*, and *LIF* polymorphisms will be essential to sustain prolificacy, maintain genetic diversity, and secure long-term reproductive success in the Markaduke population. These strategies will ensure that favorable alleles are not only maintained but also strategically fixed, thereby enhancing reproductive efficiency while safeguarding the genetic integrity of the breed.

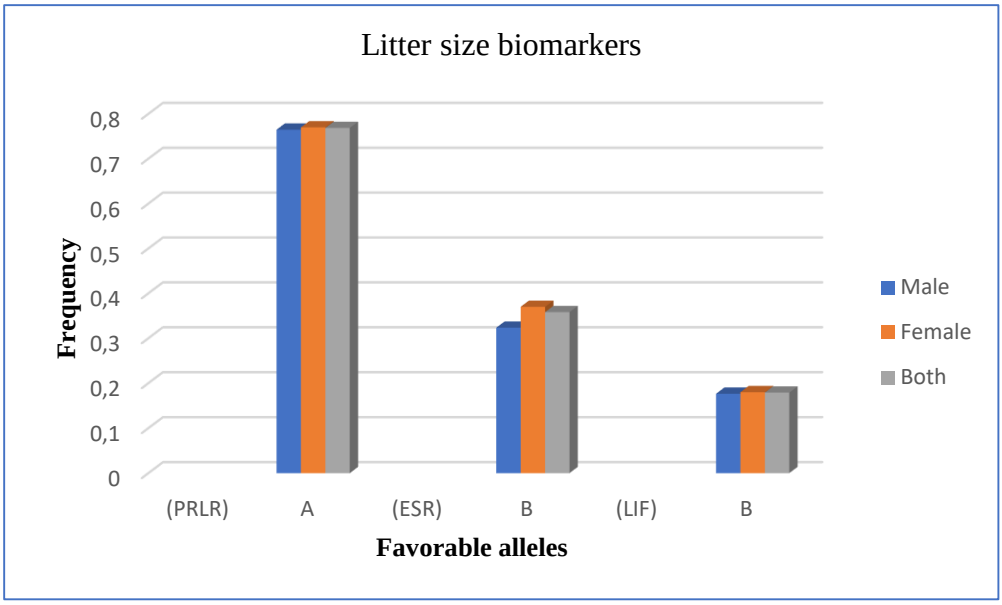

Figure 2. Frequency of favorable alleles of biomarkers (PRLR, p=0.05; ESR, p>0.05; LIF, p=0.05) for litter size traits or number of pigs born traits.

3.3. Adaptation markers

Two biomarkers for adaptation revealed the presence of favorable alleles within the population (Fig. 3 and Table A4). The most prominent was the *N* allele of the halothane (*HAL*) gene, which confers stress tolerance, observed at a frequency of 0.97 in the combined dataset across sexes. This near fixation of the N allele indicates strong resilience against porcine stress syndrome (PSS) and pale, soft, exudative (PSE) meat. However, the persistence of the unfavorable n allele, detected at frequencies of 0.06 in males and 0.02 in females, highlights the need for deliberate breeding efforts to eliminate susceptibility alleles. Given that the population conforms to HWE ($p > 0.05$), the continued presence of the *n* allele suggests that without targeted selection, stress-sensitive genotypes may persist across generations.

Resistance to *Escherichia coli* (*E. coli*) was demonstrated through the favorable allele of the *α(1,2)-fucosyltransferase* (*FUT1*) gene, observed at a frequency of 0.31 in the combined dataset. Notably, males were the primary carriers of the favorable allele, with a frequency of 0.50, deviating significantly from HWE ($p < 0.05$). This deviation suggests potential non-random mating or selective pressures acting on *FUT1*, which may influence allele distribution. Since *FUT1* variants provide defense against enterotoxigenic *E. coli* infections, a major cause of neonatal diarrhea and piglet mortality, maintaining and increasing the frequency of this allele is critical for productivity in smallholder systems. Structured breeding programs, marker-assisted introgression, and continuous monitoring of allele frequencies are essential to conserve disease-resistant traits while ensuring genetic diversity for long-term sustainability.

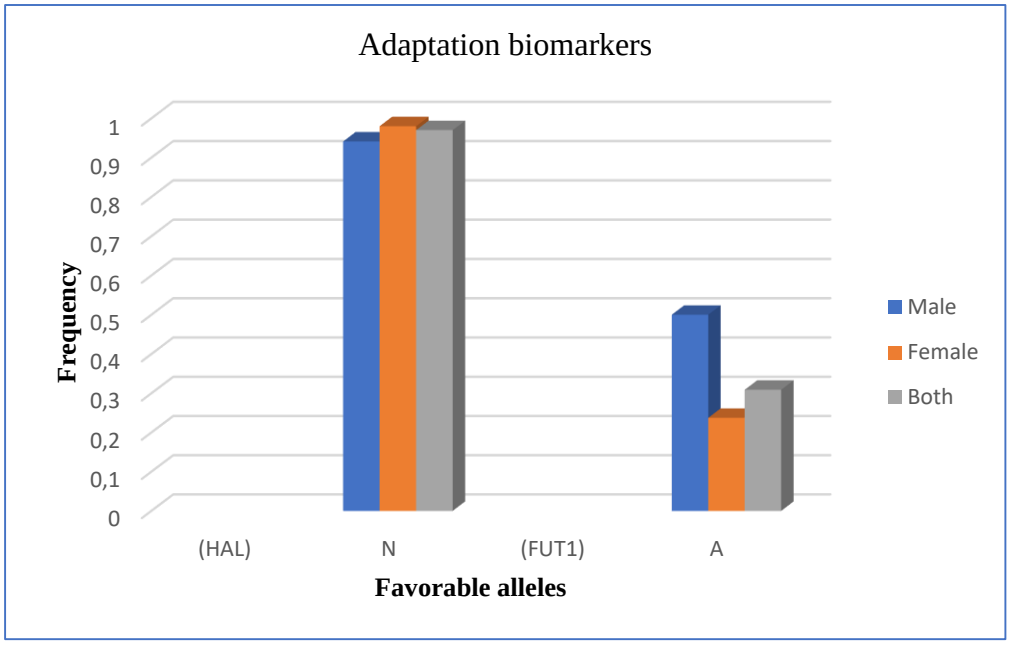

Figure 3. Frequency of favorable alleles of biomarkers (HAL, $p>_{0.05}$ and FUT1, $p=_{0.05}$) for adaptation traits.

3.4. Growth marker

The favorable allele for the *myogenic transcription factor* (*MYOG*) was detected only in heterozygous individuals, with low frequencies of 0.08 in males, 0.14 in females, and 0.13 in the combined dataset (Fig. 4 and Table A4). This limited occurrence suggests that the advantageous allele is not yet widely distributed within the population, potentially reflecting historical breeding practices or genetic drift. Despite its low prevalence, the presence of heterozygotes indicates that the allele remains part of the genetic pool and may contribute to muscle differentiation and growth-related traits when expressed in combination with other loci.

Importantly, both genotype and allele frequencies conform to HWE, suggesting that the *MYOG* allele is likely to persist in the population under current conditions, provided no strong evolutionary forces act upon it. This equilibrium implies genetic stability and the potential for the allele to be maintained across generations. From a breeding perspective, the persistence of heterozygotes highlights opportunities for marker-assisted selection to increase the frequency of favorable alleles, thereby enhancing growth efficiency and carcass quality while preserving genetic diversity.

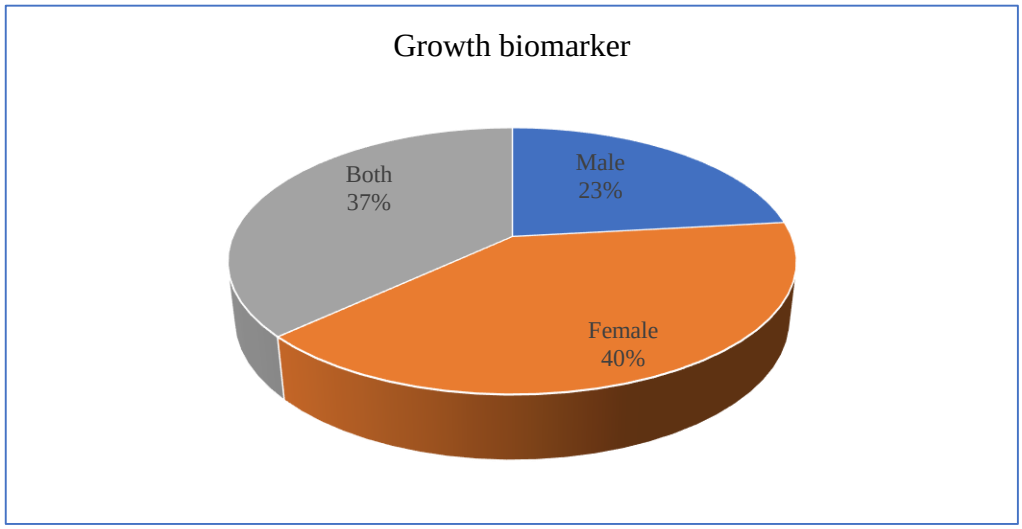

Figure 4. Frequency of favorable alleles of biomarker (MYOG, p>0.05) for growth traits.

4. Discussion

4.1. Favorable alleles for meat quality

The fixation (100%) of the homozygous recessive genotype (*rnrn*) of the *rendement napole* (*RN*) gene within the Markaduke population is unusual, given its relatively low allele frequencies (0.25–0.37) reported in other swine genetic groups (Table A5). The *rnrn* genotype serves as a marker for estimating yield and quality of cured and cooked ham, with the best products scoring highest in color, firmness, marbling, and shear force [27]. In contrast, the dominant *RN* allele is associated with paler meat, reduced water-holding capacity, low ultimate *pH* or "acid meat," and high slicing loss [27–28]. The fixation of *rnrn* in Markaduke supports empirical observations of its exceptional lechón qualities and may reflect historical or ongoing selection pressures favoring superior meat quality. Compared with commercial breeds, where *RN* allele frequencies are moderate (25–37%) and fixation often leads to pale, soft, exudative (PSE) meat [27], the Markaduke's fixation of *rnrn* reflects sustained phenotypic selection for consistent meat quality. This suggests that despite its closed nucleus classification and moderate inbreeding, the population has preserved and enhanced favorable phenotypes through deliberate selection focused on sensory and culinary characteristics.

The elevated frequencies of favorable alleles for *CTSD* and *LEPR* further strengthen the genetic profile underlying Markaduke's exceptional meat qualities. Similar findings have shown that *CTSD* is fixed in certain swine breeds [28]. As a lysosomal protease, *CTSD* contributes to postmortem proteolysis by breaking down myofibrillar proteins, thereby improving tenderness [31]. The higher frequencies observed, particularly among females, might suggest sex-biased selection or differential expression linked to reproductive energy allocation that influences muscle physiology [31]. Moreover, polymorphisms in *LEPR* are recognized as significant modulators of feed intake, energy utilization, and fat storage [32–33]. Their influence on carcass fatness corresponds with the elevated intramuscular fat levels typically found in native swine breeds, enhancing flavor and moisture [34]. Variations in the *LEPR* gene also affect fat distribution and fatty acid profiles, traits that are critical for both health-related qualities and consumer preferences in pork [35]. This study revealed allele frequencies similar to those reported in Landrace (0.88) [39]. The balance of favorable alleles suggests an equilibrium between fat and lean tissue deposition, enabling precise genotyping and targeted selection within the Markaduke population.

Genetic markers such as *LPL* and *CAST* exhibited low but measurable frequencies of favorable alleles, particularly among females, suggesting possible unoptimized sex-specific genetic patterns or selective forces. *LPL* plays a critical role in lipid metabolism, influencing intramuscular fat deposition and fatty acid composition, while *CAST* regulates *calpain* activity, which is essential for post-slaughter muscle tenderness [37–38]. The low frequency of carrier alleles indicates that fixation is unlikely under current conditions, most likely due to limited selection intensity and genotyping efforts. However, the application of marker-assisted selection targeting these loci, combined with systematic genotyping and planned selective mating, could accelerate the fixation of desirable alleles and thereby improve meat texture and flavor [39–41].

Additionally, heterozygosity observed in *insulin-like growth factor binding proteins* (*IGFBP3* and *IGFBP7*) denotes the presence of genetic variation that is essential for regulating muscle growth and development [40]. The *insulin-like growth factor* (*IGF*) pathways play a critical role in muscle hypertrophy, while the relative proportions of different muscle fiber types are key determinants of meat quality and growth efficiency [41]. Retaining heterozygosity at these loci may confer adaptive advantages by maintaining flexibility in morphology and physiology, thereby supporting both genetic resilience and phenotypic diversity within the population.

4.2. Favorable alleles for litter size

The *AA* genotype of the *prolactin receptor* (*PRLR*) *gene* was the most predominant (55.22%) among all samples, consistent with previous findings that associate this genotype with higher litter size. The favorable *A* allele (76.78%) substantially exceeded the *B* allele (23.13%), suggesting either strong selection pressure or a naturally high prevalence of the favorable allele in the studied population. Earlier studies reported that the *PRLR-A* allele was positively correlated with increased total number born (TNB) and number born alive (NBA) in Large White and Landrace pigs [42–45]. Similarly, literature indicates that the *AA* genotype is significantly superior to *AB* and *BB* in terms of TNB, further supporting the findings of this study. These results highlight *PRLR* as a key marker gene for reproductive success, consistent with the observed litter size of eight (8) piglets in the Markaduke population.

The high frequency of favorable *PRLR* alleles, coupled with deviations from HWE, suggests the influence of non-random mating patterns such as assortative mating. Assortative mating, where individuals with similar genotypes are preferentially paired, can amplify the frequency of favorable alleles across generations. In this case, the predominance of *AA* genotypes may reflect deliberate or natural assortative mating that reinforced reproductive efficiency traits. While this mechanism is beneficial for increasing litter size, it may reduce genetic diversity and limit adaptability in the long term [46]. The correlation between *PRLR* allele frequency and the observed reproductive phenotype underscores the importance of balancing allele fixation with genetic variability.

The *estrogen receptor* (*ESR*) gene, long regarded as a major gene influencing reproductive traits, showed notable variation. The *AB* genotype was slightly more frequent among females (46%) compared to *AA* (40%) and *BB* (14%), with the *A* allele (64.18%) still dominating over ***B***. Literature consistently identifies the *ESR-B* allele as favorable for increased ovulation rate and larger litter sizes, especially in European commercial breeds. However, local studies often show inconsistent trends, likely due to differences in linkage disequilibrium or genetic background. For instance, while the *BB* genotype is common in Large White pigs, subsequent studies found the *AB* genotype more productive in terms of piglets weaned [47]. The intermediate genotype findings here may reflect a heterozygote advantage under local environmental or genetic contexts, which assortative mating could either reinforce or diminish depending on breeding strategies.

The moderate frequencies of *ESR* polymorphisms, consistent with equilibrium expectations, indicate genetic stability and polygenic influence on reproductive traits. *ESR* is involved in mediating uterine receptivity and estrogen-related follicular development, both essential for fertility. However, its effects are often indirect, interacting with other loci such as *PRLR* and *LIF* [49]. Assortative mating that favors specific *ESR* genotypes may enhance reproductive efficiency but could also disrupt beneficial heterozygote balances. Careful management of mating strategies is therefore required to avoid narrowing genetic variability while still capitalizing on favorable alleles.

The *leukemia inhibitory factor* (*LIF*) gene exhibited a high frequency of the *AA* genotype (64.18%) and no occurrence of the *BB* genotype, with the *A* allele reaching 82.09%. *LIF* plays a critical role in uterine receptivity and embryo implantation, and its polymorphisms have been significantly associated with litter size traits [18, 49–50]. The low heterozygous frequency and deviations from HWE suggest that assortative mating may be accelerating the loss of genetic variation at this locus. If unmanaged, this reduction in allelic diversity could negatively influence adaptability and compromise reproductive performance. Importantly, the correlation between favorable *PRLR* and *LIF* alleles and the observed litter size of eight (8) piglets, alongside carcass yield of 47.54%, demonstrates the functional link between genotype and phenotype. These findings underscore the importance of systematic genotyping and structured assortative mating to preserve essential reproductive alleles while ensuring that carcass quality traits remain aligned with genetic potential.

4.3. Favorable alleles for adaptation

The *halothane* (*HAL*) *gene* is well known for its role in porcine stress syndrome (PSS), which is associated with malignant hyperthermia, reduced survivability under stress, and poor meat quality such as pale, soft, exudative (PSE) meat. In the present study, the *NN* genotype (non-carrier of the stress allele) was predominant across sexes (94.03%), while the n allele, linked to susceptibility to PSS, was found at only 2.99% of the population. This distribution is highly favorable, indicating a strong presence of stress-resilient genetics in the study group. Indigenous swine populations have frequently demonstrated higher adaptive capacity to harsh conditions, which is advantageous in developing countries facing climatic and disease challenges [7].

The near fixation (97%) of the stress-tolerant *N* allele in the Markaduke population reflects strong selection for resilience against stress-induced disorders. This genetic profile supports stable muscle metabolism under environmental and management stressors, thereby reducing the incidence of PSE meat and sudden death syndrome that are common in susceptible breeds [51]. Populations fixed for the N allele maintain consistent meat quality and survivability, traits that are particularly beneficial in local management systems with limited infrastructure. Such resilience enhances both productivity and animal welfare, reinforcing the importance of *HAL* genotyping in breeding programs.

Immune response-related adaptations were revealed by the presence of the favorable *A* allele for *α(1,2)-fucosyltransferase* (*FUT1*), particularly in males, where allele frequency deviations from equilibrium were observed. *FUT1* variants confer resistance against *enterotoxigenic E. coli* infections, a major cause of neonatal diarrhea and high piglet mortality in smallholder systems [25]. The presence of this allele is critical for productivity, as it reduces reliance on antibiotics and aligns with international antimicrobial stewardship

efforts. However, the observed imbalance in allele frequencies suggests potential risks if breeding management does not actively conserve these adaptive traits.

The combined findings on *HAL* and *FUT1* highlight the importance of structured breeding strategies that preserve both stress-resilient and disease-resistant alleles. Marker-assisted selection and controlled assortative mating can help maintain genetic diversity while promoting adaptability. Ongoing monitoring of allele distributions is essential to prevent genetic drift or loss of favorable alleles. Incorporating genomic selection frameworks that integrate stress tolerance (*HAL*) and disease resistance (*FUT1*) loci will provide a robust foundation for sustainable pig production systems, ensuring resilience, productivity, and meat quality in diverse environments.

4.4. Favorable alleles for growth

The *MYOG* gene, which regulates muscle fiber differentiation, was observed with a high frequency of the *AA* genotype (73.53%), followed by heterozygous *AB* (26.47%), and no occurrence of the *BB* genotype. The dominance of the *A* allele (86.76%) is generally associated with enhanced muscle development, higher average daily gain, and improved carcass quality. These results closely resemble allele distributions in Pietrain and Large White pigs [53]. However, the low frequency of favorable heterozygous *MYOG* alleles suggests that historical breeding practices prioritized meat quality and adaptability traits over growth performance. This pattern parallels findings at the *RN* locus, where fixation of *RN* alleles for superior meat quality inadvertently constrained variability in growth-related alleles, underscoring the genetic trade-offs between quality and efficiency [54].

MYOG functions as a myogenic transcription factor essential for muscle differentiation and fiber-type specification. Variants of *MYOG* are linked to differential muscle hypertrophy and intramuscular fat deposition, both of which influence growth efficiency and product quality. Similarly, *RN* alleles at the *PRKAG3* locus affect glycogen metabolism and ultimate *pH*, traits directly tied to meat quality. However, fixation of *RN* alleles has been shown to reduce allelic diversity for growth traits, highlighting the antagonistic pleiotropy between loci that favor meat quality and those that promote growth efficiency [59-60].

Breeding strategies that integrate *MYOG* polymorphisms may enhance growth rates while maintaining high-quality meat and adaptability traits [52-53]. This aligns with studies advocating balanced breeding objectives that preserve native genetic resources while improving production efficiency [7]. Evidence from *RN* allele studies reinforces this need: intense selection for meat quality can reduce allelic diversity for growth traits, thereby limiting the genetic potential for faster growth and leaner carcass yield. Sustainable breeding programs must therefore adopt multi-trait genomic selection frameworks to balance these competing objectives.

The absence of beneficial heterozygous *MYOG* alleles indicates that growth-associated traits require deliberate selective breeding. Muscle fiber composition, growth rate, and intramuscular fat levels are influenced by variations in myogenic regulatory factors such as *MYOG* and *MYH3* (myosin heavy chain), which collectively affect both growth efficiency and meat quality [57-58]. Marker-assisted selection targeting these loci offers potential to improve growth performance while safeguarding adaptability and meat quality. However, caution is warranted as demonstrated in *RN* allele fixation, single-trait selection may lead to unintended consequences such as increased stress sensitivity or compromised meat quality.

A comprehensive genomic selection framework that integrates multiple trait loci and genomic estimated breeding values (GEBVs) provides a robust foundation for achieving balanced improvement [57]. By simultaneously considering *MYOG*, *RN*, and other regulatory loci, breeders can optimize both growth and meat quality traits. This approach mitigates the risk of allelic suppression and ensures that genetic diversity is preserved for long-term adaptability. Ultimately, the integration of *MYOG* polymorphisms with RN allele management exemplifies the importance of multi-trait selection in modern pig breeding, where efficiency, quality, and sustainability must coexist.

5. Conclusion

This study highlights the genetic potential of Markaduke native swine for sustainable breeding programs and food security. The breed exhibits favorable alleles for meat quality, litter size, adaptation, and growth traits. Notably, the complete fixation of the *rnrn* genotype of the *RN* gene and high frequencies of *CTSD* and *LEPR* alleles underscore the breed's exceptional meat quality, making it highly sought after for premium pork products like *lechón*. Additionally, the presence of favorable alleles for *PRLR*, *ESR*, and *LIF* genes contributes to the breed's reproductive efficiency, with litter sizes of eight or more piglets. Adaptation

traits, such as the stress-tolerant *N* allele of the *HAL* gene and the disease-resistant *FUT1* allele, further emphasize the breed's resilience to environmental challenges, including stress and disease outbreaks.

Despite these strengths, the study identified areas for improvement, particularly in growth traits associated with the *MYOG* gene, which showed limited favorable allele frequencies. This suggests the need for targeted breeding strategies to enhance growth efficiency while maintaining the breed's unique meat quality and adaptability traits. The findings emphasize the importance of integrating marker-assisted selection and genomic frameworks to balance the fixation of favorable alleles with the preservation of genetic diversity. Future breeding programs will implement structured mating designs to minimize inbreeding, thereby sustaining genetic diversity while simultaneously enhancing performance traits. By addressing these genetic gaps, the Markaduke breed can continue to serve as a valuable resource for food security, cultural heritage preservation, and sustainable swine production in the Philippines.

Author Contributions: Conceptualization, E.B.F. and A.M.M.; methodology, E.B.F., A.M.M., and G.M.P.; software, A.M.M.; validation, E.B.F., and G.M.P.; formal analysis, AMM; investigation, G.M.P. and E.B.F.; resources, E.B.F. and A.M.M.; data curation, E.B.F. and A.M.M.; writing-original draft preparation, A.M.M.; writing-review and editing, E.B.F., G.M.P., and A.M.M.; visualization, A.M.M.; supervision, E.B.F. and A.M.M.; project administration, A.M.M.; funding acquisition, E.B.F. and A.M.M.; All authors have read and agreed to the published version of the manuscript.

Funding: This research was funded by the Department of Science and Technology – Philippine Council for Agriculture, Aquatic and Natural Resources Research and Development (DOST-PCAARRD).

Institutional Review Board Statement: The management practices for the native swine are in accordance with the prescribed husbandry standards while the sample collection and laboratory analyses followed the published protocols. Ethics approval was under the code PCC-IACUC-06-2024. In addition, the PCC-National Water Buffalo Gene Pool is a registered facility recognized by DA-RFO III and the Bureau of Animal Industry pursuant to the provisions of the Republic Act 8485 otherwise known as the Animal Welfare Act of 1998 as amended by Republic Act 10631.

Acknowledgments: The authors hereby acknowledge the Department of Science and Technology – Philippine Council for Agriculture, Aquatic and Natural Resources Research and Development (DOST-PCAARRD), and the Department of Agriculture – Philippine Carabao Center (DA-PCC) for the funding assistance, and laboratory analyses, respectively.

Conflicts of Interest: "The authors declare no conflict of interest."

References

1. Piper, P.J.; Campos, F.Z.; Hung, H.C. A study of the animal bone recovered from pits 9 and 10 at the site of Nagsabaran in Northern Luzon, Philippines. *Hukay* **2009**, *14*, 47-90.

2. Piper, P.J.; Hung, H.C.; Campos, F.Z.; Bellwood, P.; Santiago, R. A 4000-year-old introduction of domestic pigs into the Philippine archipelago: implications for understanding routes of human migration through island Southeast Asia and Wallacea. *Antiq* **2009**, *83*, 689-695.

3. Cabanas, A.J.C.; de Guia, A.P.O.; Vega, R.S.A.; Dimalibot, J.C. Occurrence and distribution of Philippine warty pig (*Sus philippensis* Nehring 1886) in Mt. Banahaw de Tayabas, Luzon Island, Philippines. *Phil J Sci* **2022**, *151(5)*, 1605-1621.

4. Banayo, J.B.; Manese, K.L.V.; Salces, A.J.; Yamagata, T. Phylogeny and genetic diversity of Philippine native pigs (*Sus scrofa*) as revealed by mitochondrial DNA analysis. *Biochem Genet* **2023**, *61*, 1401–1417.

5. Banayo, J.B.; Manese, K.L.V.; Furusho, K.O.; Salces, A.J.; Yamagata, T. Genetic diversity and population structure analysis of Philippine native pigs highlight five priority populations for conservation. *Ecol Evol* **2023**, *13(11)*, 1-19.

6. Lingao, J.Q.; Rofes, J.; Eusebio, M.S.; Baretto, G. This little piggy: Pig-human entanglement in the Philippines. *Int J Hist Arch* **2024**, *29(1)*, 40-71.

7. Banayo, J.B.; Manese, K.L.V.; Furusho, K.O.; Kingan, M.S.; Ayomen, J.P.; Saliw-an, M.G.; Nicholas, K.M.G.; Petipit, K.J.S.; Pagbilao, D.P.; Arellano, V.R.E.; Santiago, R.C.; Caguicla, F.A.; Monleon, A.M.; Perlas, G.M.; Ortego, R.P.A.; Singzon, S.B.; Salces, A.J.; Yamagata, T. Production objectives and trait preferences of smallholder farmers in the Philippines: Implications for designing breeding schemes utilizing indigenous swine genetics. *Phil Agric Scient* **2024**, *107(4)*, 318-332.

8. Sto. Domingo, D.A.M. State College R&D Center launches its native pork processed products as African Swine Fever and COVID-19 Pandemic continue to cripple the Philippine swine industry. *Agric Mag 2021, ttps://agriculture.com.ph/2021/05/23/state-college-rd-center-launches-its-native-pork-processed-products-as-african-swine-fever-and-covid-19-pandemic-continue-to-cripple-the-philippine-swine-industry/*

9. Medenilla, V. Markaduke: A native pig recognized as the best lechon in the Philippines. *Manila Bull 2022, https://mb.com.ph/2022/05/14/markaduke-a-native-pig-recognized-as-the-best-lechon-in-the-philippines/*

10. Larga-Loto, J.O.; Perlas, G.M.; Seño, M.; Lozano, S.J.M.; Monleon, A.M. Productivity of markaduke native pig at the farmers' care during the pandemic. *Asian Intel Res Educ J* **2021**, *19*, 63-66.

11. Perlas, G.M.; Robles, J.R. Reproductive performance of markaduke in different parities. *Phil J Vet Anim Sci* **2022**, 48(1), 88-93.

12. Robles, J.R.; Perlas, G.M. Optimizing carcass recovery in markaduke native pigs: insights from Marinduque State College nucleus farm. *Ignatian Int J Mult Res* **2024**, *2(5)*, 467-478.

13. Davoli, R.; Braglia, S. Molecular approaches in pig breeding to improve meat quality. *Brief Funct Genom Prot* **2008**, *6(4)*, 313-321.

14. Rohrer, G.A.; Nonneman, D.J.; Miller, R.K.; Zerby, H.; Moeller S.J. Association of single nucleotide polymorphism (SNP) markers in candidate genes and *QTL* regions with pork quality traits in commercial pigs. *Meat Sci* **2021**, *92*, 511–518.

15. Matias S, Gajeton M, Flores E. Genetic screening of halothane gene on selected Philippine native pig herds. *Open J Genet* **2023**, *13*, 105-113.

16. Rothschild, M.F.; Larson, G.R.; Jacobson, C.D; Pearson P. *PvuII* polymorphism at the porcine estrogen receptor locus (*ESR*). *Anim Genet* **1991**, *22*, 448.

17. Serrano, A.B.; Herrera Haro, J.G; Hori-Oshima, S.; Gutierrez Espinosa, A.; Ortega Cerrilla M.E.; Perez Perez, J.; Lemus Flores, C.;Kinejara Espinosa, A.L.; Gonzalez, A; Soto Avila, J.G. *Prolactin receptor* (*PRLR) gene* polymorphism and associations with reproductive traits in pigs. *J Anim Vet Adv* **2009**, 8 (3): 469-475

18. Spotter, A.; Muller, S.; Hamann, H.; Distl, O. Effect of polymorphisms in the genes for *LIF* and *RBP4* on litter size in two German pig lines. *Reprod Dom Anim* **2008**, 44, 100–105.

19. Te Pas, M.F.W.; Soumillion A.; Van Den Bosch, T.J.; Veninga, G.; Meuwissen, T.H.E. Association between polymorphism in the porcine *myogenin gene* locus and growth traits. EAAP 47th Annual Meeting, Lillehammer, Norway, 25-29 August **1996**.

20. Flores, E.B.; Herrera, J.R.V.; Fernando, T.C.; Matias, S.D.; Labonite, L.M.; Uy, M.R.D.; Pablo, J.C. *Swine Genetic Analytical Service Laboratory Reference Manual*, 2nd ed,; Philippine Carabao Center National Headquarters, Science City of Muñoz, Nueva Ecija, Philippines, **2022**, pp.1-100.

21. Buys, N. IGF2: The use of a paternally expressed *QTL* influencing muscle mass in marker assisted selection in commercial pig populations. *Proc 28th Ann Nat Swine Impt Fed*. Des Moines, Iowa, USA, **2003**, 117, 43-55.

22. Kuryl, J.; Kapelanski W., Pierzchala M., Grajewska S., Bocian M. Preliminary observations on the effect of calpastatin gene (*CAST*) polymorphism on carcass traits in pigs. Anim Sci Pap Rep **2003,** *21(2)*, 87-95

23. Russo, V., Fontanesi, L., Scotti, E., Beretti, F., Davoli, R., Nanni Costa, L., Virgili, R., Buttazzoni, L. Single nucleotide polymorphisms in several porcine cathepsin genes are associated with growth, carcass, and production traits in Italian Large White pigs. J Anim Sci **2008**, *86*, 3300-3314.

24. Perez-Montarelo D., Fernandez A., Folch J.M., R.N. Pena. Joint effects of *porcine leptin* and *leptin receptor* polymorphisms on productivity and quality traits. Anim Genet **2012,** *43*, 805-809.

25. Bao, W.-B. Ye, L. Pan, Z.-Y. Zhu, J. Zhu, G.-Q. Huang, X.-G., Wu S.-L. Beneficial genotype of swine *FUT1 gene* governing resistance to E. coli *F18* is associated with important economic traits. J Genet **2011**, *90*, 315–318.

26. Manalaysay J.G., Antonio N.D., Apilado R.L.R., Bambico J.F., Mingala C.N. Screening of the acid meat condition in the *rendement napole gene* using polymerase chain reaction - restriction fragment length polymorphism. Indones. J Agric Sci **2019,** *20(1)*, 29–34

27. Hamilton, D.N.; Ellis, M.; Miller, K.D.; McKeith, F.K.:Parrett, D.F. The effect of the *halothane* and *rendement napole genes* on carcass and meat quality characteristics of pigs. *J Anim Sci*. **2000**, *78*, 2862-2867.

28. Lundström, K.; Andersson, L. The effect of the RN-allele on meat quality and how the gene was discovered. *54th Ann Recip Meat Conf* **2001**, 143-147.

29. Miller K.D.; Ellis, M.; McKeith, F.K.; Bidner, B.S.; Meisinger D.J. Frequency of *rendement napole RN*-allele in a population of American hampshire pigs. *J Anim Sci* **2000**, *78*, 1811-1815.

30. Russo, V.; Fontanesi, L.; Scotti, E.; Beretti, F.; Davoli, R.; Nanni Costa, L.; Virgili, R.; Buttazzoni, L. Single nucleotide polymorphisms in several porcine cathepsin genes are associated with growth, carcass, and production traits in Italian Large White pigs. *J. Anim Sci* **2008**, 86, 3300–3314.

31. Han, X.; Jiang, T.; Yang, H.; Zhang, Q.; Wang, W.; Fan, B.; Liu, B. Investigation of four porcine candidate genes (*H-FABP, MYOD1, UCP3* and *MASTR*) for meat quality traits in large white pigs. *Mol Bio Rep* **2012**, *39*, 6599–6605.

32. Galve, A.; Burgos, C.; Silió, L.; Varona, L.; Rodríguez, C.; Ovilo, C.; López-Buesa, P. The effects of leptin receptor (*LEPR*) and melanocortin-4 receptor (*MC4R*) polymorphisms on fat content, fat distribution and fat composition in a Duroc × Landrace/Large White cross. *Livest Sci* **2012**, 145, 145–152.

33. Ros-Freixedes, R.; Gol, S.; Pena, R.N.; Tor, M.; Ibáñez-Escriche, N.; Dekkers, J.C.M.; Estany, J. Genome-wide association study singles out *SCD* and *LEPR* as the two main loci influencing intramuscular fat content and fatty acid composition in Duroc pigs. *PLOS ONE* **2016**, *11(3)*, 1-18.

34. Jeremiah, L.E. Marbling and pork tenderness. *Pork Info Gateway* 2006, 1-5.

35. Muñoz, G.; Alcázar, E.; Fernández, A.; Barragán, C.; Carrasco, A.; de Pedro, E.; Silió, L.; Sánchez, J.L.; Rodríguez, M.C. Effects of porcine MC4R and LEPR polymorphisms, gender and Duroc sire line on economic traits in Duroc × Iberian crossbred pigs. *Meat Sci* **2011**, *88*, 169–173.

36. Balatsky, V.N.; Bankovska, I.B.; Saienko, A.M. Association between *leptin receptor gene* polymorphism and quality of both meat and backfat in large white pigs of Ukrainian breeding. *Agric Sci Pract* **2016**, *3(2)*, 42-48.

37. Kuryl, J.; Kapelański, W.; Pierzchała, M.; Grajewska, S.; Bocian, M. Preliminary observations on the effect of *calpastatin gene* (*CAST*) polymorphism on carcass traits in pigs. *Anim Sci Pap Rep* **2003**, *21(2)*, 87-95.

38. Xue, W., Wang, W.; Jin, B.; Zhang, X.; Xu, X. Association of the *ADRB3, FABP3, LIPE*, and *LPL* gene polymorphisms with pig intramuscular fat content and fatty acid composition. *Czech J Anim Sci* **2015**, *60(2)*, 60–66.

39. Davoli, R.; Braglia S. Molecular approaches in pig breeding to improve meat quality. *Brief Funct Gen Prot* **2008**, *6(4)*, 313-321.

40. Clark, D.L.; Clark, D.I.; Beever, J.E.; Dilger, A.C. Increased prenatal *IGF2* expression due to the porcine *IGF2* intron3-G3072A mutation may be responsible for increased muscle mass. *J Anim Sci* **2015**, *93*, 2546–2558.

41. Kolaøíková, O.; Putnová, L.; Urban, T.; Adámek, J.; Knoll, A.; Dvoøák, J. Associations of the *IGF2* gene with growth and meat efficiency in Large White pigs. *J Appl Genet* **2003**, *4(44)*, 509-513.

42. Vincent, A.L.; Tuggle, C.K.; Rothschild, M.F.; Evans, G.; Short, T.H.; Southwood, O.I.; Plastow, G.S. The prolactin receptor gene is associated with increased litter size in pigs. *6th World Cong Genet Appl Livest Prod* **1998**, 1-2.

43. Sun, Y.X.; Zeng, Y.Q.; Tang, H.; Fan, X.Z.; Chen, Q.M.; Li, H.; Qian, Y.; Song, Y.P. Relationship of genetic polymorphism of *PRLR* and *RBP4* genes with litter size traits in pig. *Hereditas* (Beijing) **2009**, *31(1)*, 63-68.

44. Wu, Y.; Xie, J.; Zhong, T.; Shen, L.; Zhao, Y.; Chen, L.; Gan, M.; Zhang, S.; Zhu, L.; Niu L. Genetic diversity of porcine PRLR gene and its relationship to litter size in large white pigs. *Folia Biol (Kraków)* **2023**, *71*, 28-36.

45. Yurina, A.; Skovorodin, E.; Dolmatova, I. Evaluation of reproductive traits and ovarian and uterine morphology of sows with different genotypes for the estrogen receptor, prolactin receptor, and follicle-stimulating hormone subunit beta genes. *Can J Vet Res* **2021**, *85(3)*, 186-192.

46. Trenhaile, M.D.; Petersen, J.L.; Kachman, S.D.; Johnson, R.K.; Ciobanu, D.C. Long-term selection for litter size in swine results in shifts in allelic frequency in regions involved in reproductive processes. *Anim Genet* **2016**, *47(5)*, 534-542.

47. Rothschild, M.; Jacobson, C.; Vaske, D.; Tuggle, C.; Wang, L.; Short, T.; Eckardt, G.; Sasaki, S.; Vincent, A.; McLaren, D.; Southwood, O.; van der Steen, H.; Mileham, A.; Plastow, G. The estrogen receptor locus is associated with a major gene influencing litter size in pigs. *Proc Natl Acad Sci USA* **1996**, *93(1),* 201-5.

48. Vega, R.S.A.; Castillo, M.R.C.; Barrientos, N.N.B.; Llanes-Autriz, M.M.; Wook Cho, B.; de la Viña, C.B.; Villa, N.O. Leptin (*T3469C*) and estrogen receptor (*T1665G*) gene polymorphisms and their associations to backfat thickness and reproductive traits of large white pigs (*Sus scrofa* L.). *Phil J Sci* **2018**, *147(2)*, 293-300.

49. Lin, H.C.; Liu, G.F.; Wang, A.G.; Kong, L.J.; Wang, X.F.; Fu, J.L. Effect of polymorphism in the leukemia inhibitory factor gene on litter size in large white pigs. *Mol Biol Rep* **2008**, 36:1833-1838.

50. Ding, Y.; Ding, C.; Wu, X.; Wu, C.; Qian, L.; Li, D.; Zhang, W.; Wang, Y.; Yang, M.; Ding, J.; Zhang, X.; Gao, Y.; Yin, Z. Porcine LIF gene polymorphisms and their association with litter size traits in four pig breeds. *Can. J Anim Sci* **2018**, *100*, 85–92.

51. Silveira, A.C.P.; Freitas, P.F.A.; Cesar, A.S.M.; Antunes, R.C.; Guimarães, E.C.; Batista, D.F.A.; Torido, L.C. Influence of the halothane gene (*HAL*) on pork quality in two commercial crossbreeds. *Genet Mol Res* **2011**, *10(3)*, 1479-1489.

52. Stupka, R.; Citek, J.; Sprysl, M.; Okrouhla, M.; Brzobohaty, L. The impact of *MYOG, MYF6* and *MYOD1* genes on meat quality traits in crossbred pigs. *African J Biotech* **2012**, *11(88)*, 15405-15409.

53. Cho, I.-C.; Park, H.-B.; Ahn, J.S.; Han, S.-H.; Lee, J.-B.; Lim, H.-T.; Yoo, C.-K.; Jung, E.-J.; Kim, D.-H.; Sun, W.-S.; Ramayo-Caldas, Y.; Kim, S.-G.; Kang, Y.-J.; Lee, J.-W. A functional regulatory variant of *MYH3* influences muscle fiber-type composition and intramuscular fat content in pigs. *PLOS Genet* **2019**, *15(10)*, 1-26.

54. Kolaøíková, O.; Putnová, L.; Urban, T.; Adámek, J.; Knoll, A.; Dvoøák, J. Associations of the *IGF2* gene with growth and meat efficiency in Large White pig. *J Appl Genet* **2003**, *4(44)*, 509-513.

55. Zhao, T.; Tian, T.; Yu, H.; Cao, C.; Zhang, Z.; He, Z.; Ma, Z.; Cai, R.; Li, F.; Pang W. Identification of porcine fast/slow myogenic exosomes and their regulatory effects on lipid accumulation in intramuscular adipocytes. *J Anim SciBiotech* **2024**, *15(73)*,1-16.

56. Rodrigueza, V.R.; Maffiolya, J.I.; Zdanovicza, L.A.; Fabrea, R.M.; Barrandeguy, M.E.; García, M.V.; Lagadaria, M. Genetic diversity of meat quality related genes in Argentinean pigs. *Vet Anim Sci* **2022**, *15*, 100237.

57. Trakovická, A.; Moravčíková, N.; Kasarda, R. Genetic polymorphisms of leptin and leptin receptor genes in relation with production and reproduction traits in cattle. *Acta Biochim Pol* **2013**, *60(4)*, 783-7.

58. Kováčik, A.; Bulla, J.; Trakovická, A.; Lieskovská, Z.; Žitný, J. Effects of the porcine *LEPR* polymorphism (Hpaii) on carcass traits in large white × landrace crossbred pigs. *Sci Papers Anim Sci Biotech* **2011**, *44(1)*, 260-262.

59. Burgos, C.; Carrodeguas, J.A.; Moreno, C.; Altarriba, J.; Tarrafeta, L.; Barcelona, J.A.; López–Buesa, P. Allelic incidence in several pig breeds of a missense variant of pig melanocortin-4 receptor (*MC4R*) gene associated with carcass and productive traits; its relation to *IGF2* genotype. *Meat Sci* **2005**, *73*, 144–150.

60. Carrodeguas, J.A.; Burgos, C.; Moreno, C.; Sánchez, A.C.; Ventanas, S.; Tarrafeta, L.; Barcelona, J.A.; López, M.O.; Oria, R.; López-Buesa, P. Incidence in diverse pig populations of an *IGF2* mutation with potential influence on meat quality and quantity: An assay based on real time PCR (RT-PCR). *Meat Sci* **2005**, *71(3)*, *577*-82.

CVJ CLUJ VETERINARY JOURNAL

Research article

Comparative Efficacy of Combined Mesenchymal Stem Cell and Platelet-Rich Plasma Therapy with ESWT/Hydrotherapy in Equine Superficial Digital Flexor Tendinopathy: A Prospective Clinical Trial

Alexandru Florin Lupșan [1], Denisa Bungărdean [2], Emoke Pall [3], Zsofia Daradics [4], Maria Popescu [5], Florin Dumitru Bora [6,7], Liviu Oana [1], Adrian Todor [8], Cristian Mihăiță Crecan [1*]

1 Department of Anesthesiology and Surgery, Faculty of Veterinary Medicine, University of Agricultural Sciences and Veterinary Medicine Cluj-Napoca, Mănăştur Street 3–5, 400372 Cluj-Napoca, Romania
2 Department of Pathophysiology, Faculty of Veterinary Medicine, University of Agricultural Sciences and Veterinary Medicine Cluj-Napoca, Mănăştur Street 3–5, 400372 Cluj-Napoca, Romania
3 Department of Infectious Diseases, Faculty of Veterinary Medicine, University of Agricultural Sciences and Veterinary Medicine Cluj-Napoca, Calea Mănăştur nr. 3–5, 400372 Cluj-Napoca, Romania
4 Department of Internal Medicine, Faculty of Veterinary Medicine, University of Agricultural Sciences and Veterinary Medicine Cluj-Napoca, Mănăştur Street 3–5, 400372 Cluj-Napoca, Romania
5 Equine Clinic, Faculty of Veterinary Medicine, University of Agricultural Sciences and Veterinary Medicine Cluj-Napoca, Mănăştur Street 3–5, 400372 Cluj-Napoca, Romania
6 Laboratory of Chromatography, Advanced Horticultural Research Institute of Transylvania, Faculty of Horticulture and Business for Rural Development, University of Agricultural Sciences and Veterinary Medicine, 400372 Cluj-Napoca, Romania
7 Viticulture and Oenology Department, Advanced Horticultural Research Institute of Transylvania, Faculty of Horticulture and Business in Rural Development, University of Agricultural Sciences and Veterinary Medicine Cluj-Napoca, Mănăştur Street 3–5, 400372 Cluj-Napoca, Romania
8 Iuliu Hațieganu University of Medicine and Pharmacy, Department of Orthopedics and Traumatology
* Correspondence: cristian.crecan@usamvcluj.ro Tel.: + 4 0732556462

Abstract: Equine superficial digital flexor tendon (SDFT) tendinopathy is a frequent cause of reduced athletic performance and prolonged lameness in sport horses, characterized by limited intrinsic healing capacity, fibrosis, and high recurrence rates after return to exercise. Regenerative and adjunctive therapies such as mesenchymal stem cells (MSCs), platelet-rich plasma (PRP), extracorporeal shockwave therapy (ESWT), and hydrotherapy have been increasingly used, yet comparative clinical evidence remains limited. This prospective clinical trial evaluated the efficacy of combined MSC-PRP therapy compared with PRP-ESWT and MSC-hydrotherapy in horses with naturally occurring SDFT lesions managed under a standardized rehabilitation program. Twelve horses with ultrasonographically confirmed SDFT tendinopathy and grade 2–4/5 forelimb lameness were randomly allocated to three treatment groups (n = 4/group): Group 1 received intralesional MSC followed by PRP injections, Group 2 received PRP combined with ESWT, and Group 3 received MSC combined with underwater treadmill hydrotherapy. Clinical and ultrasonographic assessments were performed at baseline, days 14 and 28, and weeks 12 and 24. All groups showed significant improvement in lameness scores by week 12 ($p < 0.01$ versus baseline), with mean AAEP scores decreasing from 3.0 ± 0.8 to 1.2 ± 0.4 in Group 1, 1.5 ± 0.5 in Group 2, and 1.3 ± 0.4 in Group 3. Lesion cross-sectional area decreased significantly over time ($p < 0.001$), reaching reductions of 85%, 72%, and 78% in Groups 1, 2, and 3, respectively, by week 24. Echogenicity and fiber alignment improved most markedly in the MSC-PRP group. Return to previous performance level at 6 months was achieved in 100% of horses in Group 1 and 75% in Groups 2 and 3. No adverse events were recorded. Combined MSC-PRP therapy within a structured rehabilitation protocol may provide superior structural and functional recovery in equine SDFT tendinopathy, while PRP-ESWT and MSC-hydrotherapy represent effective alternative treatment strategies.

Keywords: equine tendinopathy, mesenchymal stem cells, platelet-rich plasma, extracorporeal shockwave therapy, hydrotherapy, superficial digital flexor tendon

Received: 15.02.2026
Accepted: 24.04.2026
Published: 29.04.2026

DOI:10.52331/v31i2rs08

1. Introduction

Tendinopathy constitutes a principal cause of locomotor morbidity among equine athletes, predominantly affecting the superficial digital flexor tendon (SDFT) and deep digital flexor tendon (DDFT). These tendons are particularly susceptible to overload injuries due to their pivotal biomechanical roles in force transmission and elastic energy storage during locomotion [1,2]. Healing of such injuries remains suboptimal, primarily attributable to inherent avascularity and hypocellularity, which culminate in the deposition of fibrotic scar tissue exhibiting inferior mechanical properties and recurrence rates as high as 67% upon return to athletic competition [3].

Emerging regenerative therapies—including mesenchymal stem cells (MSCs), platelet-rich plasma (PRP), extracorporeal shockwave therapy (ESWT), and hydrotherapy—hold considerable promise by augmenting angiogenesis, facilitating collagen remodeling, and promoting functional tissue recovery [4–7]. Established protocols, such as those delineated by Denoix and Smith, advocate phased rehabilitation paradigms incorporating imaging-guided interventions to optimize outcomes [6,7]. Nevertheless, therapeutic consensus remains elusive, particularly regarding comparative efficacy between proximal SDFT lesions (benefiting from superior vascularization) and distal SDFT lesions (predisposed to compressive pathology).

The present study evaluates the efficacy of combined MSC-PRP therapy adjunctive to ESWT and hydrotherapy in proximal versus distal SDFT tendinopathies, employing serial ultrasonography and standardized lameness scoring.

2. Materials and Methods

2.1. Study Population

Twelve horses of mixed breeds and both sexes (mean age: 9.1 ± 2.7 years; range: 4 – 14 years) presenting with grade 2–4/5 forelimb lameness, per the American Association of Equine Practitioners (AAEP) scale, were prospectively enrolled. All subjects were actively competing in carriage driving, endurance, or show jumping disciplines. Lameness was attributed to ultrasonographically confirmed superficial digital flexor tendon (SDFT) lesions, diagnosed by characteristic clinical signs (lameness, swelling, localized heat) and verified via high-resolution ultrasonography (7.5–12 MHz linear transducer).

Horses were randomly allocated to three treatment groups (n = 4 per group) using block randomization stratified by lesion location (proximal vs. distal) and baseline lameness grade.

2.2. Rehabilitation Protocol

All subjects followed a standardized 28-week rehabilitation program with serial assessments comprising lameness scoring (AAEP scale) and ultrasonography at baseline (day 0), days 14 and 28, and weeks 12 and 24. The phased protocol progressed as follows:

- Phase 1 (days 0–3): Strict box rest
- Phase 2 (days 4–14): Hand-walking (5–10 min twice daily)
- Phase 3 (weeks 3–8): Controlled walking (15–35 min daily)
- Phase 4 (weeks 9–12): Trot introduction (2–5 min)
- Phase 5 (weeks 13–20): Progressive trot-canter (duration escalated weekly)
- Phase 6 (weeks 21–28): Lunging or paddock turnout
- Phase 7: Gradual return to discipline-specific training

Phase advancement required clinical stability (AAEP ≤1/5) and ultrasonographic CSA reduction ≥20% from prior evaluation.

2.3. Treatment Interventions

Group 1 (MSC-PRP): Ultrasound-guided intralesional injection of autologous synovial-derived mesenchymal stem cells (MSCs; 10×10^6 cells) on day 7, followed by platelet-rich plasma (PRP; double-spin preparation, leukocyte-poor) injections on days 14 and 28.

Group 2 (PRP-ESWT): PRP injections (days 7 and 14) combined with extracorporeal shockwave therapy (ESWT; 3–5 sessions at 7–10 day intervals during proliferative phase; parameters: 2000–3000 shocks/site, 0.12–0.18 mJ/mm², 4 Hz).

Group 3 (MSC-Hydrotherapy): MSC injection (days 7 and 14) adjunctive to underwater treadmill hydrotherapy (magnesium-enriched water; 28°C; water depth 40 cm; belt speed 3.4 km/h; incline 3–5°; 10–25 min/session, 2–3 times weekly from week 3).

2.4.Outcome Measures and Statistical Analysis

Primary outcomes included AAEP lameness scores and lesion cross-sectional area (CSA; % tendon area). Secondary endpoints comprised echogenicity grade, return-to-performance (month 6), and adverse events. Data were analyzed using repeated-measures ANOVA with Tukey post-hoc testing ($\alpha = 0.05$; SPSS v.27). Results are reported as mean ± SD.

3. Results

3.1. Clinical Outcomes

Clinical lameness improved across all groups by week 12, with mean AAEP scores dropping from 3.0±0.8 at baseline to 1.2±0.4 (Group 1), 1.5±0.5 (Group 2), and 1.3±0.4 (Group 3) ($p<0.01$ vs. baseline for all; no intergroup difference). By week 24, 75% (3/4) in Group 1 and 50% (2/4) in Groups 2 and 3 were sound at walk/trot; one Group 2 horse showed mild recurrence.

3.2. Ultrasonographic Findings

Lesion cross-sectional area (CSA) reduced significantly over time ($p<0.001$). Baseline CSA was 25±8% of tendon area in all groups. At week 12, reductions were 68% (Group 1), 55% (Group 2), and 62% (Group 3); by week 24, 85%, 72%, and 78%, respectively (Table 1). Echogenicity improved markedly in Group 1 (heterogeneous to near-normal fiber alignment by week 24), with Groups 2 and 3 showing moderate gains but persistent hypoechoic foci.

Table 1. Clinical and ultrasonographic outcomes by group

Timepoint	Group 1	Group	Group 3	Intergroup p-value (ANOVA)
AAEP Score				
Baseline	3.0 ± 0.8	3.0 ± 0.8	3.0 ± 0.8	>0.05
Week 12	1.2 ± 0.4	1.5 ± 0.5	1.3 ± 0.4	0.42
Week 24	Sound: 75% (3/4)	Sound: 50% (2/4)	Sound: 50% (2/4)	0.31
Lesion CSA (% tendon area)				
Baseline	25 ± 8	25 ± 8	25 ± 8	>0.05
Week 12	32% (↓68%)	45% (↓55%)	38% (↓62%)	0.28
Week 24	15% (↓85%)	28% (↓72%)	22% (↓78%)	0.19
Return to Performance (Month 6)	100% (0% recurrence)	75% (25% recurrence)	75% (25% recurrence)	0.45

Values are mean ± SD. ↓ indicates % reduction from baseline. $p < 0.01$ for all groups vs. baseline (paired t-test). No significant intergroup differences.

3.3. Safety and Functional Recovery

No adverse events, including injection-site reactions or systemic complications, were observed in any group. By month 6, 100% of Group 1 horses returned to their previous level of performance, compared to 75% in Groups 2 and 3. These findings correspond to recurrence rates below 25% across all cohorts.

4. Discussion

The findings of this study indicate that combined regenerative therapies, when integrated within a standardized functional rehabilitation protocol, yield substantial clinical benefits in the management of equine tendinopathies [8]. Specifically, the multimodal approach encompassing mesenchymal stem cells (MSCs) and platelet-rich plasma (PRP), adjunctive to extracorporeal shockwave therapy (ESWT) and hy-

drotherapy, demonstrated superior outcomes in lameness resolution and lesion remodeling compared to single-modality treatments.

The combined MSC-PRP regimen, embedded in a structured functional recovery protocol, emerges as a particularly promising strategy for equine tendon injury management [9,10]. This approach conferred significant clinical advantages, including accelerated healing timelines and enhanced tissue regeneration quality, as evidenced by the 85% reduction in lesion cross-sectional area (CSA) and 100% return to prior performance levels by month 6 in Group 1 (Table 1; $p < 0.001$ vs. baseline). These results align with prior reports on the synergistic effects of MSCs and PRP in promoting tenocyte proliferation, extracellular matrix remodeling, and angiogenesis [11,12], while mitigating fibrotic scarring commonly observed in avascular tendon regions [13,14].

Notably, MSC-PRP combination therapy proved most efficacious in driving structural regeneration, particularly in proximal and distal superficial digital flexor tendon (SDFT) lesions [15], with marked improvements in fiber alignment and echogenicity by week 24. In contrast, PRP-ESWT and MSC-hydrotherapy pairings offered viable alternatives [16,17], achieving 72-78% CSA reductions and 75% return-to-performance rates. These options may be tailored based on lesion chronicity, patient tolerance, and available therapeutic resources, underscoring the value of individualized protocols as advocated by Denoix and Smith.

Despite these advances in equine regenerative medicine, several limitations warrant consideration [18]. The modest sample size (n=4 per group) precludes definitive power for intergroup comparisons, and long-term recurrence beyond 6 months remains to be evaluated. Furthermore, while clinical and ultrasonographic improvements were robust, histological confirmation of tendon architecture was not feasible in this clinical setting.

5. Conclusions

Combined regenerative therapies integrated into standardized rehabilitation protocols represent a promising direction for equine tendinopathy management. MSC-PRP combination yields optimal structural regeneration, while adjunctive ESWT or hydrotherapy provides effective alternatives. Future research should elucidate underlying mechanisms, optimize dosing regimens, and delineate synergistic interactions to establish evidence-based clinical standards.

Author Contributions: Conceptualization, A.F.L.; methodology, A.F.L., C.C. and F.D.B.; software, A.F.L., C.C., F.D.B. and M.P.; validation, C.C., D.B., E.P. and S.D.; formal analysis, A.F.L., C.C., F.D.B. and M.P.; investigation, A.F.L., C.C., D.B., E.P. and S.D.; resources, C.C., D.B., E.P. and S.D.; data curation, C.C., D.B., E.P. and S.D.; writing—original draft preparation, A.F.L.; writing—review and editing, L.O. and C.C.; visualization, A.F.L.; supervision, L.O. and C.C.; project administration, A.F.L.; funding acquisition, A.F.L. All authors have read and agreed to the published version of the manuscript.

Funding: This research received no specific grant from funding agencies in the public, commercial, or not-for-profit sectors.

Institutional Review Board Statement: Not applicable.

Acknowledgments: The authors express gratitude to the horse owners who participated in this study and entrusted their equine athletes to our care. Special thanks to the clinical staff at Equine Clinic of Cluj-Napoca FVM for their dedicated support during the 28-week rehabilitation period, particularly in administering ESWT sessions.

Conflicts of Interest: The authors declare no conflict of interest.

References

1. Carvalho A.M.; Badial P.R.; Álvarez L.E.C.; Yamada A.L.M.; Borges A.S.; Deffune E.; Hussni C.A.; Garcia Alves A.L. Equine tendonitis therapy using mesenchymal stem cells and platelet concentrates: a randomized controlled trial. *Stem Cell Res Ther* **2013**, *4(4),* 85. https://doi.org/10.1186/scrt236.
2. Bosch, G.; Moleman, M.; Barneveld, A.; van Weeren, P.R.; van Schie, H.T.M. The effect of platelet-rich plasma on the neovascularization of surgically created equine superficial digital flexor tendon lesions. *Scand J Med Sci Sports* **2011**, *21*, 554–561. https://doi.org/10.1111/j.1600-0838.2009.01070.x
3. Carvalho, A.M.; Badial, P.R.; Álvarez, L.E.C.; Yamada, A.L.M.; Borges, A.S.; Deffune, E.; Hussni, C.A.; Alves, A.L.G. Equine tendonitis therapy using mesenchymal stem cells and platelet concentrates: a randomized controlled trial. *Stem Cell Res Ther* **2013**, *4*, 85. https://doi.org/10.1186/scrt236

4. Dakin, S.G.; Dudhia, J.; Smith, R.K.W. Science in brief: resolving tendon inflammation. A new perspective. *Equine Vet J* **2013**, *45*, 398–400. https://doi.org/10.1111/evj.12030
5. Reis I.L.; Lopes B.; Sousa P.; Sousa A.C.; Caseiro A.R.; Mendonça C.M.; Santos J.M.; Atayde L.M.; Alvites R.D.; Maurício A.C. Equine Musculoskeletal Pathologies: Clinical Approaches and Therapeutical Perspectives-A Review. *Vet Sci* **2024**, *26;11(5)*, 190. https://doi.org/10.3390/vetsci11050190.
6. Filomeno, P.; Dayan, V.; Touriño, C. Stem cell research and clinical development in tendon repair. *Muscles Ligaments Tendons J* **2012**, *2*, 204–211.
7. Daglish, J., Mama, K.R. Pain Its Diagnosis and Management in the Rehabilitation of Horses. *Vet Clin North Ame Equine Pract* **2016** *32(1)*, 13–29. https://doi.org/10.1016/j.cveq.2015.12.005
8. Ortved, K.F. Regenerative Medicine and Rehabilitation for Tendinous and Ligamentous Injuries in Sport Horses. *Vet Clin North Ame Equine Pract* **2018**, *34*, 359–373. https://doi.org/10.1016/j.cveq.2018.04.012
9. Smith, R.K.W.; Werling, N.J.; Dakin, S.G.; Alam, R.; Goodship, A.E.; Dudhia, J. Beneficial effects of autologous bone marrow-derived mesenchymal stem cells in naturally occurring tendinopathy. *PLoS One* **2013**, *8*, e75697. https://doi.org/10.1371/journal.pone.0075697
10. Reed, S.A., Leahy, E.R. Stem cell therapy in equine tendon injury. *J Anim Sci* **2013**, *91(1)*, 59-65. doi.org/10.2527/jas.2012-5736
11. Schnabel, L.V.; Lynch, M.E.; van der Meulen, M.C.H.; Yeager, A.E.; Kornatowski, M.A.; Nixon, A.J. Mesenchymal stem cells and insulin-like growth factor-I gene-enhanced mesenchymal stem cells improve structural aspects of healing in equine flexor digitorum superficialis tendons. *J Orthop Res* **2009**, *27*, 1392–1398. https://doi.org/10.1002/jor.20887
12. Bungărdean, D.; Pall, E.; Daradics, Z.; Popescu, M.; Tripon, M.A.; Lupșan, A.F.; Crecan, C.M.; Morar, I.A.; Nicolescu, A.; Bora, F.D.; et al. In Vitro Effects of PRP, Ozonized PRP, Hyaluronic Acid, Paracetamol, and Polyacrylamide on Equine Synovial Fluid-Derived Mesenchymal Stem Cells. *Life* **2025**, *15*, 1558. https://doi.org/10.3390/life15101558
13. Patterson-Kane J.C., Firth EC. The pathobiology of exercise-induced superficial digital flexor tendon injury in Thoroughbred racehorses. Vet J **2009**, *181(2)*:79-89. https://doi.org/10.1016/j.tvjl.2008.02.009
14. Thomopoulos, S.; Parks, W.C.; Rifkin, D.B.; Derwin, K.A. Mechanisms of tendon injury and repair. *J Orthop Res* **2015**, *33*, 832–839. https://doi.org/10.1002/jor.22806
15. Murata, D.; Miyakoshi, D.; Hatazoe, T.; Miura, N.; Tokunaga, S.; Fujiki, M.; Nakayama, K.; Misumi, K. Multipotency of equine mesenchymal stem cells derived from synovial fluid. *Vet J* **2014**, *202*, 53–61. https://doi.org/10.1016/j.tvjl.2014.07.029
16. Morawska-Kozłowska, M.; Pitas, M.; Zhalniarovich, Y. Mesenchymal Stem Cells in Veterinary Medicine—Still Untapped Potential. *Animals (Basel)* **2025**, *15*, 1175. https://doi.org/10.3390/ani15081175
17. Qiu Z, Wang J, Zhang Y, Liu X, Wei C, Ma T. Extracorporeal shock wave therapy for equine musculoskeletal disorders: from biological mechanisms to clinical applications. Front Vet Sci **2025**, *12*:1719123. https://doi.org/10.3389/fvets.2025.1719123.
18. Smith, R.K.W. Physiology of Tendon and Ligament. In: Chuit, P.; Montavon, S., Eds.; *9th Congress on Equine Medicine & Surgery*; International Veterinary Information Service: Geneva, 2005; pp. 1903–1905.

CVJ CLUJ VETERINARY JOURNAL

Case Report

Cervical Infectious Panniculitis in a Dog: Successful Treatment with En Bloc Excision Including Jugular Vein Resection and Omentopexy

Tom Ablassmaier [1], Lucia Bel [1,*], Liviu Oana [1], Iosif Vasiu [1], Raluca Marica [2], Robert Purdoiu [3] and Adrian Todor [4]

[1] Department of Anesthesiology and Surgery, Faculty of Veterinary Medicine, University of Agricultural Sciences and Veterinary Medicine Cluj-Napoca, 3-5 Mănăştur Street, 400372 Cluj-Napoca, Romania tom-adrian.ablassmaier@usamvcluj.ro; lucia.bel@usamvcluj.ro; iosif.vasiu@usamvcluj.ro;
[2] Department of Pathology, Faculty of Veterinary Medicine, University of Agricultural Sciences and Veterinary Medicine Cluj-Napoca, 3-5 Mănăştur Street, 400372, Cluj-Napoca, Romania; raluca.marica@usamvcluj.ro
[3] Department of Imagistics and Internal Diseases, Faculty of Veterinary Medicine, University of Agricultural Sciences and Veterinary Medicine Cluj-Napoca, 3-5 Mănăştur Street, 400372 Cluj-Napoca; robert.purdoiu@usamvcluj.ro
[4] Department of Pediatric Orthopedics and Trauma Orthopedics, Faculty of Medicine, "Iuliu Haţieganu" University of Medicine and Pharmacy, 8 Victor Babeş Street, 400012 Cluj-Napoca, Romania; atodor81@gmail.com
* Correspondence: lucia.bel@usamvcluj.ro

Abstract: Panniculitis is an inflammation of the *panniculus adiposus* rarely seen in dogs and cats. In this case, the dog developed multiple cervical nodules, some forming fistulas that discharged serosanguineous or purulent fluid. Preoperative CT scans showed the mass was closely attached to the right jugular vein, and microbiological tests detected *Staphylococcus pseudintermedius*. Due to inadequate response to conservative treatment, the mass and part of the jugular were surgically removed *en bloc*. To address the large defect post-removal, an omental pedicle flap was created, tunneled under the skin to the neck, and covered with a skin flap. Follow-up ultrasonography and Doppler exams confirmed the flap's vascularization remained intact. The dog recovered well despite minor postoperative complications. At eight months post-surgery, the omentum remained in place, with no recurrence or complications.

Keywords: cervical panniculitis, jugular vein resection, omental pedicle flap

Received: 24.02.2026
Accepted: 25.02.2026
Published: 19.03.2026

DOI:10.52331/v31i1qy72

1. Introduction

Panniculitis is characterized by inflammation of the subcutaneous fat, which can lead to the formation of single or multiple nodules and is caused by infectious or non-infectious agents. The non-infectious causes may also be idiopathic, resulting in sterile nodular panniculitis (SNP) [1–3]. The pathogenesis and clinical progression of SNP are not well understood, although clinicians often suspect a systemic origin, such as pancreatic or liver diseases. Treatment for SNP typically involves oral glucocorticoids used as immunosuppressive agents [1,2]. Infectious panniculitis is usually triggered by agents like Actinomyces spp., *Staphylococcus pseudintermedius*, or *Mycobacterium* spp. [3]. Other causes include fungal, viral, or parasitic infections, as well as post-injection site inflammation, vasculitis, drug eruptions, thermal reactions, or insect bites, which can cause inflammation of the adipose tissue leading to non-sterile nodular panniculitis (NSNP). This condition often results in ulcerated or fistulous skin lesions [1–3].

These skin lesions can be localized or generalized, may vary in size and consistency, and, while they are more often found on the trunk in dogs, they are more commonly found on the ventral abdomen in cats. The skin may appear normal or change color to yellow, brown, or red, and it may become necrotic [3]. Histologically, sterile panniculitis often

shows granulomatous inflammation, whereas pyogranulomatous or suppurative infiltrates suggest an infectious cause [4]. Treating panniculitis can be lengthy and challenging; moreover, conservative approaches do not always yield satisfactory results. Rapidly progressing nodules of infectious origin or with secondary infection may require special attention, such as surgical removal of the masses. The resulting defects can slow recovery, increase costs, and delay healing.

Transposing the greater omentum as a pedicle flap offers the opportunity not only to support but also to accelerate healing. Its ability to enhance angiogenesis through vascular endothelial growth factor (VEGF)-mediated mechanisms, promote lymphatic and tissue fluid drainage, and support immune function via its milky spots and fat-associated lymphoid clusters (FALCs), along with its regenerative potential due to resident stem cells, has made the greater omentum a valuable tool in the surgical management of traumatic tissue defects and substance loss [5–9]. The greater omentum consists of three major compartments: the bursal, splenic, and, in carnivores, the veil portion, each with a unique vascularization pattern [10–13]. In addition to the previously described properties, it provides mechanical stability and has been used in chest wall reconstruction and to support abdominal hernia repairs [14,15]. The objective of this retrospective case report is to describe the management and evolution of a dog after resection of multiple nodules caused by panniculitis in the cervical region, combined with the use of an omental pedicle flap, and the follow-up involving frequent ultrasonographic examinations to ensure an intact vascularization of the omental pedicle flap.

2. Material and Methods

2.1 Case Description

A four-year-old female mixed-breed dog weighing 24 kg was presented to the Surgical Clinic at the University of Agricultural Sciences and Veterinary Medicine Cluj-Napoca (USAMV) in mid-May 2025. According to the owner, a swelling in the right cervical region had first been noticed in early January 2025 (Fig. 1A). A few days later, the enlarging mass began draining serosanguineous and purulent discharge.

In early March, an exploratory surgery was performed at another veterinary clinic to investigate the possible presence of a foreign body. Postoperatively, the dog was treated with metronidazole, amoxicillin-clavulanic acid and drotaverine. Shortly after the surgery, a second mass appeared adjacent to the first. The surgical wound healed slowly and additional masses subsequently developed (Fig. 1B).

A microbiological examination performed in April identified an infection with *S. pseudintermedius*. Based on culture and antimicrobial susceptibility testing, the dog was prescribed amoxicillin-clavulanic acid. By the time of presentation at USAMV in mid-May 2025, multiple masses had developed, discharging serosanguineous and purulent fluid, consistent with fistula formation (Fig. 1C and D).

2.2 Imaging Modalities

A 20G catheter (B. Braun Melsungen, Germany) was inserted into the left cephalic vein, and a blood sample was collected for biochemistry and a complete blood count (CBC) analysis, which showed no abnormalities. To check for metastases, a full-body contrast-enhanced CT scan was performed (SOMATOM Scope Siemens, Germany). An intravenous contrast medium (Iohexol; Omnipaque 35%, GE Healthcare AS, Norway; 2 ml/kg IV) was administered. The dog received lactated Ringer's solution (Ringer-Lactate, B. Braun Melsungen, Germany; 10 ml/kg/h IV) throughout the procedure.

The CT scan revealed a subcutaneous mass infiltrating the dermis and subcutaneous adipose tissue, extending to the right jugular vein. The mass was well-defined, showed marked contrast enhancement, and exhibited increased vascularization. Furthermore, no evidence of metastasis was detected (Fig. 2A and D).

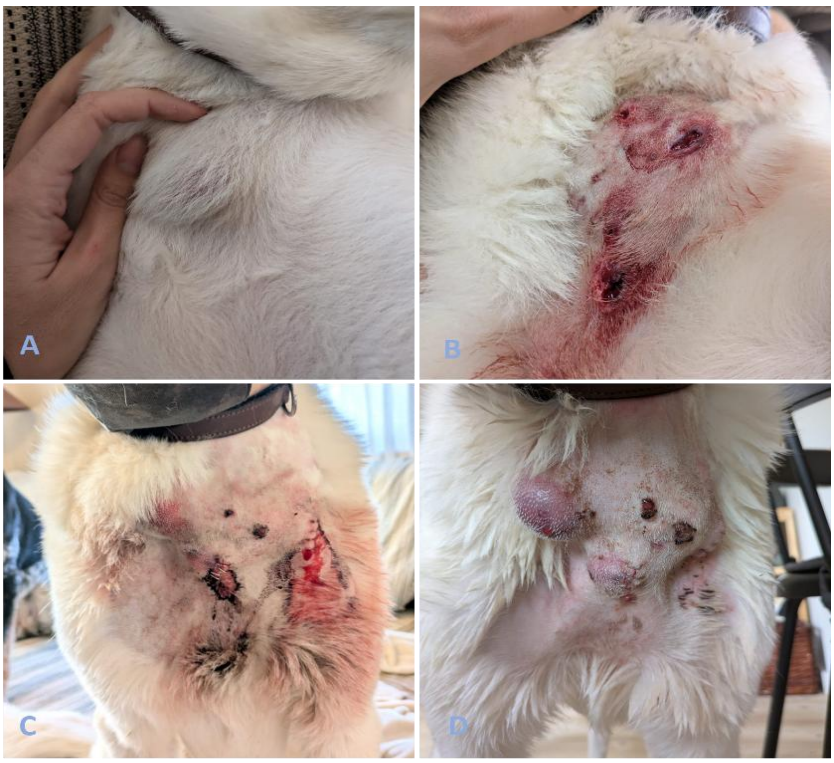

Figure 1. Appearance of the cervical mass before surgery: (**A**) Initial mass observed in early January 2025; (**B**) Development of new masses following the first exploratory surgery, with ulceration and formation of draining tracts; (**C**) Lesions at the first visit to the surgery clinic of USAMV Cluj-Napoca; (**D**) Rapid growth of additional nodules observed just two days after the initial presentation.

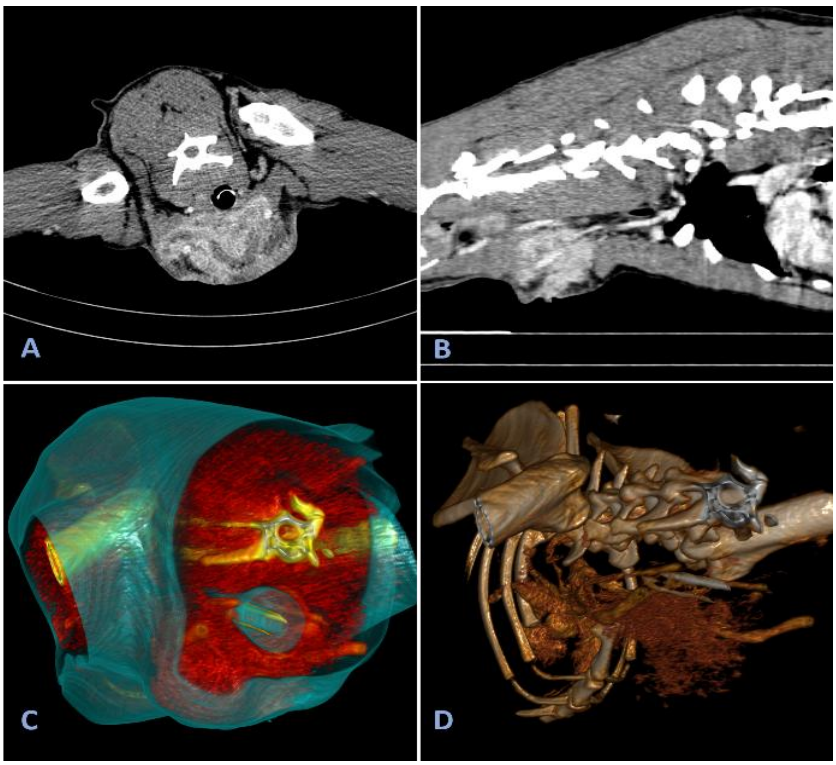

Figure 2. Axial (**A**) and sagittal (**B**) views of the cervical region. Mild to moderate fat stranding and heterogeneous contrast enhancement of the soft tissues in the ventral part of the caudal cervical area. Contrast enhancement emphasizes the left and right jugular veins, which are surrounded by inflamed soft tissue. (**C and D**) Volume-rendered images showing increased contrast enhancement of the inflamed soft tissue.

2.3 Biopsy and Histopathology

Under the same anesthesia, following the CT scan, a biopsy of the mass was sent for histopathological analysis of the lesion. The histological examination of the biopsy specimen showed severe inflammatory and necrotic changes. More than 70% of the dermis and subcutaneous fat tissue were replaced and distended by multiple coalescent pyogranulomas of various sizes, centered on large bacterial colonies embedded in hyalinized, eosinophilic material with a radiating appearance, consistent with the Splendore-Hoeppli phenomenon (immune complexes) (Fig. 3A and B). The pyogranulomatous lesions exhibited central necrosis and contained numerous intact and degenerated neutrophils, along with epithelioid macrophages, multinucleated giant cells, and a moderate number of lymphocytes and plasma cells. The inflammatory infiltrate was associated with fibrosis and was accompanied by multifocal hemorrhage, fibrin deposition, interstitial edema, and a moderate number of siderophages. Inflammation extended into the musculature, where muscle fiber fascicles were separated by interstitial edema, fibrin, and inflammatory cells. A diagnosis of severe, multifocal, pyogranulomatous dermatitis and panniculitis was made, with intralesional bacterial colonies and associated Splendore-Hoeppli material (Fig. 3C and D).

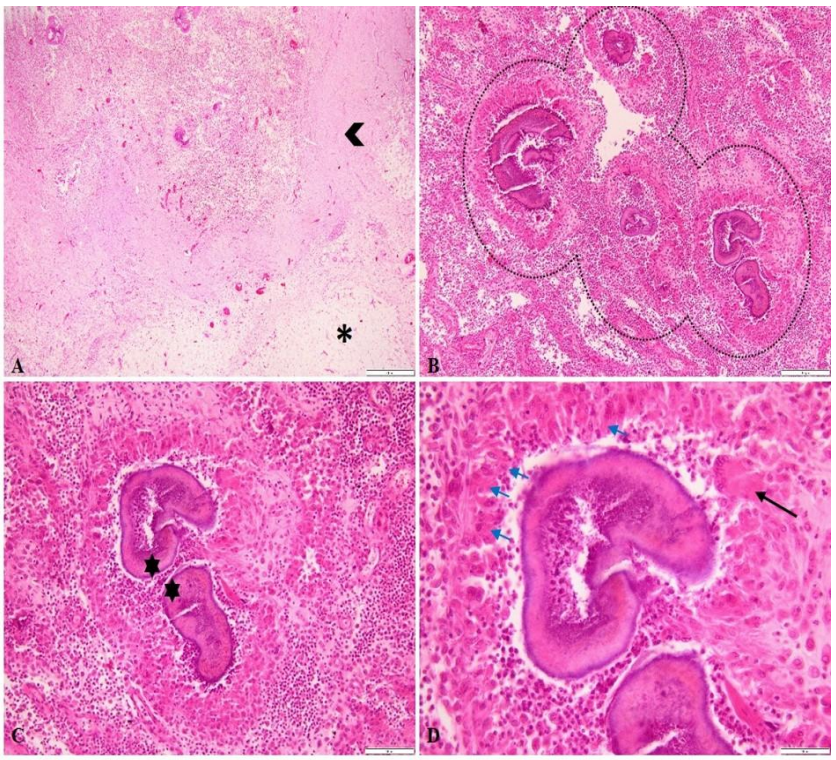

Figure 3. Histological appearance of severe, multifocal, pyogranulomatous dermatitis and panniculitis: (**A**) inflammation in the dermis is accompanied by congestion, interstitial edema, and extensive fibrosis (arrowhead), with infiltrates into the subcutaneous adipose tissue (asterisk), bar=500μm; (**B**) multiple coalescing pyogranulomatous lesions centered on immune complexes, bar=200μm; (**C**) Splendore-Hoeppli phenomenon (stars) observed in the center of the inflammatory infiltrate, bar=100μm; (**D**) bacterial colonies surrounded by an inflammatory infiltrate dominated by macrophages and neutrophils, with a moderate number of epithelioid cells (blue arrows) and multinucleated giant cells (black arrow), bar=20μm; HE stain.

2.4 Anesthetic and Surgery Protocol

After the histopathological examination results ruled out malignancy, the animal was prepared for surgery. The dog was premedicated with methadone (0.2 mg/kg IV) and dexmedetomidine (4 μg/kg IV), and induced with ketamine (3 mg/kg IV) and propofol (30 mg IV given slowly). Following intubation, anesthesia was maintained with isoflurane in oxygen. To ensure a painless procedure, the dog also received a constant rate infusion (CRI) containing lidocaine (1.2 mg/ml) and ketamine (0.1 mg/ml).

The dog was placed in lateral recumbency, and the cervical to abdominal areas were clipped and prepared aseptically. The mass was surgically removed *en bloc* along with the affected segment of the jugular vein and overlying skin. The jugular vein was ligated cranially and caudally beforehand. Afterwards, the

greater omentum was accessed through a midline laparotomy and externalized (Fig. 4A). An omental pedicle flap was prepared from the bursal portion (Fig. 4B) and brought to the cervical region via a subcutaneous tunnel, passing over the thorax at the sternal level (Fig. 4C). The omentum was then double-folded over the exposed tissue (Fig. 4D) and covered with a skin flap (Fig. 4E and F). The abdominal wall was then carefully closed to preserve the vascularization of the omental pedicle flap while reducing the risk of abdominal organ herniation.

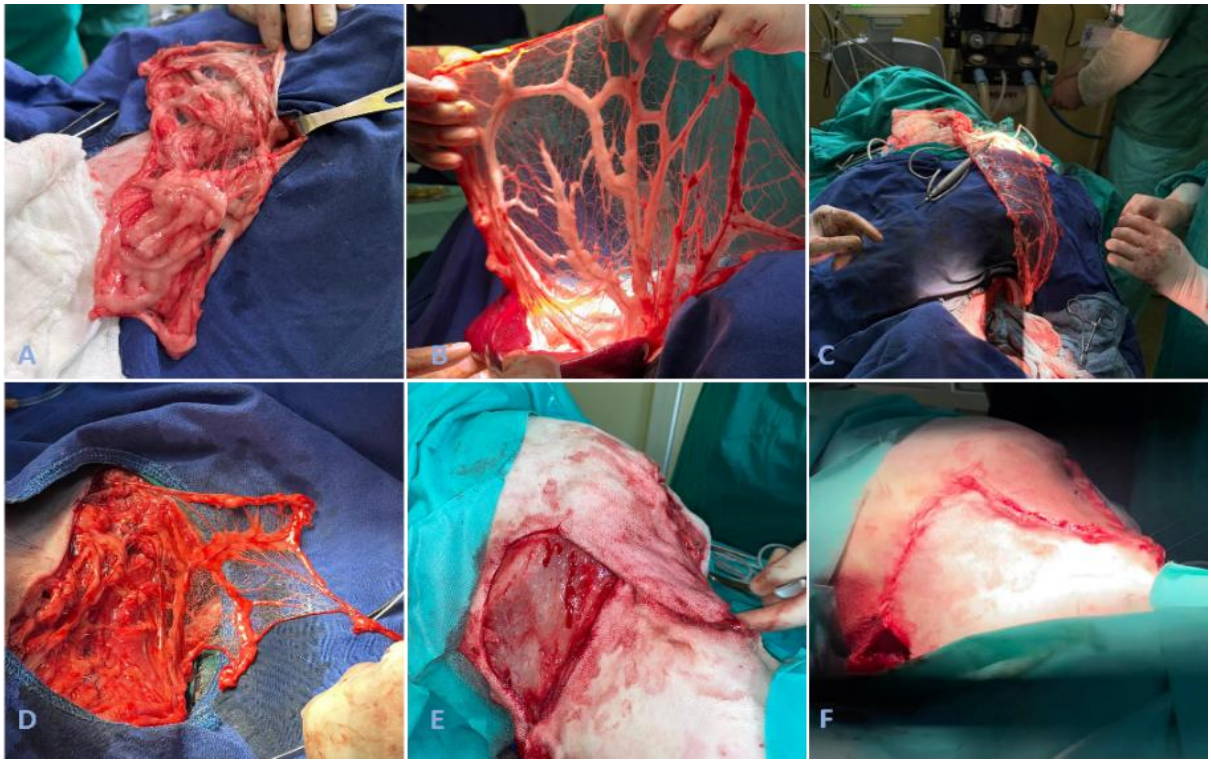

Figure 4. Preparation of the omental pedicle flap after excising the mass: (**A**) Exposure of the bursal part of the greater omentum; (**B**) Dorsal elongation of the bursal part; (**C**) After further elongation, the omental pedicle flap was placed on the surgical drapes to check if enough length was achieved to reach the cervical area; (**D**) Placement of the omental pedicle flap onto the excision site in the cervical area. Note that the flap is double-folded; (**E**) Preparation of a skin flap for covering the omental pedicle flap; (**F**) Final closure of the cervical area after flap transposition.

2.5 Postoperative Treatment Plan

The post-operative protocol focused on pain control and minimizing the dog's activity and stress levels. Medications included paracetamol (10 mg/kg PO), gabapentin (300 mg PO), pentoxifylline (400 mg PO), meloxicam (initial dose 0.2 mg/kg SC followed by 0.1 mg/kg SC), and tramadol (2 mg/kg PO), along with preventive antibiotic therapy with amoxicillin–clavulanic acid. Regular blood tests were scheduled to monitor for systemic changes. A primary focus was the assessment of proper vascularization of the omental pedicle flap, with Doppler ultrasonography scheduled three times a week during the first two weeks, then weekly if the outcome was favorable.

3. Results

3.1 Post-op outcome

Three days post-operatively, multiple hematomas appeared across the entire cervical region (Fig. 5A). A hematological examination revealed inflammatory leukocytosis (WBC 21.0 × 10^9/L) with neutrophilia (16.65 × 10^9/L). One week after surgery, small parts of the sutured tissue began to dehisce, accompanied by purulent fluid (Fig. 5B and C). A microbiological examination identified infections with *S. pseudintermedius* and *Pseudomonas aeruginosa*. As a result, the antibiotic protocol was changed to Amikacin (15 mg/kg IM for 12 days), based on culture and sensitivity results. The wound was cleaned daily with diluted chlorhexidine along with NaCl (0.9%) and rinsed with pure NaCl (0.9%). Over the following month, progressive wound closure with complete epithelialization was observed, and the small dehiscence closed via secondary intention, while the other stitches around the skin flap were safely removed. By two weeks postoperatively, the

hematomas had completely resolved (Fig. 5D). The abdominal incision uneventfully, with no evidence of incisional hernia. The omental pedicle flap remained in situ without complications.

Figure 5. Postoperative appearance of the cervical region (**A, B and C**) and abdomen (**D**): (**A**) Three days postoperative, minor hematomas are present, extending to the incision site on the abdomen; (**B**) One week postoperative: the cervical region has been reconstructed using a skin flap; (**C**) Two weeks postoperative: caudally, a small portion of the suture line shows early signs of dehiscence with purulent discharge; (**D**) Abdomen two weeks postoperative: note the resolution of the postoperative hematomas.

Moreover, periodic follow-up ultrasonography with Doppler was performed to confirm vascularization of the omental pedicle flap (Fig. 6). Throughout the recovery period, the pedicle flap maintained healthy blood flow and showed no significant complications, except for a small seroma, which was drained under ultrasound guidance.

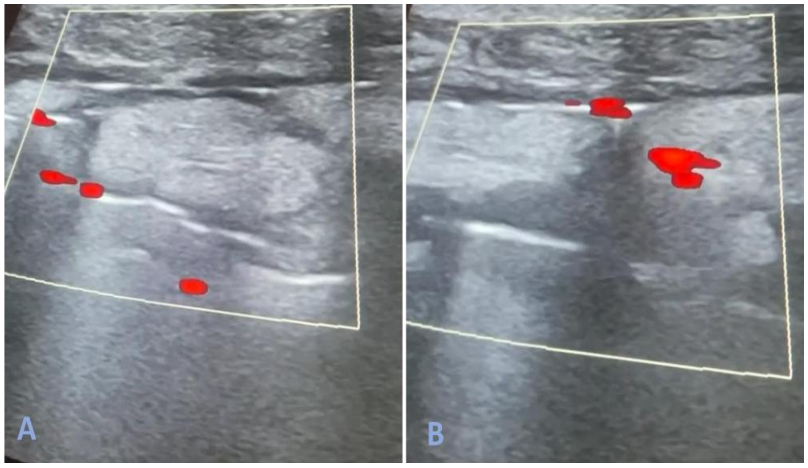

Figure 6. Power Doppler – mild panniculitis and fat presence from the omentum tissue positioned during surgery at the level of the jugular vein, with normal Power Doppler flow at the same level.

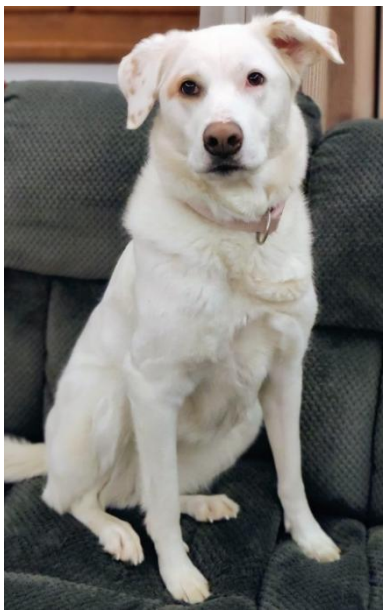

Figure 7. The clinical appearance of the dog eight months post-surgery.

4. Discussion

The following case involved severe, rapidly progressive cervical panniculitis requiring surgical excision, with additional support from an omental pedicle flap. While SNP can sometimes be managed conservatively, NSNP may be more challenging due to its potential for quick expansion, ongoing dispersion, and tendency to produce painful nodules [4]. These nodules may become necrotic and ulcerate or develop fistulas, discharging serosanguineous or purulent fluid, which is typical of lesions caused by infectious agents [1,2].

The literature often describes NSNP spreading to the dermis, subcutis, and sometimes musculature—especially in chronic infectious processes [4]. Neuber et al. (2011) stated that these lesions can extend deeper and into adjacent muscles, and another study highlighted the importance of removing as much abnormal tissue as possible, a procedure that often leads to significant loss of subcutaneous fat [3,16]. The loss of dermal tissue from large mass removals, whether the lesion is benign or malignant, challenges the surgeon—particularly in the sternal region—and requires preparation of a left omocervical flap to cover the defect while reducing tension [17].

The dog presented with severe, multifocal pyogranulomatous dermatitis and panniculitis, with bacterial involvement within the lesions. The nodules grew rapidly and involved a large part of the right jugular vein. Therefore, the surgeon decided to perform a wide excision of the mass along with removal of the right jugular vein. Previous studies have shown that dogs can survive with only one jugular vein, even in severe cases [18,19].

To support tissue regeneration, an omental pedicle flap was routed through a subcutaneous tunnel to the cervical region and sutured onto the defect. The greater omentum is not merely a passive fat deposit but an immunologically active organ; it contains milky spots and FALCs, which are rich in macrophages, B- and T-cells, and dendritic cells, thereby functioning as an immune filter and site of immune response [9]. In addition, it promotes angiogenesis through VEGF-mediated mechanisms, thereby contributing to tissue regeneration [7].

A post-surgical infection involving *P. aeruginosa* and *S. pseudintermedius* slowed the healing process and caused a minor dehiscence of the caudal part of the skin flap. Antimicrobial therapy with an antibiotic based on culture and sensitivity was crucial for treating the infection; however, in this case, the potential supportive role of the omental pedicle flap in managing the local infection cannot be excluded [5,7,9].

The initial infection with *S. pseudintermedius* was deemed the primary suspected trigger. Nonetheless, given the complex pathophysiology of panniculitis, other etiopathogenic factors cannot be entirely excluded. Although mycobacterial involvement seems less likely, it cannot be definitively ruled out, especially without a Ziehl–Neelsen stain [16].

However, the histological features observed, including pyogranulomatous inflammation and Splendore–Hoeppli material, along with the results of the initial microbiological examination, align with pathogens described in the literature and strongly suggest infectious panniculitis caused by *S. pseudintermedius* [3].

Periodic follow-up ultrasonography with color Doppler was performed to evaluate the vascular integrity of the omental pedicle flap, confirming adequate perfusion. Doppler sonography has been proven to be a safe, non-invasive technique for assessing tissue perfusion and vascular patency in soft tissues [20,21]. Eight months after surgery, the dog exhibited no signs of new nodules or complications related to omentopexy or resection of the right jugular vein (Fig. 7). The omental pedicle flap remained in place.

5. Conclusion

The case report describes a dog suffering from severe and severe, rapidly progressing infectious cervical panniculitis near the right jugular vein that required surgical treatment. Conservative management showed no results, and new masses appeared adjacent to the original one. After a CT scan, which revealed the size of the masses encasing the jugular vein as well, the decision for *en bloc* resection, including the jugular, was justified. An omental pedicle flap was placed to enhance perfusion, support local immune regulation, and promote tissue repair. Serial Doppler ultrasonography allowed non-invasive monitoring of the vascularization of the omental pedicle flap throughout the postoperative period. The dog showed no signs of recurrence or procedure-related complications at an eight-month follow-up.

Author Contributions: Conceptualization, T.A. and L.B.; methodology, L.B. I.V. and T.A.; investigation, R.M. and R.P.; data curation, T.A.; writing—original draft preparation, T.A.; writing—review and editing, I.V.; visualization, T.A., R.M. and R.P.; supervision, L.B., A.T. and L.O.; All authors have read and agreed to the published version of the manuscript".

Funding: This research received no external funding

Institutional Review Board Statement: Ethical review and approval were waived for this study, due to its nature as a retrospective clinical case report describing standard diagnostic and therapeutic procedures. No experimental protocols were involved, and informed owner consent was obtained for treatment and publication of anonymized data.

Data Availability Statement: The data supporting the findings of this study are available within the article. No additional datasets were generated or deposited in a publicly available repository.

Acknowledgments: The author gratefully acknowledges the support of the staff of the Surgery and Anesthesiology Departments, as well as the teams from the Emergency, Radiology, Microbiology, and Pathology Departments. This work would not have been possible without their interdisciplinary collaboration.

Conflicts of Interest: The authors declare no conflict of interest.

References

1. O'Kell, A.L.; Inteeworn, N.; Diaz, S.F.; Saunders, G.K.; Panciera, D.L. Canine sterile nodular panniculitis: A retrospective study of 14 cases. *J Vet Intern Med* **2010**, *24*, 278–284.
2. Contreary, C.L.; Outerbridge, C.A.; Affolter, V.K.; Kass, P.H.; White, S.D. Canine sterile nodular panniculitis: A retrospective study of 39 dogs. *Vet Dermatol* **2015**, *26*.
3. Neuber, A. Panniculitis in dogs and cats. *Companion Anim* **2011**, *16*, 27–30.
4. Gross, T.L.; Ihrke, P.J.; Walder, E.J.; Affolter, V.K. Skin Diseases of the dog and cat: Clinical and Histopathologic Diagnosis.; 2nd ed.; Blackwell Publishing: Ames, IA, USA, **2005**.
5. Huyghe, S.; De Rooster, H.; Doom, M.; Van den Broeck, W. The microscopic structure of the omentum in healthy dogs: The mystery unraveled. *Anat Histol Embryol* **2016**, *45*.
6. Karl, S.; Dupré, G. Omentalisation of the head in cats: A cadaver study. *J. Feline Med. Surg.* **2012**, *14*, 295–298.
7. Morawska-Kozłowska, M.; Wilkosz, A.; Zhalniarovich, Y. The omentum—A forgotten structure in veterinary surgery in small animals' surgery. *Animals* **2024**, *14*, 1848.
8. Ablassmaier, T.; Zăvoi, A.; Gog-Bogdan, S.; Bel, L.; Oana, L. The use of an L-shaped omental pedicle flap to facilitate healing in a cat with a dehiscent surgical wound after a tibial fracture repair. *Bull UASVM Vet Med* **2025**, *82*, 10–16.
9. Liu, M.; Silva-Sanchez, A.; Randall, T.D.; Meza-Perez, S. Specialized immune responses in the peritoneal cavity and omentum. *J Leukoc Biol* **2021**, *109*, 717–729.
10. Zietzschmann, O. Das Mesogastrium dorsale des Hundes mit einer schematischen Darstellung seiner Blätter. *Morph Jahrb* **1939**, *83*, 327–358.
11. Doom, M.; De Rooster, H.; Van Bergen, T.; Gielen, I.; Kromhout, K.; Simoens, P.; Cornillie, P. Morphology of the canine omentum part 1: Arterial landmarks that define the omentum. *Anat Histol Embryol* **2014**, *45*, 37–43.
12. Ablassmaier, T.A.; Bel, L.V.; Oana, L.I. Evaluation of the morphological and vascular structure of the feline greater omentum. *Rev Rom Med Vet* **2024**, *34*, 54–58.

13. Grävenstein, H. Über die Arterien des grossen Netzes beim Hunde. *Morph Jahrb* **1938**, *82*, 1–26.
14. Jurkiewicz, M.J.; Arnold, P.G. The omentum: An account of its use in the reconstruction of the chest wall. *Ann Surg* **1977**, 548–554.
15. Sato, R.; Kim, S.; Okada, S.; Ikedo, T.; Satoh, H.; Steiner, A. Case report: Abdominal hernia repair using a surgical wire and an autologous omental graft in a Japanese Black calf. *Front Vet Sci* **2023**, *10*, 1119034.
16. Malik, R.; Shaw, S.E.; Griffin, C.; Stanley, B.; Burrows, A.K.; Bryden, S.L.; Titmarsh, J.; Stutsel, M.-J.; Carter, S.-A.; Warner, A.; et al. Infections of the subcutis and skin of dogs caused by rapidly growing mycobacteria. *J Small Anim Pract* **2004**, *45*, 485–494.
17. Tobias, K.M.; Johnston, S.A. Veterinary Surgery: Small Animal; 2nd ed.; Elsevier: St. Louis, MO, USA, **2017**.
18. Holsworth, I.G.; Kyles, A.E.; Bailiff, N.L.; Hopper, K.; Long, C.; Ilkiw, J.E. Use of a jugular vein autograft for reconstruction of the cranial vena cava in a dog with invasive thymoma and cranial vena cava syndrome. *J Am Vet Med Assoc* **2004**, *225*, 1920–1922.
19. Salmeri, K.R.; Bella, J.R.; Ackermann, N.; Homer, B. Unilateral congenital aneurysm of the jugular, linguofacial, and maxillary veins in a dog. *J Am Vet Med Assoc* **1991**, *198*, 101–103.
20. Reetz, J.A.; Seiler, G.; Mayhew, P.D.; Holt, D.E. Ultrasonographic and Color-Flow Doppler Ultrasonographic assessment of direct cutaneous arteries used for axial pattern skin flaps in dogs. *J Am Vet Med Assoc* **2006**, *228*, 1361–1365.
21. Van Wingerden, J.J.; Collins, J.M.P.; Coret, E.H.; Schröder, P.J.J. Early monitoring of the viability of the buried intrathoracic omental flap: A feasibility study. *Ann Thorac Surg* **2010**, *90*, 1332–1336.

CVJ CLUJ VETERINARY JOURNAL

Case report

Septic Osteitis and Osseous Sequestration of the Distal Phalanx Associated with a Coronary Band Lesion in a Draft Horse: Clinical, Radiographic and Surgical Findings

Constantin Lazăr [1], Gheorghe Solcan [1], Vasile Vulpe [1], Iulia Straton [1*], and Iulian Mihăilă [1]

[1] Department of Clinics, Faculty of Veterinary Medicine, "Ion Ionescu de la Brad" University of Life Sciences, Iași, Romania; margivet_srl@yahoo.com; iulian.mihaila@iuls.ro; iulia.straton@iuls.ro; vasile.vulpe@iuls.ro; gsolcan@yahoo.com;
* Correspondence: iulia.straton@iuls.ro;

Abstract: Inflammatory disorders of the distal phalanx (P3) associated with lesions of the coronary region of the hoof may involve reactive periosteal bone proliferation and focal osseous separation. This report describes a case of focal inflammatory osteal pathology of P3 in a draft horse presenting with severe forelimb lameness and a localized lesion of the coronary region. Radiographic examination revealed a longitudinal radiopaque formation with irregular margins on the dorsal aspect of P3, associated with a corresponding radiolucent area and a tract containing fluid and gas extending toward the coronary region. Surgical intervention was performed under general anesthesia. A progressive distal hoof wall resection was carried out with preservation of the coronary region, followed by evacuation of purulent material and curettage of the affected bone. A detached lamellar bone fragment consistent with focal osseous sequestration was removed, and debridement was continued until macroscopically viable bone was obtained. The excised tissues were submitted for histopathological evaluation. Hematoxylin–eosin-stained sections demonstrated lamellar bone with periosteal thickening and adjacent fibrous connective tissue showing hemorrhagic infiltration and a mixed inflammatory infiltrate composed predominantly of neutrophils and macrophages. No histological evidence of neoplastic proliferation was identified. The findings were consistent with periostitis and osteitis associated with reactive exophytic bone formation and focal osseous sequestration. This case highlights the diagnostic value of radiography and the importance of complete surgical debridement in inflammatory conditions of the distal phalanx associated with lesions of the coronary region.

Keywords: distal phalanx; equine; coronary region; osseous sequestration; reactive exostosis; periostitis; osteitis; hoof surgery; draft horse

Received: 06.03.2026

Accepted: 20.03.2026

Published: 09.04.2026

DOI:10.52331/v31i2m363

1. Introduction

Osseous sequestration is defined as the separation of a segment of necrotic bone from adjacent viable osseous tissue as a consequence of vascular compromise, septic inflammation, or direct traumatic insult [1]. Interruption of the intraosseous blood supply results in cortical necrosis, followed by progressive demarcation of the devitalized fragment from surrounding healthy bone. In the horse, sequestrum formation is a recognized sequela of septic and traumatic osteal pathology, and surgical removal of the necrotic fragment is frequently required to achieve definitive resolution [2].

Within the equine digit, the anatomical configuration of the hoof capsule—characterized by its rigid, non-distensible keratinized wall and the close apposition of the dermal lamellae to the distal phalanx (P3)—predisposes to propagation of infectious processes to the underlying bone when drainage is inadequate or delayed [3]. Subsolar abscessation and penetrating solar or coronary injuries may extend beyond the epidermal and dermal layers, leading to septic involvement of deeper structures, including the distal phalanx.

Septic conditions affecting the hoof complex may culminate in septic osteitis or osteomyelitis of P3, radiographically manifested by focal osteolysis, cortical irregularity,

and, in chronic cases, periosteal reaction and sequestrum formation [4]. The pathophysiological progression involves bacterial contamination, inflammatory osteolysis, compromise of local perfusion, and eventual necrosis of cortical bone.

Septic osteitis of the distal phalanx is a well-documented clinical entity in both adult horses and foals and is typically associated with severe weight-bearing lameness, radiographic evidence of bone lysis, and, in advanced stages, separation of necrotic osseous fragments [5]. When medical management and drainage are insufficient, surgical debridement and curettage of devitalized bone are considered essential to eliminate the septic focus and restore functional integrity of the digit.

The present report describes a case of focal septic osteal pathology of the distal phalanx associated with osseous sequestration in a mature draft horse, detailing the clinical presentation, radiographic findings, surgical management, and histopathological confirmation, and discussing the pathophysiological mechanisms implicated in sequestrum formation within the equine hoof.

2. Materials and Methods

A 6-year-old intact male draft horse (Greu de Bucovina type) was presented for evaluation of severe lameness of the left hindlimb. A complete general and orthopedic clinical examination was performed, and the degree of lameness was assessed using a standard lameness grading scale. The distal region of the affected limb was inspected and palpated, and the coronary region was clipped to allow direct evaluation of the skin and underlying structures.

Standard radiographic examination of the distal segment of the affected forelimb was performed using appropriate projections to assess the distal phalanx and adjacent structures.

The horse was placed under general anesthesia and positioned in lateral recumbency. A progressive dorsal hoof wall resection was performed in a distal direction while preserving the coronary region. The area corresponding to the radiographically identified lesion was approached through controlled removal of the hoof wall. After accessing the pathological focus, the contents were evacuated and curettage of the affected region of the distal phalanx was performed. Curettage was continued until all macroscopically altered tissue was removed, and intraoperative assessment of osseous vitality was based on the gross appearance and consistency of the bone.

At the end of the procedure, a topical cicatrizing ointment was applied locally, followed by placement of a compressive bandage. Postoperative management included periodic bandage changes.

The retrieved osseous fragment and associated soft tissue samples were submitted for histopathological examination. The specimens were processed using standard laboratory techniques, and representative serial sections were stained with hematoxylin and eosin for microscopic evaluation.

3. Results

3.1. General Clinical Examination

A 6-year-old intact male draft horse (Greu de Bucovina type), used for forestry traction work in mountainous terrain, was presented on March 14, 2025, for acute-onset lameness of the left hindlimb. According to the anamnesis, the lameness developed suddenly immediately after returning from timber extraction activities. No obvious wound had been identified initially at the hoof level, most likely due to the abundant hair covering the coronary region. Conservative treatment administered for approximately two weeks prior to referral (local cooling and topical anti-inflammatory therapy) resulted in no improvement and progressive worsening of clinical signs.

Orthopedic examination revealed severe lameness of the left hindlimb, graded 4.5–5/5 on the AAEP lameness scale. The horse demonstrated minimal weight-bearing on the affected limb and exhibited a marked pain response during locomotion, particularly when the limb was loaded during the stance phase. At rest, the animal frequently attempted to unload the limb by intermittently lifting the hoof or shifting weight to the contralateral hindlimb.

Following clipping of the hair at the distal portion of the limb to allow better visualization of the integument, a well-demarcated hyperemic area was identified at the dorsolateral aspect of the coronary band (Fig. 1a). The affected region presented mild, diffuse oedema and was markedly painful upon palpation, eliciting a clear withdrawal response. Local tissue temperature appeared mildly increased compared with adjacent areas, suggesting an active inflammatory process. No fluctuation suggestive of a mature abscess cavity was detected on digital palpation, and careful inspection did not reveal spontaneous drainage, purulent exudate, or a visible fistulous tract. The coronary surface remained relatively dry and intact, with no obvious disruption of the epidermal continuity.

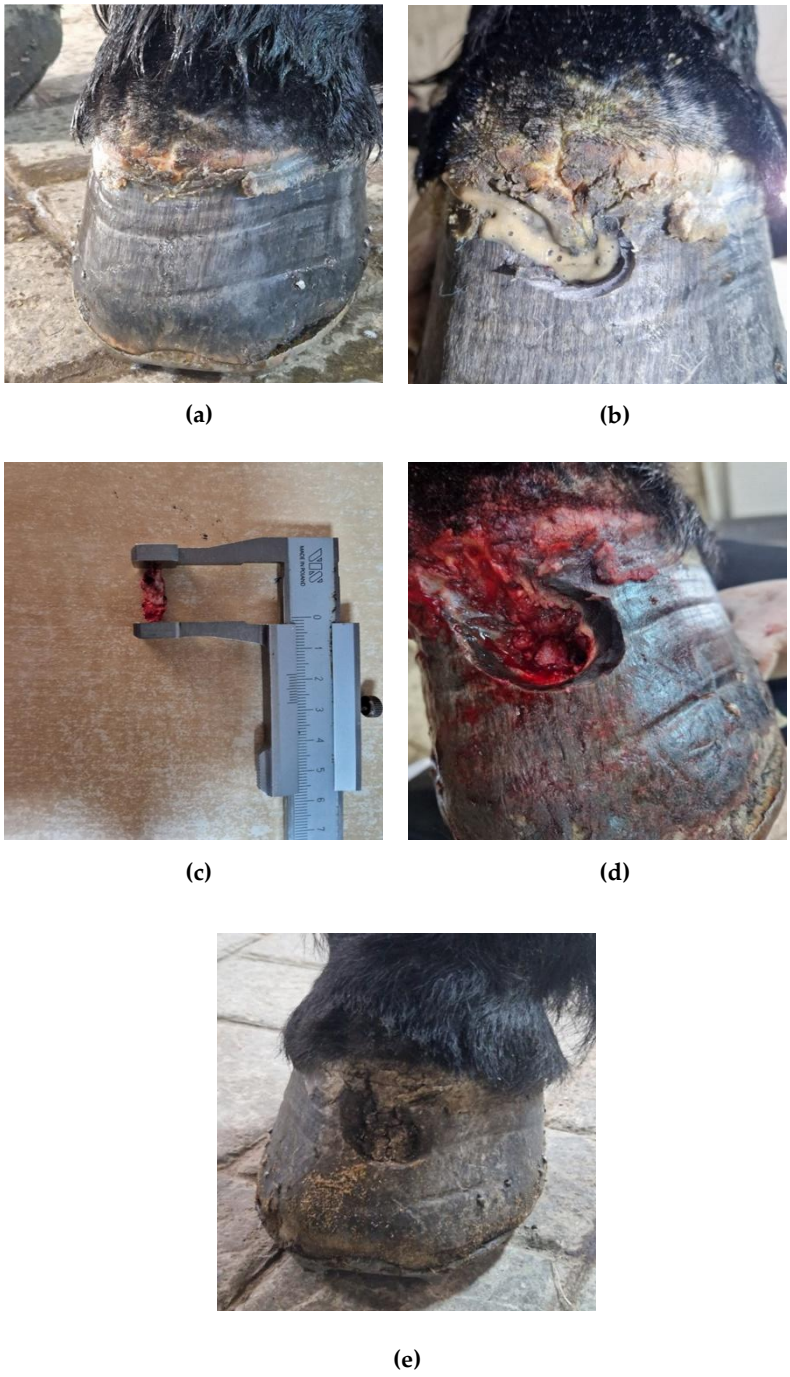

Figure 1. (**a)** Preoperative clinical aspect of the dorsolateral coronary band of the left hindlimb after clipping, showing localized hyperemia and mild oedema; **(b**) Intraoperative view of the subparietal cavity following dorsal hoof wall resection and evacuation of pressurized purulent material; (**c**) Macroscopic appearance of the extracted osseous fragment; (**d)** Dorsal cortical defect of the third phalanx after complete curettage, demonstrating viable bleeding bone; (**e**) Cicatrized lesion located adjacent to the radiographic site at 27 days post-procedure.

Gross inspection of the dorsal hoof wall did not reveal visible cracks, deformities, or structural defects. The hoof capsule maintained a normal conformation and there were no evident defects or discoloration that could immediately suggest an external penetration point or chronic wall pathology. Application of hoof testers elicited a pronounced pain response localized to the dorsal aspect of the hoof capsule. The most intense reaction occurred in the region topographically corresponding to the coronary lesion observed during the clinical inspection (Fig. 1a). Compression in this area provoked a strong withdrawal reflex and behavioral signs of discomfort, indicating increased sensitivity of the underlying structures. In contrast, application of the hoof testers to the lateral quarters, heel region, and frog elicited either a mild or absent response.

This localized pain pattern suggested the presence of a focal pathological process involving the dorsal hoof wall and/or the adjacent subsolar or subcoronary structures.

The clinical appearance of the cicatrized lesion observed at 27 days post-procedure indicates a favorable healing process. The formation of a stable scar adjacent to the radiographic site suggests that the local tissue response progressed normally, with resolution of the initial inflammatory signs and gradual restoration of tissue integrity. Such evolution is consistent with the expected healing pattern following surgical or therapeutic intervention in the affected region. The absence of visible complications, such as excessive swelling, discharge, or tissue necrosis, further supports the effectiveness of the applied treatment and the satisfactory recovery of the area.

3.2 Radiographic Examination

Radiographic examination of the left hindlimb was performed in a latero-medial projection, with careful positioning to optimize visualization of the third phalanx and its relationship to the dorsal hoof wall. The images revealed a distinct longitudinal radiopaque structure located on the dorsal surface of the third phalanx, extending proximodistally along the anterior cortical margin. This structure exhibited irregular, poorly defined margins and heterogeneous opacity, features suggestive of reactive or devitalized osseous tissue rather than organized periosteal proliferation.

Beneath this radiopaque formation, a focal radiolucent area was identified within the dorsal aspect of the third phalanx. The radiolucency was relatively well delineated but irregular in contour, consistent with localized osteolysis. The dorsal cortical bone appeared thinned and focally interrupted, with loss of the normal continuous radiopaque cortical line. The adjacent trabecular bone demonstrated reduced radiodensity and partial disruption of its normal architecture, indicating inflammatory bone rarefaction and remodeling.

In addition, a radiolucent tract extending from the dorsal cortical lesion toward the coronary band was identified. This tract contained discrete radiolucent foci consistent with intralesional gas within the soft tissues and subparietal space, supporting the presence of an active septic process. The orientation of this channel indicated communication between the osseous lesion and the coronary region, compatible with a fistulous tract or drainage pathway through the subparietal tissues. No complete fracture lines, articular surface involvement, or displacement of the distal phalanx were observed, and the distal interphalangeal joint space appeared preserved.

Overall, the radiographic examination revealed changes consistent with a focal inflammatory osteitic process affecting the dorsal surface of the third phalanx (P3). The most prominent findings included focal cortical disruption of the dorsal margin of the distal phalanx accompanied by a well-defined area of localized osteolysis. The lytic region appeared irregular and slightly radiolucent relative to the surrounding cortical bone, suggesting active bone resorption associated with inflammation or infection.

Additionally, a radiolucent tract-like area was visible extending from the dorsal margin of the distal phalanx toward the inner surface of the hoof wall. This radiographic feature was compatible with a subparietal septic cavity located between the dorsal hoof wall and the underlying structures. The presence of this radiolucent pathway suggested a possible drainage route or communication channel between the infected bone surface and the surrounding soft tissues. The cavity appeared to communicate proximally with the region of the coronary band, corresponding topographically with the hyperemic and painful area observed during the clinical examination.

Taken together, these findings were highly suggestive of a localized septic process involving the dorsal aspect of the distal phalanx, characterized by focal osteitis, cortical bone destruction, and secondary reactive bone formation. The radiographic appearance also indicated communication between the osseous lesion and the subcoronary soft tissues, supporting the hypothesis of a septic focus originating from or extending toward the coronary band (Fig. 2a and b). These combined clinical and radiographic findings highlight the importance of early diagnostic imaging in identifying septic involvement of the distal phalanx and guiding appropriate therapeutic management.

3.3 Intraoperative Findings and Surgical Management

Surgical intervention was performed under general anesthesia, with the horse positioned in lateral recumbency. The affected limb was carefully prepared and aseptically draped. Particular attention was given to precise identification and preservation of the coronary band in order to prevent secondary disturbances in horn growth. A progressive distal resection of the dorsal hoof wall was carried out in a controlled, stepwise manner, allowing continuous assessment of the underlying corium and limiting tissue removal to the affected area.

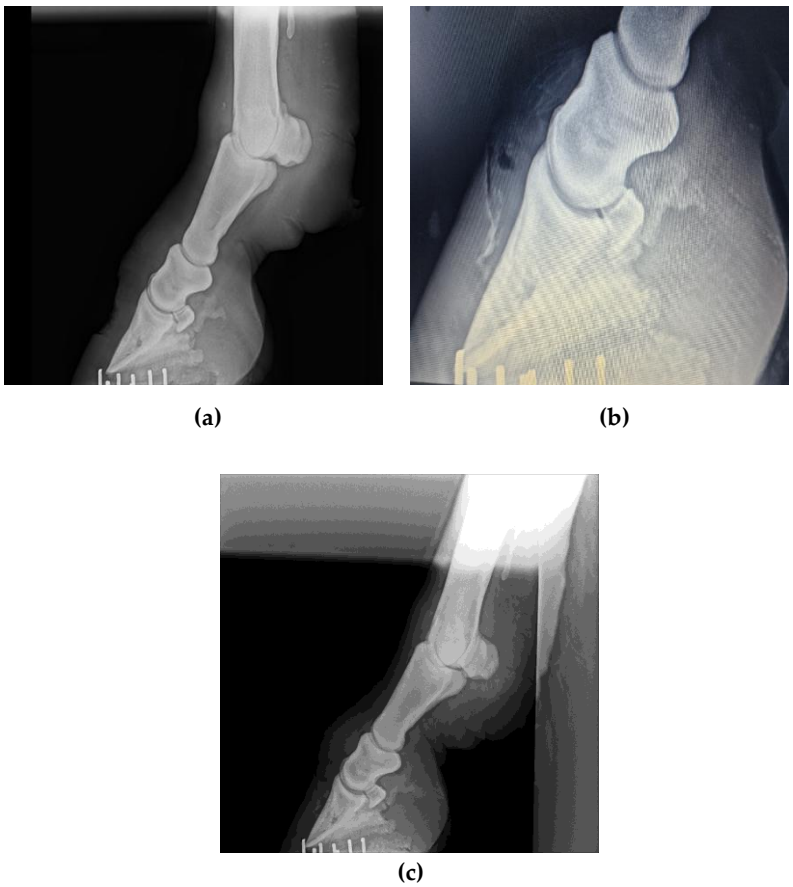

Figure 2. Preoperative latero-medial radiograph of the left hindlimb showing (**a**) dorsal radiopaque lesion of the third phalanx with associated osteolysis; (**b**) Gas-containing tract toward the coronary band; (**c**) Latero-medial radiograph obtained 27 days postoperatively showing restoration of the dorsal cortical margin of the third phalanx and complete disappearance of the previously observed radiolucent lesion.

The purulent material had accumulated within a confined subparietal compartment located between the dorsal hoof wall and the underlying corial tissues. This space had been effectively sealed by the rigid hoof capsule, preventing spontaneous drainage and allowing progressive accumulation of exudate. As a result, substantial internal pressure had developed within the lesion prior to surgical decompression.

The pressurized evacuation of purulent exudate, together with the presence of intralesional gas, strongly confirmed the existence of an active septic process within an anatomically inextensible compartment. Such conditions are characteristic of deep subparietal abscessation, where the rigid structure of the hoof capsule limits expansion and promotes the buildup of pressure, thereby exacerbating pain and facilitating the extension of infection toward adjacent soft tissues and osseous structures. The sudden decompression achieved through dorsal wall resection therefore represented both a diagnostic confirmation of the septic focus and a critical therapeutic step in relieving intracompartimental pressure and enabling thorough drainage and debridement of the infected cavity.

Following complete evacuation of the purulent content, a well-defined subparietal cavity became clearly visible within the dorsal aspect of the hoof capsule (Fig. 1b). The cavity was located between the inner

surface of the dorsal hoof wall and the underlying corial tissues, extending proximally toward the coronary band. Its margins were relatively distinct, indicating the presence of a localized pathological compartment formed as the septic process progressed. Careful inspection revealed that this cavity communicated directly with the dorsal cortical surface of the third phalanx (P3), confirming the radiographic suspicion of osseous involvement.

The internal surface of the cavity was lined by markedly inflamed soft tissue characterized by hyperemia and friable inflammatory granulation tissue. In several areas, partially organized necrotic debris adhered to the surrounding tissues and the exposed bone surface. The dorsal cortex of the distal phalanx was directly visible through the surgical window and presented evident pathological alterations, including focal cortical irregularity, superficial bone erosion, and localized loss of cortical continuity. These macroscopic findings were consistent with an inflammatory osteitic lesion affecting the dorsal margin of P3.

Thorough surgical debridement was subsequently performed. Curettage of the affected osseous surface was carried out using sharp bone curettes in order to remove all infected and devitalized material. Necrotic bone fragments, inflammatory granulation tissue, fibrinous deposits, and other devitalized debris were meticulously excised until a clean and stable bone surface was obtained. The curettage was continued carefully until only firm, viable bone remained, characterized by a more uniform appearance and resistance to the curette.

During this process, a free osseous fragment measuring approximately 1.83 cm in length was identified within the cavity and subsequently extracted (Fig. 1c). The fragment was irregularly shaped, with rough and heterogeneous surfaces and poorly defined margins. It was not firmly attached to the surrounding bone structures and could be removed without resistance, suggesting that it had previously detached from the dorsal cortical surface of the third phalanx. Macroscopic examination indicated that the fragment was composed of devitalized or reactive bone. Based on its appearance and location, it was considered compatible either with a sequestrum formed secondary to focal septic osteitis or with a reactive exophytic bone fragment that had subsequently become detached during the progression of the inflammatory process.

The removal of this fragment was considered a critical step in the surgical management of the lesion, as retained sequestra or devitalized bone can act as persistent foci of infection and significantly impair the resolution of septic processes within the hoof. Necrotic or poorly vascularized bone fragments provide an ideal substrate for bacterial colonization, protecting microorganisms from both host immune responses and antimicrobial therapy. Consequently, failure to remove such fragments may lead to chronic infection, delayed healing, or recurrence of clinical signs.

Complete elimination of the fragment, combined with thorough curettage of the surrounding tissues, allowed effective decontamination of the cavity and facilitated the establishment of a viable environment for subsequent healing. Careful curettage ensured the removal of infected and devitalized tissue, while preserving as much healthy bone and surrounding structures as possible. This approach promotes the formation of healthy granulation tissue and supports progressive tissue regeneration within the affected area.

Furthermore, the removal of the sequestrum reduces mechanical irritation and prevents continued inflammatory stimulation of the adjacent tissues. By eliminating the primary source of infection and restoring adequate drainage and aeration of the cavity, the procedure enhances the effectiveness of postoperative treatments and significantly improves the prognosis. In cases involving the distal phalanx and hoof structures, such surgical debridement is particularly important, given the limited vascular supply and the enclosed anatomical environment that can favor the persistence of septic material.

Curettage was continued until all visibly altered bone tissue had been eliminated and a uniformly bleeding cortical surface was obtained. The presence of punctate hemorrhage from the bone surface was considered an important indicator of adequate debridement and tissue viability, suggesting that the remaining bone retained an intact vascular supply. Achieving this endpoint is essential in the surgical management of septic osseous lesions, as it indicates that devitalized or infected bone has been successfully removed.

At this stage, contact between the curette and the remaining bone produced a clear, resonant sound, consistent with healthy and structurally stable osseous tissue (Fig. 1d). This auditory feedback is frequently used intraoperatively as an additional indicator that the curettage has reached viable cortical bone, distinguishing it from the dull sound typically associated with necrotic or weakened bone.

Careful inspection of the surgical cavity confirmed the absence of residual purulent material, sinus tracts, or necrotic bone fragments. The margins of the defect appeared regular and clean, with no evidence of further cortical instability or ongoing bone destruction. Ensuring complete removal of infected and devitalized tissues at this stage is crucial to minimize the risk of persistent infection and to create favorable conditions for subsequent healing, granulation tissue formation, and gradual restoration of the affected structures.

Following extensive lavage of the surgical cavity with sterile isotonic solution, a topical antimicrobial and cicatrizing ointment was applied to the exposed corial and osseous surfaces. A sterile compressive bandage was placed to protect the surgical site and to support controlled healing. Postoperatively, systemic anti-inflammatory therapy was administered to control pain and inflammation, and broad-spectrum antimicrobial therapy was instituted to address the septic component of the lesion. The bandage was scheduled for regular changes, with local cleansing and reapplication of topical medication. Strict environmental hygiene and limited activity were recommended during the initial healing phase to prevent contamination and mechanical stress on the regenerating hoof wall.

3.4 Histopathological examination

Histopathological examination of the extracted osseous fragment was performed on serial sections stained with Hematoxylin–Eosin. At low magnification (4× objective), the specimen consisted predominantly of mature lamellar bone with largely preserved cortical architecture, although focal surface irregularities were evident (Fig. 3a). The periosteum was markedly thickened and expanded by oedema, with partial loss of the normal distinction between the outer fibrous and inner osteogenic layers. In certain areas, the external cortical surface appeared uneven, consistent with reactive bone remodeling in an inflammatory context.

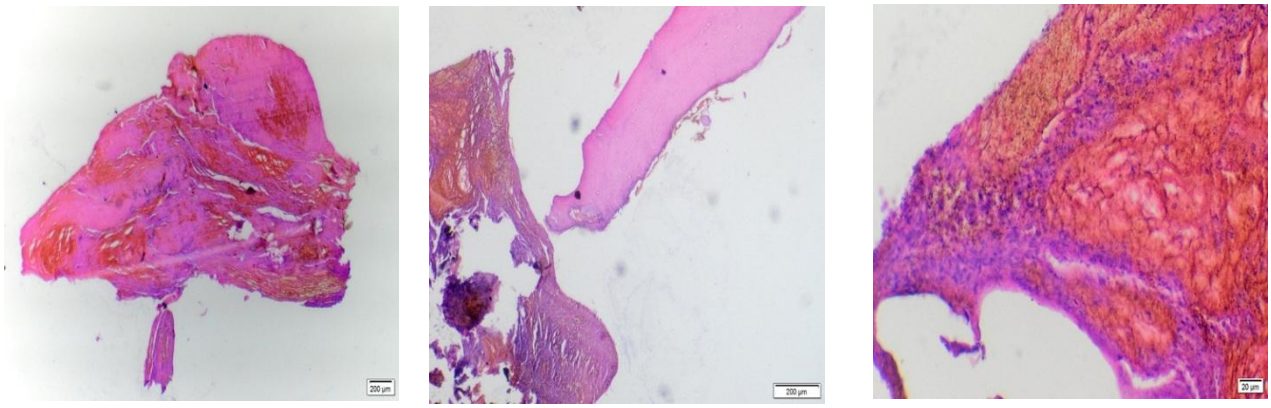

(a) **(b)** **(c)**

Figure 3. Representative histological section showing (**a**) Mature lamellar bone with marked periosteal thickening; (**b**) Periosteal oedema, vascular congestion, and mixed inflammatory infiltrate; (**c**) Dense neutrophilic and macrophagic inflammatory infiltration without evidence of neoplastic changes

At intermediate magnification (10× objective), the periosteum appeared markedly thickened due to pronounced interstitial oedema and cellular infiltration. The periosteal connective tissue was expanded by clear spaces separating collagen bundles, consistent with fluid accumulation within the extracellular matrix. Within this edematous stroma, a mixed inflammatory infiltrate was evident, composed predominantly of neutrophils and macrophages, with occasional scattered lymphocytes (Fig. 3b). The neutrophils were often arranged in small aggregates or diffusely distributed throughout the periosteal tissue, indicating an active acute inflammatory component, while the presence of macrophages suggested ongoing phagocytosis and tissue cleanup associated with a subacute inflammatory stage.

The vascular component of the periosteum and adjacent connective tissue was markedly altered. Numerous small and medium-sized blood vessels were dilated and congested with erythrocytes, reflecting vascular hyperemia and increased local blood flow typical of inflammatory reactions. Endothelial cells lining these vessels appeared mildly swollen, and in some areas the perivascular space was expanded by inflammatory cells and oedema fluid.

Multifocal areas of recent hemorrhage were also observed within the periosteal tissue. These consisted of small accumulations of extravasated erythrocytes dispersed within the connective stroma, likely resulting from increased vascular permeability and minor vascular damage associated with the inflammatory process. The hemorrhagic foci were generally limited in extent and did not show evidence of significant organization.

In addition to the previously described inflammatory alterations, a mild fibroblastic proliferation was also evident within the periosteal connective tissue layer. Numerous spindle-shaped fibroblasts were identified interspersed among the collagen fibers of the periosteum. These cells appeared elongated with tapered

cytoplasmic processes and oval nuclei, and they were arranged in small aggregates as well as short, interlacing bundles, indicating an increase in fibroblastic activity within the connective tissue matrix.

The surrounding extracellular matrix exhibited moderately organized collagen fibers, between which these fibroblasts were distributed, suggesting the initiation of reactive connective tissue remodeling. Such fibroblastic proliferation is commonly associated with the early stages of tissue repair, where fibroblasts actively participate in the synthesis of new extracellular matrix components, particularly collagen, as part of the reparative response.

This proliferative fibroblastic response likely represents an early reparative mechanism triggered by the adjacent inflammatory and destructive processes affecting the periosteal surface and underlying bone tissue. The presence of activated fibroblasts in the periosteal connective tissue indicates that the tissue is attempting to restore structural integrity and stabilize the affected area, counteracting the damage induced by the ongoing inflammatory reaction.

Furthermore, the coexistence of inflammatory changes and fibroblastic proliferation reflects the dynamic interplay between tissue injury and the activation of local reparative mechanisms, a process that is commonly observed in periosteal reactions associated with osteitic or osteomyelitic conditions. In the presence of inflammatory stimuli, the periosteum responds through a cascade of cellular and molecular events that aim to contain tissue damage and initiate structural repair.

The periosteum is a highly vascularized and metabolically active connective tissue layer, composed of an outer fibrous layer and an inner cambium layer rich in mesenchymal progenitor cells. Due to this cellular composition, it plays a crucial role in bone homeostasis, repair, and remodeling. When exposed to inflammatory mediators released during infection or bone injury, the periosteum becomes activated, leading to proliferation of fibroblasts and recruitment of progenitor cells capable of differentiating into osteogenic lineages.

In such conditions, fibroblasts within the periosteal connective tissue increase their synthetic activity, producing extracellular matrix components, particularly collagen fibers, which contribute to the formation of a provisional reparative framework. This early fibroplastic response not only stabilizes the affected tissue but also creates a microenvironment that supports subsequent phases of tissue repair, including osteoblastic activity and potential new bone formation.

Additionally, inflammatory mediators and local vascular changes may stimulate angiogenesis and enhanced cellular turnover within the periosteum, further supporting the regenerative process. These mechanisms represent a coordinated attempt by the periosteal tissue to counteract the destructive effects of inflammation and restore structural integrity to the affected bone surface.

Therefore, the simultaneous presence of inflammatory infiltrates and fibroblastic proliferation in the periosteal connective tissue is indicative of an active and ongoing reparative response, reflecting the intrinsic capacity of the periosteum to participate in both inflammatory defense and early stages of bone tissue regeneration.

At higher magnification (20× objective), the inflammatory infiltrate was more clearly characterized by dense aggregates of neutrophils distributed within the periosteal connective tissue and adjacent inflammatory stroma (Fig.3c). Many of these neutrophils exhibited morphological features consistent with degenerative change, including nuclear swelling, karyolysis, and fragmentation of nuclear material. In several areas, neutrophils appeared partially disintegrated, forming small accumulations of cellular debris intermixed with fibrin and inflammatory exudate. These findings were indicative of an intense acute inflammatory response associated with tissue destruction.

Interspersed among the neutrophilic aggregates were numerous activated macrophages. These cells displayed abundant eosinophilic cytoplasm and enlarged, often vesicular nuclei, consistent with a reactive and phagocytically active phenotype. In some macrophages, cytoplasmic vacuoles containing cellular debris or erythrocyte remnants were observed, reflecting ongoing phagocytosis of necrotic tissue and inflammatory detritus. The coexistence of neutrophils and macrophages suggested a transition between acute suppurative inflammation and early stages of tissue clearance and repair.

Despite the abundance of inflammatory cells, no well-organized abscess structure was identified at this magnification. Specifically, there was no clear central cavity surrounded by a defined pyogenic membrane or a peripheral fibrous capsule. Instead, the inflammatory process appeared relatively diffuse and infiltrative within the affected periosteal and connective tissues.

Importantly, careful examination of the cellular morphology revealed no evidence of nuclear atypia, abnormal mitotic figures, or pleomorphism that might indicate a neoplastic process. The nuclei of fibroblasts, inflammatory cells, and vascular endothelial cells maintained normal architecture and chromatin distribution. Furthermore, there were no atypical cellular proliferations or disorganized tissue patterns suggestive

of sarcomatous or other neoplastic transformation. These observations supported the interpretation that the lesion represented a purely inflammatory and reactive process rather than a proliferative neoplasm.

Overall, the histopathological features were consistent with inflammatory periostitis and osteitis associated with reactive bone formation. The examined sections demonstrated clear evidence of an active inflammatory process involving both the periosteum and the superficial cortical layers of the bone. The periosteum was markedly expanded by oedema and infiltrated by mixed inflammatory cells, predominantly neutrophils and macrophages, accompanied by vascular congestion and multifocal hemorrhages. These findings indicated an ongoing inflammatory reaction affecting the periosteal tissues.

In addition to the inflammatory component, the cortical surface of the bone exhibited areas of irregularity and focal resorption compatible with osteitic changes. The presence of necrotic debris, inflammatory exudate, and degenerating neutrophils further supported the diagnosis of an active infectious or septic process affecting the osseous structures. Macrophage infiltration and phagocytic activity suggested ongoing removal of necrotic material and tissue breakdown products.

Evidence of early reparative activity was also present. Mild fibroblastic proliferation within the periosteal connective tissue, together with the presence of reactive bone formation along the cortical surface, indicated that the lesion had initiated a localized reparative response. This reactive osteogenesis likely represented a biological attempt to stabilize and remodel the affected bone in response to inflammation and tissue damage.

Importantly, no histological features suggestive of neoplastic proliferation were observed. Cellular morphology remained consistent with inflammatory and reparative processes, without nuclear atypia, abnormal mitotic figures, or disorganized cellular growth patterns.

Taken together, these microscopic findings supported the diagnosis of focal inflammatory periostitis and osteitis accompanied by reactive bone formation, most consistent with a secondary response to a localized septic process affecting the dorsal aspect of the distal phalanx.

3.5 Clinical and Radiographic Outcome

The horse was re-evaluated 27 days postoperatively. The owner returned primarily for a complimentary tax-free follow-up radiographic examination, performed at the clinician's insistence in order to objectively assess lesion evolution, coinciding with a separate dental procedure scheduled for another horse.

At clinical examination, the horse showed complete resolution of lameness in the affected forelimb. No pain was elicited on palpation of the coronary band or dorsal hoof wall. The surgical defect of the hoof capsule exhibited progressive keratinization and ongoing horn regeneration, with satisfactory cicatrization and absence of purulent discharge. No signs of recurrent infection or local inflammation were observed.

Follow-up latero-medial radiography demonstrated complete resolution of the previously described radiolucent area at the dorsal aspect of the third phalanx (Fig. 2c). The dorsal cortical margin appeared continuous and well-defined, with restoration of normal radiodensity of the adjacent trabecular bone. No residual osteolysis, gas accumulation, or fistulous tract toward the coronary band was identified.

These findings indicated complete clinical recovery and radiographic resolution of the septic osteitic process within 27 days following surgical debridement. The clinical image illustrates a focal defect located on the dorsal aspect of the hoof wall in close proximity to the coronary band. The lesion appears as a vertically oriented fissure associated with localized disruption of the hoof horn and partial loss of the external keratinized layer. The surrounding horn tissue shows irregular margins and structural disorganization, suggesting previous mechanical disruption and subsequent degradation of the hoof wall architecture.

This type of defect is consistent with a penetrating or traumatic lesion of the coronary region, which may serve as an entry point for bacterial contamination into the deeper structures of the hoof capsule. In working horses, particularly those operating in forestry environments, small penetrating injuries produced by wooden splinters or sharp environmental debris may remain initially unnoticed due to the dense hair covering the coronary band and the rigid structure of the hoof capsule.

Once microbial contamination occurs, the confined anatomical environment of the hoof capsule can facilitate the accumulation of inflammatory exudate within the subparietal space, promoting the development of a localized septic process. Progressive pressure generated by purulent material within this inextensible compartment may lead to separation of the hoof wall layers and formation of a visible fissure or defect, similar to the one observed in this case.

Furthermore, the proximity of the lesion to the coronary band is of particular clinical significance. The coronary region represents the primary site of horn production, and traumatic or septic damage at this level may compromise the integrity of the newly forming hoof wall. Such lesions may therefore persist or enlarge

over time as the hoof grows, creating a pathway through which infection can propagate toward deeper tissues.

The presence of a focal defect in this region supports the hypothesis of a communication pathway between the external environment and the deeper subparietal structures, which may ultimately allow extension of the septic process to the dorsal cortical surface of the distal phalanx. This mechanism is consistent with the radiographic and intraoperative findings described in the present case, where a tract connecting the coronary region with the dorsal surface of P3 was identified.

Overall, the clinical appearance of the hoof lesion provides important evidence supporting the presumed pathogenesis of the condition, namely a traumatic coronary penetration followed by subparietal infection and secondary septic osteitis of the distal phalanx. Such lesions highlight the importance of careful inspection of the coronary band and dorsal hoof wall in horses presenting with severe lameness of unclear origin.

4. Discussion

Inflammatory conditions of the distal phalanx associated with lesions of the coronary region represent a diagnostic and therapeutic challenge due to the confined anatomical environment of the hoof capsule and the potential for rapid extension of infection into osseous structures. Penetrating injuries of the hoof, even when not immediately apparent, are well recognized as a source of deep-seated infection and subsequent osteal involvement [6]. In the present case, although a penetrating tract was not externally visible at the time of examination, radiographic evidence of a communication pathway containing gas between the dorsal cortex of P3 and the coronary region strongly supported the presence of a septic process originating from the coronary area.

Solar and subparietal penetrations have been associated with progression toward deeper structures, particularly when early drainage is inadequate or delayed [7]. The rigid, non-distensible nature of the hoof capsule favors accumulation of purulent material under pressure, leading to vascular compromise of adjacent tissues. In this case, the intraoperative finding of pressurized purulent exudate mixed with gas confirmed the existence of a septic focus within a confined subparietal compartment, consistent with mechanisms previously described in penetrating hoof injuries.

Septic pedal osteitis has been documented as a complication of penetrating wounds and subsolar abscessation, frequently requiring surgical intervention when conservative management fails [8]. In reported case series, aggressive debridement of necrotic bone and restoration of drainage were considered essential for resolution and return to function. The surgical approach adopted in the present case, consisting of progressive dorsal hoof wall resection and thorough curettage of the affected cortical bone, is in accordance with these recommendations.

Although septic osteitis of the distal phalanx has been more extensively described in foals, similar pathological mechanisms apply to mature horses when bacterial contamination results in cortical necrosis and osteolysis [9]. The radiographic findings observed in this case—focal osteolysis, cortical disruption, and a distinct radiopaque formation—are consistent with inflammatory bone remodeling and possible sequestrum formation secondary to localized vascular compromise.

The extracted osseous fragment was macroscopically detached and corresponded radiographically to the longitudinal radiopaque structure identified preoperatively. Sequestrum formation is recognized as a consequence of localized bone necrosis, followed by demarcation and separation of the devitalized fragment from surrounding viable bone [10]. The histopathological findings of lamellar bone with periosteal thickening and mixed inflammatory infiltration support the interpretation of an inflammatory osteal process associated with reactive bone proliferation rather than neoplastic transformation.

Furthermore, marginal cortical devitalization has been reported in association with traumatic or septic processes, leading to focal separation of bone fragments [11]. Although no fracture line was identified radiographically in the present case, the possibility of microtrauma or focal cortical disruption secondary to a penetrating wooden foreign body cannot be excluded, particularly given the horse's use in forestry traction work [12]. The absence of retained foreign material at the time of surgery does not preclude a prior transient penetrating insult that initiated the inflammatory cascade [12].

The complete radiographic resolution of the osteolytic area and restoration of a continuous dorsal cortical margin within 27 days indicate that early and thorough surgical debridement can result in favorable outcomes, even in cases involving focal osseous sequestration. These findings underscore the importance of prompt radiographic assessment in cases of unexplained severe lameness associated with coronary region

abnormalities and highlight the necessity of complete removal of necrotic and devitalized bone to prevent chronic infection or persistent osteitis.

Overall, this case reinforces the pathophysiological link between localized septic processes within the hoof capsule and focal cortical necrosis of the distal phalanx, culminating in osseous sequestration. Accurate radiographic diagnosis combined with meticulous surgical debridement appears to be critical for achieving rapid functional recovery in similar cases.

5. Conclusions

This case illustrates that inflammatory pathology of the distal phalanx associated with lesions of the coronary region may culminate in focal cortical necrosis and osseous sequestration, even in the absence of an externally visible penetrating wound. The confined anatomical environment of the hoof capsule facilitates accumulation of septic material under pressure, predisposing to vascular compromise and localized osteitis.

Radiographic examination proved essential for identifying cortical disruption, focal osteolysis, and the presence of a detached osseous fragment in communication with the coronary region. Early recognition of these changes allowed timely surgical intervention.

Complete surgical debridement, including removal of the detached lamellar bone fragment and curettage to macroscopically viable bleeding bone, resulted in rapid clinical recovery and radiographic resolution of the lesion within 27 days. Histopathological evaluation confirmed the inflammatory nature of the lesion and excluded neoplastic proliferation.

Prompt diagnostic imaging combined with meticulous surgical management appears critical for achieving favorable functional outcomes in cases of septic osteal involvement of the distal phalanx associated with coronary region lesions.

Supplementary Materials: No supplementary material is provided, as all information and data are presented in the manuscript.

Author Contributions: Conceptualization, C.L., I.M., I.S. and V.V.; methodology, C.L., I.M. and I.S.; software, I.M. and I.S.; validation, C.L., I.M., I.S. and A.-G.H.-Z.; formal analysis, C.L. and I.S.; investigation, C.L., I.M. and I.S.; resources, V.V. and A.-G.H.-Z.; data curation, I.M. and I.S.; writing—original draft preparation, C.L., I.M. and I.S.; writing—review and editing, C.L., I.M., I.S., A.-G.H.-Z. and V.V.; visualization, I.S. and I.M.; supervision, V.V. and A.-G.H.-Z.; project administration, V.V.; funding acquisition, V.V. All authors have read and agreed to the published version of the manuscript.

Funding: This research received no external funding.

Institutional Review Board Statement: Not applicable.

Data Availability Statement: The data supporting the findings of this study are available within the article. Additional information is available from the corresponding author upon reasonable request.

Acknowledgments: The authors would like to thank the technical staff of the veterinary clinic for their assistance during the surgical procedure and postoperative care of the horse. We also acknowledge the contribution of the histopathology laboratory personnel for processing and evaluating the tissue samples. The cooperation of the animal owner is gratefully appreciated.

Conflicts of Interest: The authors declare no conflict of interest.

References

1. Aßmann, A.D.; Donati, B.; Geyer, H.; Theiss, F.; Bischofberger, A.S. Fracture margin sequestration in mandibular fractures in three horses. Equine Vet Educ **2025**, *37*, e295–e305.
2. Barton, C.K.; Samol, M.A.; Nelson, B.B.; Piquini, G.; Smanik, L.E.; Goodrich, L.R. Subchondral bone sequestrum formation in the proximal intra-articular and osteochondral region of the third metatarsal bone of an Appaloosa mare treated for septic arthritis. J Am Vet Med Assoc **2023**, *262*, 1–4.
3. Cauvin, E.R.; Munroe, G.A. Septic osteitis of the distal phalanx: Findings and surgical treatment in 18 cases. Equine Vet J **1998**, *30*, 512–519.
4. Clem, M.F.; DeBowes, R.M.; Yovich, J.V.; Douglass, J.P.; Bennett, S.M. Osseous sequestration in the horse: A review of 68 cases. Vet Surg **1988**, *17*, 2–5.
5. Findley, J.A.; Pinchbeck, G.L.; Milner, P.I.; Bladon, B.M.; Boswell, J.; Mair, T.S.; Suthers, J.M.; Singer, E.R. Outcome of horses with synovial structure involvement following solar foot penetrations in four UK veterinary hospitals: 95 cases. Equine Vet J **2014**, *46*, 352–357. https://doi.org/10.1111/evj.12124
6. Firth, E.C. Bone sequestration in horses and cattle. Aust Vet J **1987**, *64*, 65–69.
7. Fürst, A.E.; Lischer, C.J. Other clinical problems of the equine foot. Vet Clin North Am Equine Pract **2021**, *37*, 695–721.

8. Gaughan, E.M.; Rendano, V.T.; Ducharme, N.G. Surgical treatment of septic pedal osteitis in horses: Nine cases (1980–1987). J Am Vet Med Assoc **1989**, *195*, 1131–1134.
9. Gift, L.J.; DeBowes, R.M. Wounds associated with osseous sequestration and penetrating foreign bodies. Vet Clin North Am Equine Pract **1989**, *5*, 695–708.
10. Lazăr, C.; Mihăilă, I.; Vulpe, V. "Hoof woodpecker" at coronary band and hoof wall level in forestry environment working horses. Sci Pap Ser Vet Med **2023**, *66*, 12-17. https://doi.org/10.61900/SPJVS.2023.02.02
11. Neil, K.M.; Axon, J.E.; Todhunter, P.G.; Adams, P.L.; Caron, J.P.; Adkins, A.R. Septic osteitis of the distal phalanx in foals: 22 cases (1995–2002). J Am Vet Med Assoc **2007**, *230*, 1683–1690.
Redding, W.R.; O'Grady, S.E. Septic diseases associated with the hoof complex: Abscesses, puncture wounds, and infection of the lateral cartilage. Vet Clin North Am Equine Pract **2012**, *28*, 423–440.